UiT The Arctic University of Norway
Faculty of Health Science, Department of Medical Biology
Research group: Molecular Cancer Research Group

Study of human PRKAR1A and its role in autophagy

Apsana Lamsal
Master thesis in Biomedicine
May 2018
Supervisor Professor Terje Johansen
Assistant supervisor Assoc. Professor Eva Sjøttem

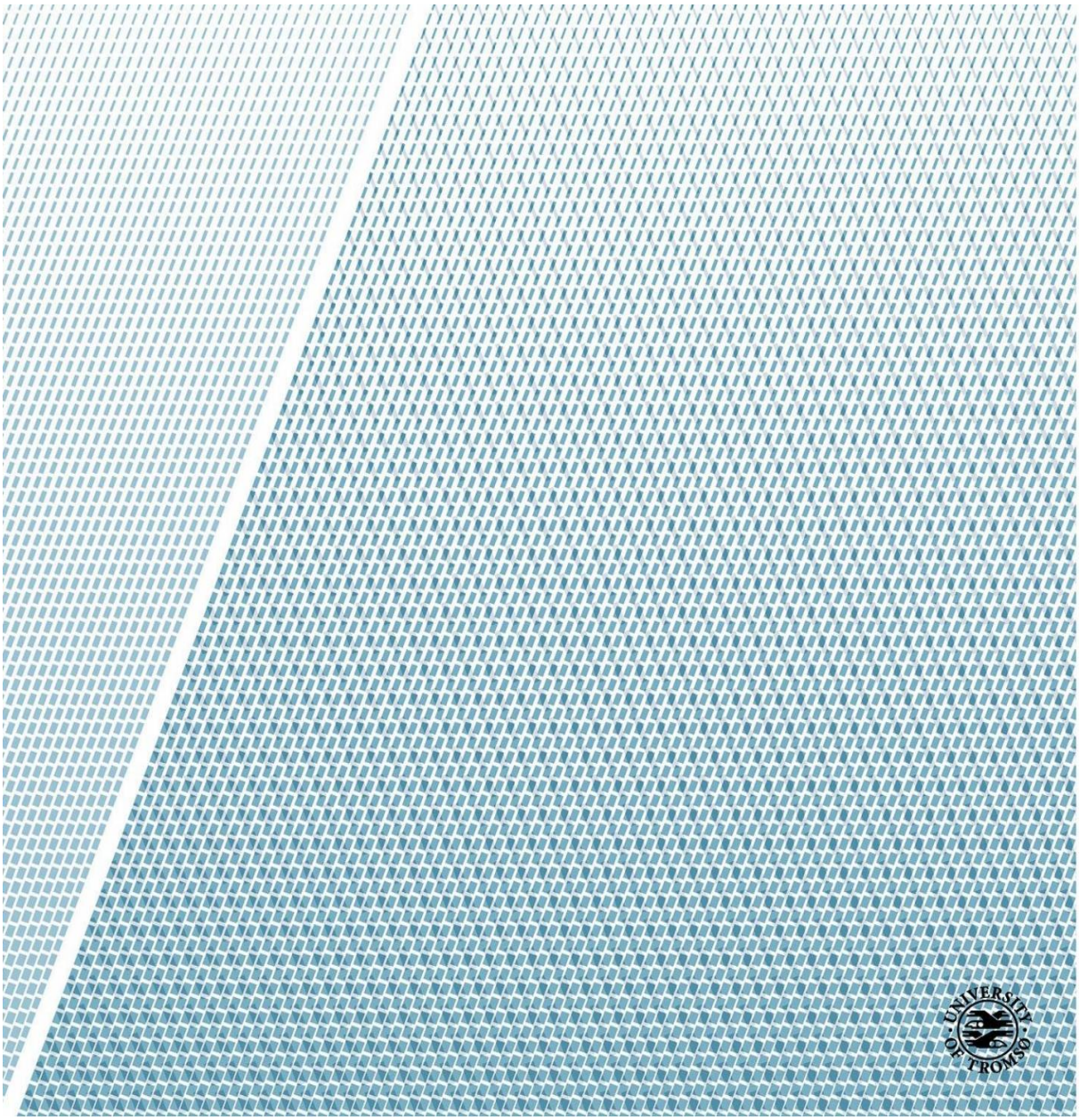

ACKNOWLEDGEMENTS

Foremost, I would like to extend my sincere gratitude to my main supervisor Professor Terje Johansen not only for his continuous support and guidance throughout my master's degree but also for his patience, motivation, enthusiasm and immense knowledge.

My deepest gratitude to my assistant supervisor, Assoc. Professor Eva Sjøttem for her nurturing supervision. I had the opportunity to strengthen my troubleshooting and analytical thinking skills, which are essential for my research career. I could not have imagined having a better advisor and mentor for my thesis.
I would like to mention a huge thanks to Dr. Pradip in assisting in my procedures, all the analytics, and encouraging me to think outside the box.

I would like to thank all the members of MCRG, Gry Evjen and Hanne Britt, Aud for your technical support and supervision especially during my pregnancy. Without your expertise, I would not have been able to complete my experiments, let alone graduate on time. Experiment days were always shorter and a bit easier having so lovely people in the lab.

I thank Kenneth Bowitz Larsen for his invaluable technical excellence in microscopy and imaging.

Finally, I am very grateful to my parents for their continuous motivation, my husband, Pushpa Shigdel, who has always been there for me. To my little daughter, Prazna who constantly tolerated my absence. You give me a chance to live a life outside of school.

I sincerely hope my work will spark further research in the field of autophagy.

LIST OF ABBREVIATIONS

aa	amino acid
Atg	Autophagy- related genes
CMA	Chaperone- mediated- autophagy
Co-IP	Co-Immunoprecipitation
DMEM	Dulbecco′s Modified Eagle′s Medium
DTT	Dithiothreitol
E. coli	*Escherichia coli*
EGFP	Enhanced Green Fluorescent Protein
ER	Endoplasmic reticulum
FA	Formaldehyde
FBS	Fetal bovine serum
FIP200	Focal adhesion kinase family interacting protein 200kD
FM	Full growth Medium
GOI	Gene of interest
GST	Glutathione S- transferase
HBSS	Hanks Balanced Salt Solution
HRP	Horse Radish Peroxidase
IPTG	Isopropyl-β-D-thiogalactopyranoside
LB	Luria-Bertani
LC3	Light Chain 3
LIR	LC3-interacting region
LSCM	Laser Scanning Confocal Microscopy
mCherry	monomeric Cherry

MEM	Minimum Essential Medium Eagle
ON	Overnight
PBS	Phosphate Buffered Saline
PPNAD	Primary pigmented nodular adrenocortical disease
PRKAR1A	Protein Kinase cAMP-dependent type I Regulatory Subunit Alpha
RT	Room temperature
RTL	Reticulocyte lysate
SDS-PAGE	Sodium Dodecyl Sulfate Polyacrylamide Gel Electrophoresis
SOC	Super optimal broth with Catabolite repression
TAX1BP1	Tax 1 Binding protein 1
TE	Tris-EDTA
TEMED	Tetramethylethylenediamine
UBA	Ubiquitin Associated Domain
UPS	Ubiquitin proteasome system
WB	Western Blot
WT	Wild Type

SUMMARY

The human PRKAR1A gene is a 381- amino acid protein encoding the regulatory subunit (RIα) of the cAMP dependent Protein Kinase A (PKA). The main function of PRKAR1A is to regulate the catalytic activity of PKA. PRKAR1A is shown to regulate autophagy via association with mTOR kinase and colocalization with the autophagy marker proteins LC3B, Rab7 and Rab9. Contradictory findings regarding the localization and function of the protein in autophagy have been reported. The main aim of this study was to investigate a functional role of the protein in relation to autophagy. Our *in vitro* and *in vivo* assays show that PRKAR1A interacts with the ATG8 family proteins, and strongest with GABARAPL2. PRKAR1A exhibits mainly diffuse cytosolic localization in the cells, and did not show a significant colocalization with LC3B, GABARAP or the autophagy receptor p62. Interestingly, colocalization of PRKAR1A with GABARAP was enhanced by the presence of the catalytic subunit of PKA. Furthermore, PRKAR1A was degraded by the proteasomal system and not by autophagy. However, PRKAR1A was involved in the regulation of autophagy as observed by a reduction in the average number of LC3B puncta in cells expressing EGFP-PRKAR1A upon starvation. It is still unclear if PRKAR1A directly regulates autophagy or has an indirect function. The strongest binding to GABARAP family members could suggest this protein might have a role during autophagosome maturation. However, further studies are crucial to identify the role of PRKAR1A in autophagy.

Table of Contents

1. Introduction

1.1 Protein Kinases

Protein kinases are a large family of enzyme proteins that catalyze the phosphoryl transfer from Magnesium Adenosine Tri-Phosphate (MgATP) to Serine/Threonine and/or Tyrosine side chains thereby changing the conformation from inactive to active form of a protein [1]. Protein kinases represent 3% of the genes in the total eukaryotic genome and more than 500 different protein kinases have been identified in human [2].With the discovery of protein kinases in 1950s, a lot have been understood regarding their roles in various signal transduction pathways and abnormal kinase activity leads to several diseases; cancer being a major concern [3].

1.1.1 cAMP dependent Protein Kinase A (PKA)

3',5'- cyclic Adenosine Monophosphate (cAMP) is a secondary messenger which mediates intracellular signal transduction in various cellular/physiological pathways and having its vital role in cell division, proliferation, hormonal homeostasis and inflammation [4, 5]. cAMP production is mediated by activated G protein–coupled receptors (GPCRs) causing the dissociation of the GPCR trimer to Gα and Gβγ subunits. The activation of GPCRs is via exchange of bound GDP to GTP upon ligand binding. The dissociated Gα activates a membrane bound enzyme Adenylyl cyclase leading to the production of cAMP from Adenosine Triphosphate (ATP) (Figure 1) [6] .

cAMP sensing Protein Kinase A (PKA) is activated by cAMP and is the best studied protein kinase to date [7]. PKA, a ubiquitous serine/threonine protein kinase holoenzyme is a hetero-tetramer containing two pairs each of regulatory (RIα or RIβ and RIIα or RIIβ), and catalytic subunits (Cα, Cβ or Cγ and Prkx) [8, 9]. PKA is inactive under low levels of cAMP, however the inactive form undergoes a conformation change into the active form when the cAMP level is upregulated. cAMP binds to the two binding sites of the regulatory subunit dimer and releases two free monomeric catalytic subunits. This activation is achieved by phosphorylating the substrate at serine/threonine residues of the protein (Figure 1) [10].

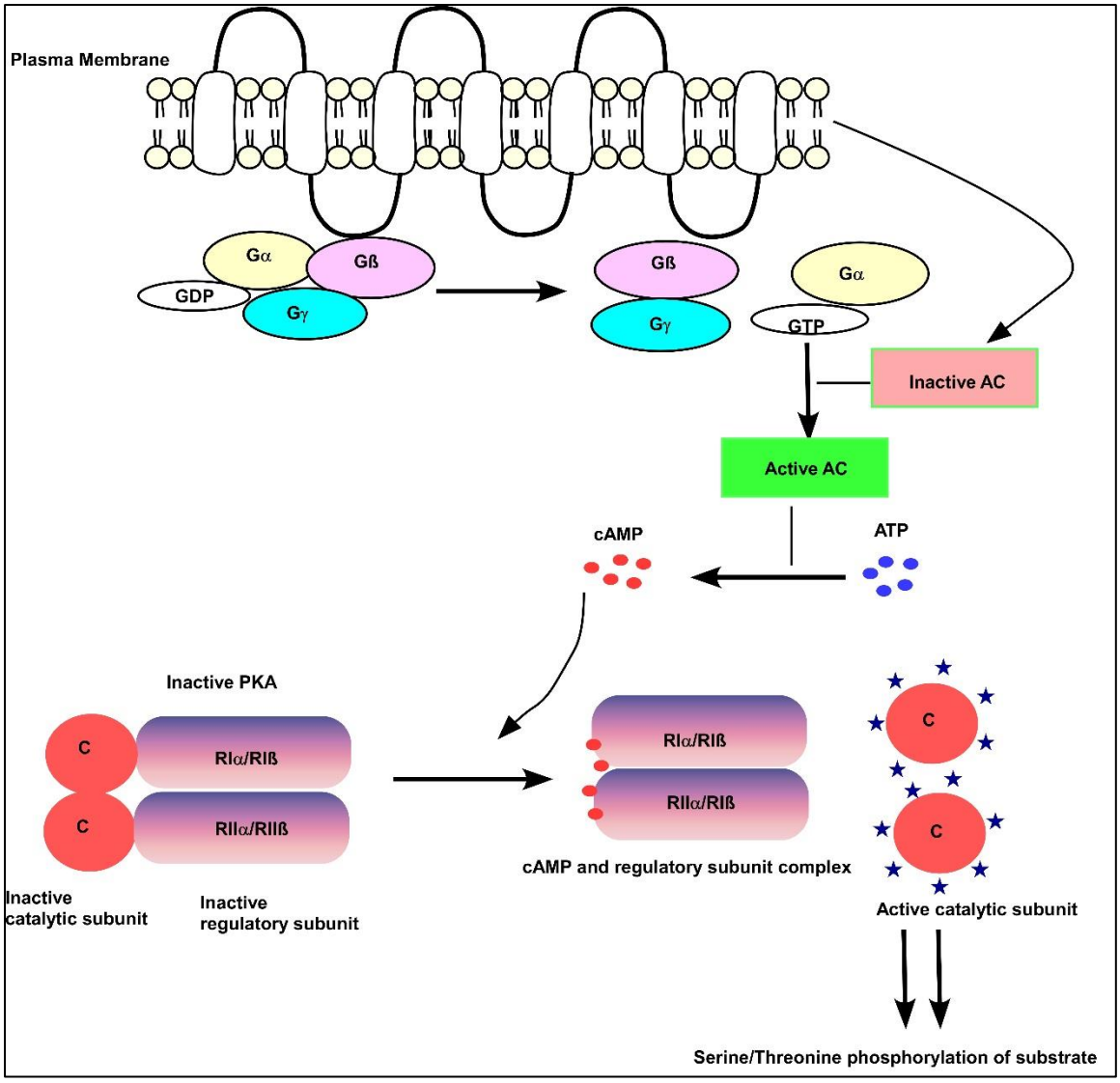

Figure 1: PKA signaling and PKA holoenzyme. Upstream signaling from GPCR leads to production of cAMP from ATP which then activates PKA. Receptor activation (ligand binding) dissociates GPCRs into Gα and Gβγ subunits. After activation, Gα-GTP subunit interacts with membrane bound Adenylyl cyclase thus leading to production of cAMP from Adenosine Triphosphate (ATP). The inactive PKA holoenzyme is a hetero-tetramer composed of two catalytic subunits and two regulatory subunits (RIα/ RIIα and RIβ/RIIβ). Two cAMP molecules bind to each regulatory subunit and release two free monomeric catalytic subunits. The activated catalytic subunits now phosphorylate/activate the downstream targets. Adapted with minor modifications from [11-13].

The catalytic subunit of PKA is well studied and has about 70% sequence similarities to all protein kinases [14]. Although, various regulatory subunits of PKA are involved in cellular processes, RI α is the most abundant regulatory subunit that regulates various cell cycle processes. Within the cell, R1α and RIβ is diffusely localized in the cytoplasm; R1α is expressed ubiquitously whereas RIβ being preferentially expressed in brain, testis, and B and T lymphocytes. RII subunits are localized to subcellular structures (RIIα being ubiquitous and

RIIβ in brain, endocrine and adipose tissues) and compartments by anchoring via A kinase anchoring proteins (AKAPs) [15-18].

1.1.1 PRKAR1A in Carney Complex disease

PRKAR1A gene is a 381- amino acid protein encoding the RIα subunit of PKA; containing an N-terminal dimerization/docking domain (1-45), linking region or hinge region (92-96), two cAMP binding domains A (145-262) and B (263-380) (Figure 2) [19].

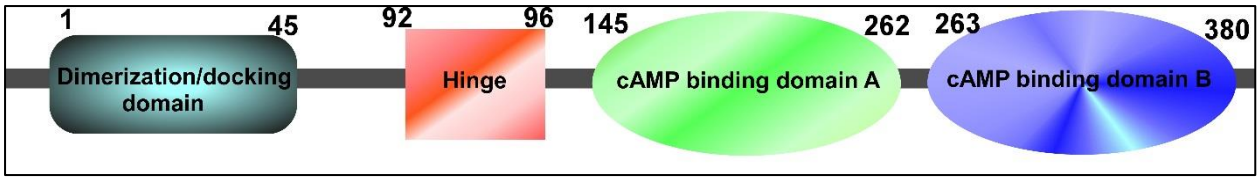

Figure 2: PRKAR1A structure PRKAR1A consists of an N-terminal dimerization/docking domain (turquoise), linking region (orange) and two cAMP binding domains A and B (green and blue). Adapted with minor modifications from (http//atlasgeneticsoncology.org//Genes/PRKAR1AID387.html).

Inactivating mutations/large deletions in PRKAR1A have been linked with Carney complex (CNC) disorder, primary pigmented nodular adrenocortical disease (PPNAD), adrenocortical adenomas and cancer [20, 21]. CNC is a multiple endocrine neoplasia syndrome; inherited in autosomal dominant manner characterized by skin pigmentation/tumors, myxomatous tumors, schwannomas, endocrine and non-endocrine neoplasms [22, 23]. More than 125 different mutations have been reported in 401 unrelated families of different origin [12]. Almost all mutations identified till date lead to premature stop codon and the mutant mRNAs are degraded due to nonsense-mediated mRNA decay [24]. PRKAR1A defects related to CNC causes PRKAR1A haploinsufficiency thereby losing the function of the regulatory subunit and making the catalytic subunit available for cAMP dependent activation (also termed as increased PKA activity) leading to cell proliferation and subsequent tumor formation in the affected tissues [25, 26].

1.2.2 Mouse models of PRKAR1A disease mutations

Mouse models have been developed to understand the molecular basis of PRKAR1A in CNC and its phenotypes. Mouse embryonic fibroblasts (MEFs) having PRKAR1A mutations had significant increased PKA activity compared to the wild type MEF cells. The PKA activity was even more elevated in the PRKAR1A knockout (KO) cells [27, 28]. Kirshner *et al.* 2005

studied mice with PRKAR1A mutations up to 2 years and revealed 85% of the population had osteoblast neoplasia, 33% had schwannomas and 10% had thyroid carcinomas. This suggests that mouse having the exact same heterozygous mutations in PRKAR1A as patients with CNC are more susceptible to tumor formation in cAMP-responsive tissues [29]. However, this model did not explain other CNC tumors associated with skin, pituitary adenomas and heart myxomas. Another mouse model with antisense transgene for PRKAR1A in exon 2 showed highly significant decrease in the protein level and increased cAMP signaling. The transgene under control of a tetracycline responsive promoter developed other CNC features, like thyroid tumors, adenoma, adrenocortical hyperplasia as well as visceral adiposity and late onset weight gain, providing more insight to the role of PRKAR1A in the disease [30, 31]. There are some studies showing mice with knock out PRKAR1A in the developing heart with lesions suggesting cardiac myxomas [32]. Another knock out mouse model with mice PRKAR1A knock out in the adrenal cortex developed the hallmarks of bilateral and adrenal hyperplasia exactly similar to Primary Pigmented Nodular Adrenocortical disease (PPNAD) caused by PKA dysregulation [33].

1.2 Cellular homeostasis

Eukaryotic cells continuously renew their components like protein, lipid and carbohydrate with the interplay between catabolic and anabolic processes thereby maintaining cellular homeostasis. This balance is a tightly regulated mechanism essential for the biosynthesis and degradation of macromolecules [34]. During shortage of nutrients, the cells fulfil their needs by recycling cellular components through degradation of macromolecules and proteolysis. Thus, proteolysis is an equally important process as uptake since it ensures the reuse of amino acids and provides protein quality control. Proteins or macromolecules are degraded by two major pathways the ubiquitin-proteasome system; that degrades single proteins and short-lived protein complexes in the cytoplasm and nucleus and the lysosomal degradation pathway that degrades long-lived proteins and damaged organelles like mitochondria, peroxisomes and Endoplasmic Reticulum (ER) [35-37].

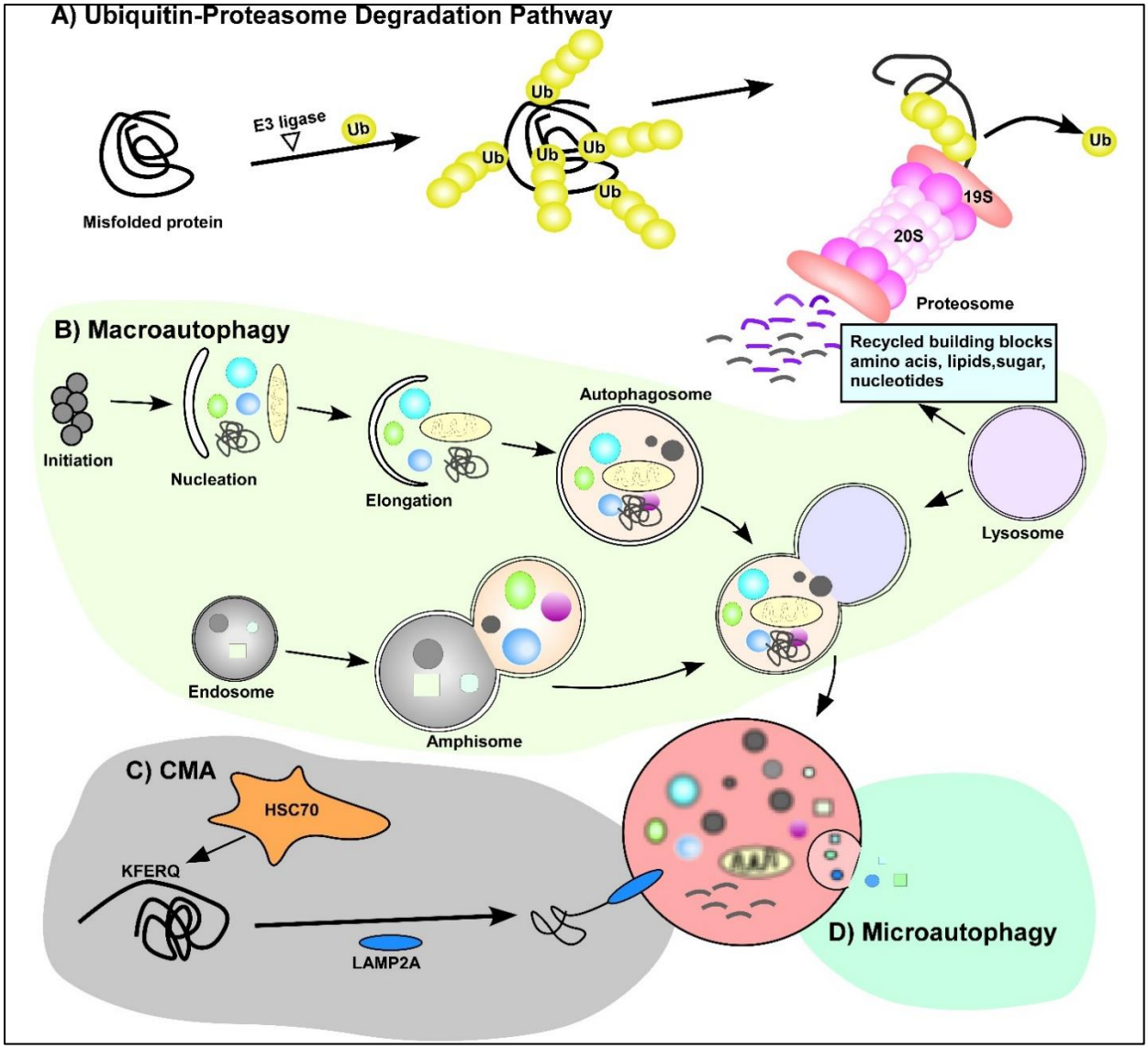

Figure 3: Eukaryotic degradation system. (A) Ubiquitin-Proteasome Degradation Pathway- misfolded protein or targeted component ubiquitinated by E3 ligase following transfer of protein to the proteasome thereby degraded by proteolysis. **B - D Autophagic pathways**. **(B) Macroautophagy** - steps in autophagy as gathering the protein complex (initiation), generation of the double membrane phagophore (Nucleation), and expansion of phagophore along with the docking of targeted organelle or proteins (elongation), after completion the phagophore closes to make autophagosome which fuses with the lysosome. Some of the autophagosomes fuse with endosome prior to fuse with lysosome making amphisomes. **(C) Chaperone Mediated Autophagy** misfolded protein recognized by HSC70 transporting directly into lysosome by a lysososmal membrane receptor LAMP2A. **(D) Microautophagy** direct invagination of the cytosolic material (micromolecules) into the lysosome. Adapted with modifications from [38].

1.2.1 Ubiquitin-Proteasome System (UPS)

The ubiquitin–proteasome system (UPS) mediates the degradation of proteins with the help of a 76- amino acid, highly conserved molecule known as ubiquitin (Ub). UPS degrades around 80-90% of the intracellular proteins and the rest 10-20% is degraded by the lysosome under optimal conditions [39]. UPS comprises of Ub, the Ub- activating enzyme (E1), Ub conjugating enzymes (E2), and Ub ligases (E3), the proteasome and deubiquitinases (DUBs) [40]. Transfer of Ub to the target protein is via a multistep enzymatic cascade and is a complex process. E1 enzyme activates Ub, an ATP dependent formation of Ubiquitin-E1 thiol ester. E2 enzyme then recognizes the E1 enzyme where the cysteine residue of E1 is transferred to E2 enzyme with an additional thioester linkage. E2 is finally recognized by E3 by binding through its conserved core. The E3 enzyme facilitates the linkage of at least four Ub monomers to the specific target protein determined for degradation (Figure 3A). The poly-ubiquitinated proteins are then directed to the 26S proteasome complex where the proteins are degraded [41-43].

The 26S proteasome complex consists of the 20S catalytic subunit and two 19S regulatory subunits. The catalytic subunit is cylindrical in shape and the regulatory subunits reside at the ends of the 20S protein core. The target protein is recognized and unfolded by the 19S subunit and transferred into 20S subunit for degradation [44].

1.3 Autophagy

Autophagy, derived from the Greek meaning ‘eating of self’ is a self-degradative process involved in the sequestration and transport of the cytosolic proteins or organelles for lysosomal degradation in response to nutrient or cellular stress [45]. The cellular autophagy process is also activated by other stress conditions like low ATP concentration, endoplasmic reticulum stress, invasion by pathogens, accumulation of damaged organelles or proteins and many more [46-49]. Autophagy is an evolutionarily conserved process which plays a vital role in maintaining cellular homeostasis [50]. Based on different mechanisms for directing the cytoplasmic content into the lysosomes for proteolytic degradation three different types of autophagy have been described macro-autophagy, micro-autophagy, and chaperone-mediated autophagy (CMA).

In both micro and macro autophagy the large structures are engulfed in selective as well as non-selective mechanisms and are best characterized in yeast. However, in CMA only soluble proteins (KFERQ peptide) are degraded via a selective mechanism which only occurs in mammals [38]. In macro autophagy, the cytoplasmic substrate (long lived proteins, damaged

organelles and invasive microbes) are sequestered into the double membrane vesicle known as autophagosome which fuses with the lysosome to form autolysosomes for the recycling and degradation of the cytoplasmic contents (Figure3B) [51]. However, in micro autophagy, the micro substrate like small macromolecules, vesicles are directly engulfed or fused to the lysosomal membrane facilitating the invagination into the lysosome (Figure 3D) [52]. In CMA, the protein to be degraded is recognized by the chaperone Hsc70 (Heat Shock Cognate-70) through KFERQ motif within the substrate and transported to the lysosomal membrane by glycoprotein LAMP2A to be degraded by the lysosome (Figure 3C). Hence CMA allows the specific removal of selected proteins without interrupting the FM and neighboring proteins [53].

The first study in the field of autophagy was made by De Duve *et al.* in 1955 with the discovery of the lysosome. Later in 1963 he and his colleagues coined the term "autophagy" as the process of delivery of cytoplasmic components for lysosomal degradation [54, 55]. The great breakthrough was made in the early 1990s, as autophagy was studied in yeast by microscopic observation under the condition of nutrient stress [56, 57]. Oshumi and colleagues identified the first 15 Atg genes in a genetic screen. Thereafter, yeast has been subsequently used as a model organism for autophagy research and pioneering genetic studies have revealed more than 41 AuTophaGy-related (*ATG*) genes involved in the formation of the core machinery of autophagosome and membrane dynamics during autophagy [58, 59]. *APG1* (now *ATG1*) was the first *ATG* gene (ULK1/ULK2 in mammals) to be identified [60]. Several mammalian *ATG* genes have been linked with diseases ranging from inflammation , cardiac diseases and neurodegeneration [61].

1.3.1 The core machinery of autophagosome formation

Autophagosome biogenesis is the hallmark of macroautophagy (hereafter referred as autophagy) involving the formation of the double membrane structure known as phagophore which expands and maturates to form a cytoplasmic double membrane vesicle, the "autophagosome' [62]. The size of autophagosome in yeast and mammalian cells slightly vary; yeast having the smaller (~500-900 nm), while mammalian having much larger (0.5-1.5 μm) autophagosomes. However, some cells like hepatocytes, embryonic stem cells and embryonic fibroblast have much larger autophagosomes that can be visualized by light microscopy [63]. Rapid molecular research in the field of autophagy peaked after the discovery of *ATG* genes and led to the more detailed characterization of various steps in autophagy. Since

autophagosome biogenesis is a complex phenomenon diverse genes and proteins involved in the process have been identified. The term “core autophagy machinery” has been coined which refers to a subgroup of approximately 18 genes that is common for all subtypes of autophagy and the corresponding gene products required for the autophagosome formation [64, 65].

The elements of the core autophagy machinery are well conserved from yeast to mammals and have been shown to act in an identical manner. The yeast counterparts are referred to as *Atg* genes and their corresponding proteins as Atg proteins whereas *ATG* genes and ATG proteins respectively for the mammalian hereafter. The mammalian core autophagy machinery is composed of (1) complex of uncoordinated 51-like kinase 1 and 2 (ULK1–ULK2); (2) Class III phosphatidylinositol 3-kinase (PI 3-kinase) complex; ATG2A and ATG2B, (3) and the mammalian Atg18 homologs WD-repeat protein interacting with phosphoinositides 1, 2, 3 and 4 (WIPI1, WIPI2, WIPI3 and WIPI4, respectively; (4) ATG9; (5) Complex of the ATG12–ATG5 conjugate and Atg16L1 and (6) Two subfamilies of at least 7 ATG8 Light chain 3 proteins (LC31A/LC31B, LC3B, LC3C) and γ-amino butyric acid associated protein (GABARAP,GABARAPL1,GABARAPL2). Autophagy involves a chain of molecular processes from initiation of autophagosome formation, nucleation, elongation to maturation and degradation of the autophagosomal contents (Figure 4A) [63, 66, 67].

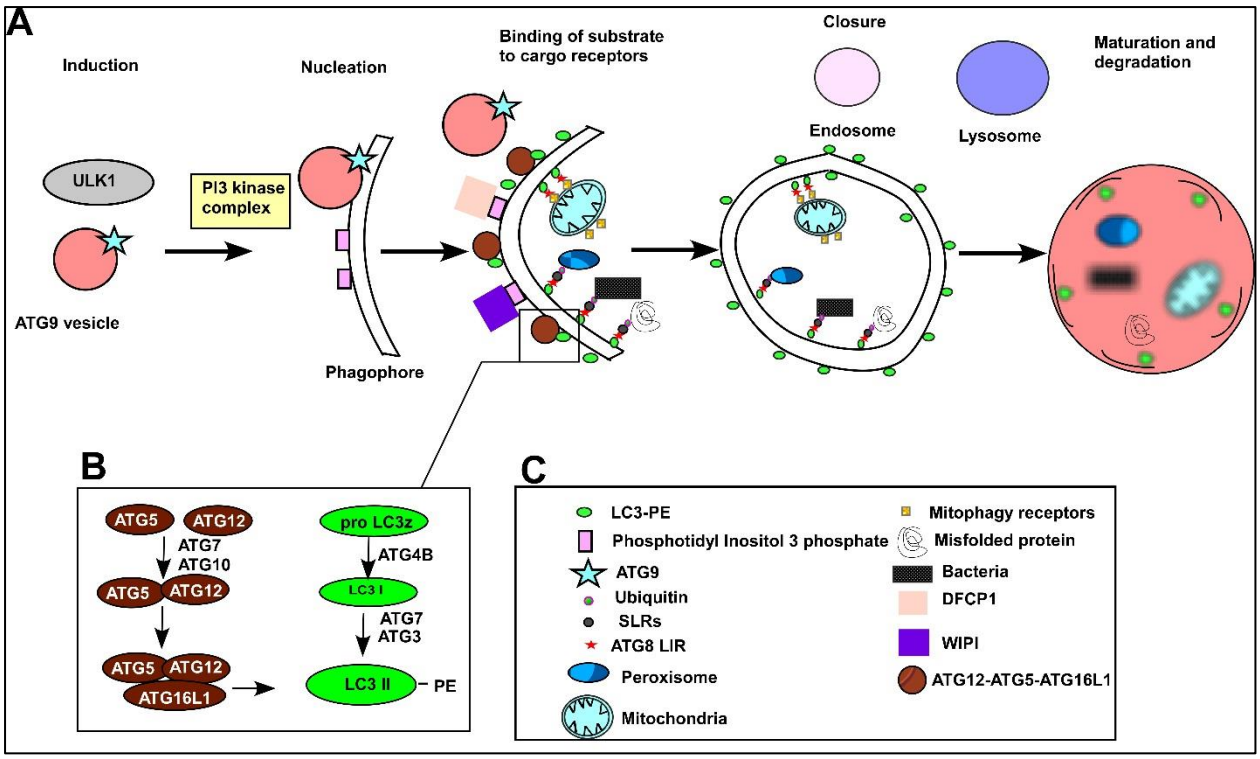

Figure 4: Steps of autophagosome formation in mammalian cells. **A**. The initiation of autophagosome formation starts when the ULK protein complex comprising ULK1/2, ATG13, FIP200 and ATG101 assemble at the isolation membrane. During the nucleation process the proteins and lipids are recruited to the phagophore and a vesicle located transmembrane protein ATG9 transports proteins and lipids to and from the phagophore. The membrane nucleation generates the Phosphotidyl Inositol 3 phosphate at the phagophore with the involvement of Beclin 1/PI3K complex, coordinated by the interaction between Beclin 1, ATG14L, Vps34, Vps15 and double FYVE-containing protein 1 (DFCP1). Phagophore expansion is mediated by the ubiquitin-like conjugated system **B**. An oligomeric complex between ATG12-ATG5 and ATG16L1 is produced via E1 like enzyme ATG7 and E2 like enzyme ATG10. ATG8/LC3 proteins are conjugated to phosphatidylethanolamine (PE) following cleavage by ATG4 which acts on naive ATG8s to expose C-terminal glycine residue essential for covalent attachment to PE. Now, the E1 like enzyme ATG7 conjugates the exposed glycine of ATG8 (LC3-I) and the activated ATG8 is transferred to E2 like enzyme ATG3 subsequently forming an ATG8-ATG3 thioester intermediate prior to conjugation of ATG8 to PE by E3 like ATG12-ATG5-ATG16 complex. The cargo for autophagy is recruited to the surface of the phagophore by cargo receptors. The expansion of the phagophore and enclosing of cargo forms the autophagosome which fuses with the late endosomes/lysosome to form autolysosome where the cargo is degraded. The representative cartoons are described in box **C**. Adapted with minor modifications from [66].

1.3.2 Events in Autophagosome formation

1.3.2.1 Initiation of autophagosome formation

The isolation membrane or phagophore; a small crescent shaped structure, is the origin of the autophagosome as well as the starting point of autophagy. The source of the phagophore can be diverse organelles like endoplasmic reticulum, Golgi apparatus, mitochondria and the plasma membrane [68-71]. The cellular nutritional level is sensed by an important regulator of autophagy; the mechanistic target of rapamycin (mTOR) which is active under nutrient-rich conditions, inhibiting autophagy and protein degradation. However, under starvation mTOR is inactivated and autophagy is induced by reduced mTOR dependent phosphorylation of ULK1 and ATG13 [72]. The formation of ULK protein complex containing ULK1/2, ATG13, FIP200 and ATG101 at the phagophore leads to the initiation of autophagosome formation (Figure 4A and 5A) [73]. In mammals mTOR regulates the ULK1 complex (ATG13, ULK1/2 and FIP200) via direct binding and phosphorylation of ATG13 and ULK1/2 whereas in yeast, TOR binds and phosphorylates Atg13, detaching it from the Atg1 complex [74]. Besides mTOR, autophagy can also be activated by reduction of the cellular level of inositol 1, 4, 5-trisphosphate (IP_3) as well as by lowering cyclic adenosine monophosphate (cAMP) level. The reduced IP_3 level is responsible for the further reduction in intra-cytosolic calcium ion concentration and calpain activity to lower the cAMP level, leading to a feedback loop for the stimulation of autophagy [75, 76].

1.3.2.2 Nucleation

The nucleation phase is induced when the dephosphorylated ULK1 dissociates from the mTOR complex and phosphorylates ATG13 and FIP200. The phagophore assembly site (PAS); a peri-vacuolar location is the proposed site for autophagosome formation. Atg9, a transmembrane protein transports proteins and lipids to the phagophore (Figure 4A). In yeast, the core machinery proteins co-localize at PAS however in mammals the proteins are found throughout the cell [77, 78]. In yeast this step is regulated by the Atg1 complex (including at least Atg1, Atg13 and the Atg17–Atg31–Atg29 ternary sub complex) [73, 77]. Atg14-containing class III phosphatidylinositol 3-kinase (PI3K) complex comprised of Vacuolar protein sorting (Vps34), Vps30/Atg6, Vps15, Atg14 and Atg38) is then recruited to the PAS [79]. In mammalian cells, autophagosome nucleation is a highly coordinated process which relies on

Beclin 1/PI3K complex that phosphorylates phosphatidylinositol to phosphatidylinositol 3-phosphate (PI3P) eventually recruiting effector proteins such as the WD-40-repeat-domain containing proteins WIPI1 and WIPI2, and the FYVE-domain containing protein (DFCP1) that are essential for the expansion of the autophagosome (Figure 4A) [80-82]. The Beclin1/PI3K complex comprises of VPS34, VPS15, ATG14 and Beclin1, associates with the ULK1/2 complex and this is regulated by post translational modifications in mammals [83]. The formation of the Beclin1/ PI3KC3 is also facilitated by UV irradiation resistance-associated gene (UVRAG) and a Beclin 1-interacting protein Ambra1 [84]. In addition to this, UVRAG and ATG14 (mammalian homolog of yeast Atg14) are exclusively found in Beclin1/PI3K complexes [85].

1.3.2.3 Phagophore expansion/elongation and closure

The nucleation step is followed by the recruitment of Atg/ATG proteins to the pre-autophagosomal membrane facilitating the elongation, expansion and completion of the autophagosome biogenesis [86, 87]. The two UBL (ubiquitin-like) conjugation systems Atg8 and Atg12 are essential for elongation of the phagophore membrane [80, 88]. ATG7 act as E1 enzyme and ATG10 (E2 enzyme) facilitates the formation of the ATG5-ATG12 complex [89]. ATG5 binds to the N –terminal of ATG16L1 via a non-covalent bond independent to its binding with ATG12 and forms a homodimer which is capable of binding to ATG12-ATG5 conjugate eventually forming a heterohexamer (Figure 4B). This ATG12-ATG5-ATG16L1 complex is responsible in ordering the site of autophagosome formation which acts as an E3 ligase in the next UBL conjugation system and for stabilization of membrane structure [89-91].

The second UBL conjugate system causes the modification of MAP1LC3 (Microtubule-associated protein 1-light chain 3), the mammalian homolog of yeast Atg8. The mammalian Atg8 homologue is a UBL protein family and consists of seven family members grouped into the LC3 and GABARAP subfamilies. However, yeast has only one Atg8 protein [92, 93]. Yeast has single Atg4 however mammalians have four ATG4 homologues (ATG4A, ATG4B, ATG4C, ATG4D) [94]. ATG4B cleaves the C-terminal Glycine-120 residues of precursor LC3 (proLC3) producing LC3-I and exposes a C-terminal glycine residue essential for the covalent attachment to phosphatidylethanolamine (PE). In contrast, a single Atg4 cysteine protease is responsible for cleaving Atg8 in yeast cells. The exposed glycine of LC3-I (ATG8) now covalently binds to E1 like enzyme ATG7 which is then transferred to E2 like enzyme ATG3

before ATG8 is conjugated to PE by the E3 like ATG12-ATG5-ATG16 complex. The lipidated LC3 (LC3-II) is then incorporated into the forming autophagosomal membrane which remains associated with the autophagosome until the dissociation of the outer membrane and degradation of the inner membrane by the lysosomal enzymes along with the enclosed cargo [91, 95, 96].

1.3.2.4 Autophagosome maturation and degradation

Elongation and closure of the autophagosome is followed by maturation where the autophagosome fuses with the lysosome for the enclosed cargo degradation. The late endosome marker protein Rab7 and lysosomal associated membrane protein-2 (LAMP-2) promote the fusion of autophagosome with different types of vesicles from endosomal/lysosomal pathways [97-100].

Rab7, a member of the large superfamily Ras-like GTPase (guanosine-5'-triphosphatases) is involved in transport of autophagosomes and endosomes for lysosomal degradation. Rab7 is the most studied Rab protein. Apart from its vital role in membrane trafficking, it is equally important for lysosomal biogenesis and maintenance [101, 102]. Two different isomers of Rab7 (Rab7a and Rab7b) with 50% similarities have been reported in mammals. However, they are different in localization; Rab7a being localized mainly to late endosomes and regulating the trafficking from early to late endosomes and from late endosomes to lysosomes. In contrast, Rab7b is localized to late endosomes as well as trans-golgi network thereby regulating endosome to Golgi transport [103-106]. The Retromer trafficking complex (sorting nexin subunits and a VPS26/29/35 trimer) regulates the Rab7 activity by regulating the endosome-lysosomal and autophagosomal membrane trafficking [107, 108]. Perinuclear aggregation of lysosomes is seen when Rab7-interacting ring-finger protein (Rabring 7) is overexpressed [109]. Inactivation or depletion of Rab7 leads to reduced lysosome biogenesis causing accumulation of autophagic vacuoles, and subsequent reduction in clearance of the protein aggregates [97].

LAMPs (lysosome associated membrane proteins) are a family of glycosylated proteins predominantly residing on the lysosomal membrane and involved in the lysosomal/endosomal membrane trafficking. Based on expression, five different LAMPs have been identified LAMP1 and LAMP2 are ubiquitously expressed whereas LAMP3, LAMP4 and LAMP5 display cell type specific expression [110]. LAMP1 and LAMP2 have 37% sequence similarity

and are major constituents of type I transmembrane proteins. LAMP1 is a single transcript whereas LAMP2 has three different isoforms (LAMP2a, LAMP2b and LAMP2c); LAMP2a being particularly involved in Chaperone mediated autophagy[111-113]. Studies have shown LAMP1 and LAMP2 deficient mice with aggregated autophagic vacuoles in many tissues suggesting its role in autophagy [114]. In addition to this, double LAMP (LAMP1 and LAMP2) deficient cells had reduced late endosomal/lysosomal fusion to autophagosomes as well as reduced recruitment of Rab7 to autophagosomes [99, 115]. The important proteins involved in the core machinery of autophagosome formation is listed in Table 1.

Table 1: Summary of Atg/ATG proteins involved in core machinery of autophagosome formation

	Yeast	Mammals	Characteristics and Functions
Atg1/ULK1 COMPLEX	Atg 1	ULK1/2	Ser/Thr kinase, Phosphorylated by mTORC1 Recruits Atg protein to PAS
	Atg 13	ATG13	Acts as a regulatory subunit and is hyper phosphorylated or dephosphorylated by mTORC1 depending upon nutrient status; Links Atg1and Atg17
	Atg17	-	Bridges Atg29 and Atg31
	Atg11	-	Scaffold for the PAS alignment in selective autophagy
	Atg29	-	Forms ternary complex with Atg17 and Atg29
	Atg31	-	Acts as scaffold protein which binds Atg1; essential for PAS organization in selective autophagy
	-	RB1CC1/FIP200	Forms ternary complex with Atg29 and Atg31. Scaffold protein for ULK1/2 and ATG13
	-	ATG101/C12orf44	Collaborate with Atg13. Might have similar functions as of yeast Atg17s, Atg29, and Atg31
Atg9 complex	Atg2	ATG2A/B	Interacts with Atg18
	Atg9	ATG9A/B	Spanning trans membrane protein; recruit proteins to PAS
	Atg18	WIPI1/2	Binds to PI3P, necessary for returning to peripheral sites from PAS
	-	DFCP1	PI3P-binding FYVE-containing protein. Essential for expansion of autophagosome.
Class III PtdIns3K complex	Vps34	PIK3C3/VPS34	PtdIns3Kinase
	Vps15	PIK3R4/VPS15	Ser/Thr kinase, essential for Vps34 membrane association
	Vps30/Atg6	Beclin1	Interacts with Bcl-2; Component of PtdIns3K complex I and II
	Atg14	ATG14	Autophagy-specific subunit. Component of PtdIns3K complex I
Atg8/LC3 Ubl conjugation system	Atg8	LC3A/B/C, GABARAP, GABARAPL1/2	Ubl protein; Forms Atg8–PE complex

	Atg4	ATG4A/B/C/D	Cysteine protease; Removes C-terminal Glycine residues of Atg8 proteins (LC3 and GABARAP)
	Atg7	ATG7	E1 like enzyme
	Atg3	ATG3	E2 like enzyme
Atg12/LC3 Ubl conjugation system	Atg12	ATG12	Ubl protein; Forms Atg12-Atg5 complex
	Atg7	ATG7	E1 like enzyme
	Atg10	ATG10	E2 like enzyme
	Atg5	ATG5	Atg5 and Atg12 interacting protein
	Atg16	ATG16L1	Homodimer; Atg5 interacting protein

Adapted from Table 1 of [116] and Table 2 of [65].

1.3.3 Regulation of autophagy

Autophagy is a complex phenomenon and is tightly regulated to prevent the unbalanced activation causing cellular damage. In yeast, nutrient depletion (based on the nature of nutrients like nitrogen depletion, glucose depletion, amino acid and phosphate depletion) is the primary stimulus inducing autophagy. However, in mammals various factors can regulate the induction of autophagy [117]. Autophagy is classified into basal and induced. Under normal conditions, the rate of basal autophagy is relatively low. Stress conditions like nutrient or energy starvation, hypoxia, pathogenic infection and ER stress trigger the induction of autophagy by degrading the cytosolic components for energy production allowing cell survival [67, 118].

The evolutionarily conserved TOR (Target of Rapamycin) kinase in yeast and mTORC1 in mammals belongs to serine/threonine kinase in the PI3K-related kinase (PIKK) and is a major sensor of nutrient depletion and a negative regulator of autophagy (Figure 5A and B) [119, 120]. mTOR contains two signaling complexes mTORC1 and mTORC2; mTORC1 is involved in regulation of autophagy whereas mTORC2 regulates cellular metabolism [121]. As discussed in initiation section for autophagosome biogenesis, TOR via phosphorylation of Atg proteins directly regulates autophagy. In addition to this, TOR exhibits its regulatory function via signaling cascades. In yeast, Tor2 phosphorylates Tap42 facilitating interaction with protein phosphatase 2A (PP2A); a phosphatase acting on various TOR substrates including Glucaminadase resulting in a decrease in PP2A enzymatic activity. During nutrient stress TOR is inhibited resulting in dephosphorylation and dissociation of Tap42 from PP2A. This leads to dephosphorylation of TOR targets and eventually the induction of autophagy [122-124]. Since multiple checkpoints are regulated during autophagy, other proteins apart

from TOR like p70S6kinase (candidate substrate of mTOR), PKA (during glucose starvation), Gcn2 (General control of nutrient), Gcn4, Pho85 (Cyclin dependent kinase), Beclin-1/PtdIns3K complex etc. are also involved in induction/inhibition of autophagy [117, 125-127].

PKA has a regulatory function on autophagy during nutrient starvation [128, 129]. Various PKA substrates directly regulate autophagy and are important in cellular processes for maintaining homeostasis in eukaryotes. PKA inhibits autophagy during nutrient-rich conditions in yeast suggesting Ras/PKA signaling activity is important for the inhibition of the autophagy during nutrient rich conditions. In contrast, upon starvation, the absence of Ras/PKA activity causes the induction of autophagy [130]. PKA inhibits phosphorylation of the Atg1 complex essential for initiation of autophagy [131]. This is mediated by Ras/PKA signaling pathway that inhibits the association of Atg1 to the phagophore assembly site. Effective regulation is achieved when the PKA signaling cascade and the mTOR signals have been combined; when mTOR signaling is inactivated, the autophagy response is accelerated by PKA inhibition [132-134]. PKA phosphorylation site on LC3 has been identified that regulates its involvement in autophagy (Figure 5C) [129].

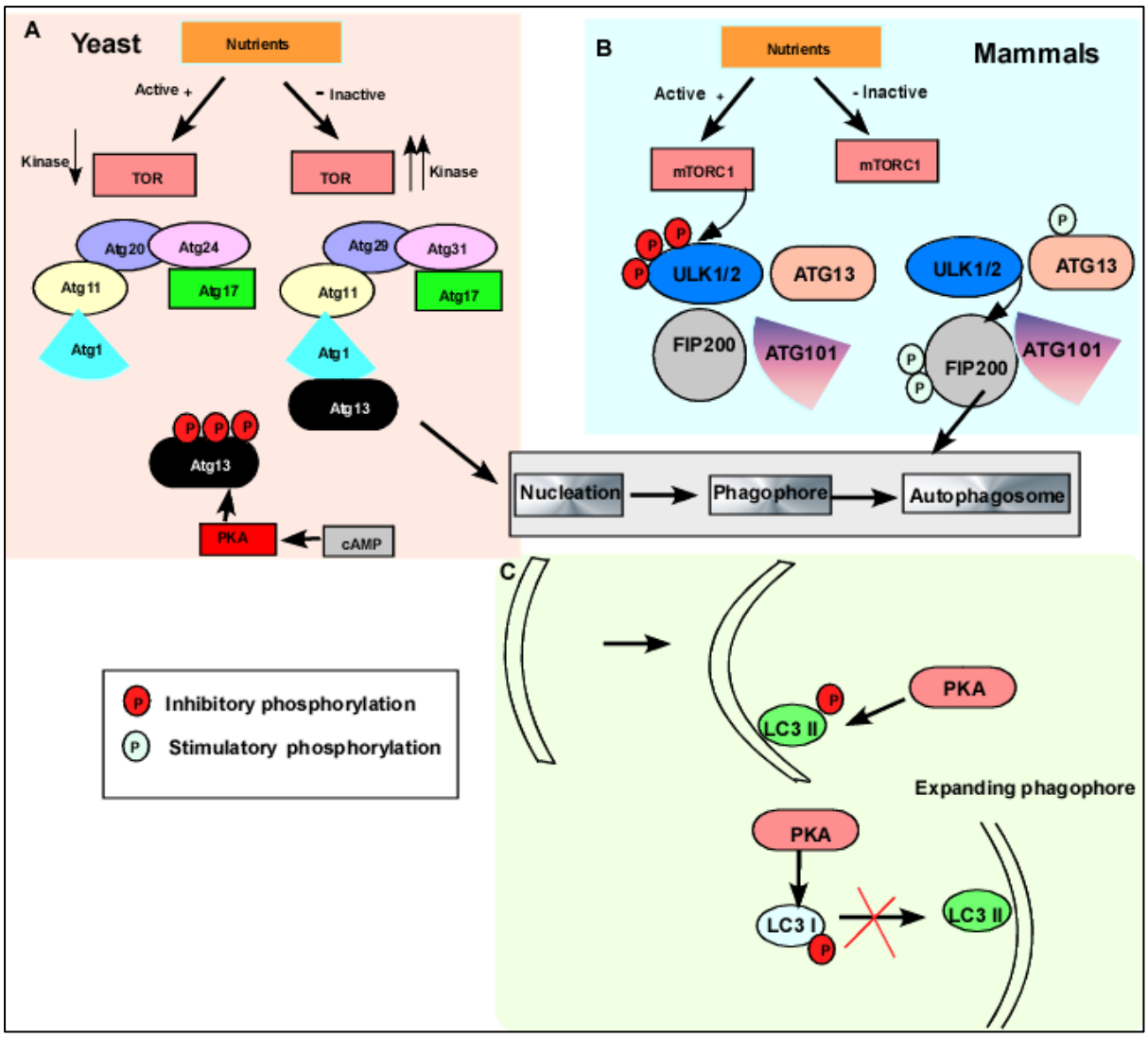

Figure 5: Regulation of autophagy by TOR in yeast and mammals. **A** During nutrient rich condition TOR is activated which leads to the phosphorylation of Atg13, eventually reducing the affinity of Atg13 for the Atg1-Atg11-Atg20-Atg24 complex. In contrast, when the yeast cell starve, TOR is inactivated, leading to dephosphorylation of Atg13 subsequently causing the assembly of Atg13 with Atg1 and with the Atg17-Atg29-Atg31 complex. This complex is responsible for increased Atg1 kinase activity and induction of autophagy. **B** Similarly, in mammals during nutrient rich conditions mTOR directly interacts with the stable ULK1/2-ATG13-FIP200-ATG101 complex, and it phosphorylates ULK1/2 and ATG13, leading to inhibition of ULK1/2 kinase activity and as well as inhibition of autophagy. In contrast, during nutrient starvation, the inactivated mTOR dissociates from the complex and leads to an inactive state causing dephosphorylation of Ulk1/2 and Atg13. Ulk1/2 kinase is now activated and causes phosphorylation of Atg13 and FIP200, and induction of autophagy. **C** PKA inhibits the incorporation of LC3 interacting protein into the autophagosome by phosphorylation. Adapted with minor modifications from [135-137].

1.3.4 Autophagy related 8 (ATG8) family proteins and the LIR motif

Atg8 gene family proteins are highly conserved eukaryotic proteins that share structural similarities to Ubiquitin [138]. Yeast have a single Atg8 protein while there are at least seven ATG8 proteins in mammals LC3A, LC3B (LC3B and LC3B2), LC3C,GABARAP,GABARAPL1 and GABARAPL2 [92]. ATG8 proteins are essential for conjugation of phosphatidylethanolamine to the phagophore which is an important step during autophagosome formation [139, 140]. ATG8 proteins also recruit different cargo to autophagosomes via cytoplasm-to-vacuole transport mediated by binding to Atg19 and Atg34 [141, 142].

ATG8 proteins contain a C-terminal ubiquitin core with four β-strands (β1, β2, β3, β4) and two α-helices (α3 and α4). ATG8 proteins also contain an N terminal domain with two α-helices (α1 and α2). All the mammalian ATG8 homologues contain an exposed β strand that makes two hydrophobic pockets (HP1 and HP2) on their surface [143]. Most of the protein interactions with ATG8s are via a short linear motif known as LIR (LC3 interacting region). LIR motif was identified for the first time in the autophagy substrate protein p62 bound to LC3B [144, 145]. The core LIR motif is also known as Autophagy Interacting Motif (AIM) or LC3 recognition sites (LRS) [144]. The core LIR motif contains four residues [W/F/Y] xx [L/I/V]. The first aromatic residue (W/F/Y) and the fourth hydrophobic residue (L/I/V) is separated by two amino acids. The (W/F/Y) binds deeply into the hydrophobic pocket (HP1) whereas the hydrophobic residue at the fourth position binds to the HP2 site [66]. Structural studies reveal that the core residues of the LIR motif dock into the hydrophobic pockets in the ubiquitin like structure located within the ATG8 family proteins, hence called LIR docking site (LDS) which determines the specificity of ATG8 interaction involved in the autophagic process [146].

Various proteins have been identified that interact via LIR motifs to ATG8 family proteins. Studies have shown the LIR motifs containing W residue at the first position have higher affinity towards LC3 family proteins whereas F residue have much more affinity towards the GABARAP family proteins [66, 93]. Mutations in LDS or LIR motifs have shown to weaken or inhibit the binding of LIR motif containing proteins like NBR1, p62 and NIX to ATG8 proteins thereby preventing the cargo transfer to the lysosome. LDS mutants (mutations in LC3B and GABARAP) can be used to test if the protein binds to ATG8 family proteins via LIR motifs. Some proteins can interact to LDS mutated ATG8 proteins suggesting ATG8 proteins also contain another interaction surface apart from the LIR motif [146, 147]. Atg1, the

first autophagy protein to be identified binds to ATG8 proteins via LIR motifs. Mutation in the core LIR motif of Atg1 results in impaired transport of autophagosome to the lysosome without affecting the initiation process. Similarly, ULK 1 and ULK2 (mammalian Atg1 homologues) also contain LIR motifs required for targeting ULK1 to the autophagosome [93, 148, 149]. Atg13 in yeast and the mammalian homologues ATG13 contain LIR motifs having more affinity towards GABARAP proteins. These proteins have an essential role in late stages during autophagosome maturation and use the LIR motif for anchorage [150]. Several other proteins like NBR1, Optineurin, NDP52 (nuclear dot protein 52 kDa), FYCO1, TBC1D25 (Tre2, Bub2, Cdc16 (TBC) 1 domain containing family member 25) are shown to have LIR motifs that have different roles in autophagic processes [66, 93].

1.3.5 Selective Autophagy and Sequestosome Like Receptors (SLRs)

Autophagy was long considered as a non-selective process. However, in the last decade it is well understood being a very selective and tightly regulated process that requires cargo recognition and recruitment to the autophagosome [151]. Different types of selective autophagy have been described based on the substrate sequestration such as aggrephagy (degradation of selective protein aggregates), mitophagy (degradation of mitochondria), pexoyphagy (degradation of peroxisomes), ribophagy (degradation of ribosomes), recticulophagy (degradation of endoplasmic reticulum), nucleophagy (degradation of parts of nucleus), lipophagy (degradation of lipid droplets) glycophagy (glycogen delivery to lysosome), ferritinophagy (selective turnover of ferritin), lysophagy (degradation of lysosome) and xenophagy (removal of intracellular pathogens) [143, 152]. Five receptors that mediate cargo selection have been identified in yeast Atg19, Atg34, Atg32, Atg36, Atg30 and more than 20 autophagy receptors have been identified in human [151, 153].

The notion regarding selective autophagy begun while studying the protein p62 which showed interaction with LC3B and degradation by the autophagosome [145, 154]. p62 contains an N-terminal self-interacting PB1 domain, a ZZ-type zinc finger domain, a LIR motif and a C-terminal Ubiquitin binding (UBA) domain. The UBA domain of p62 interacts with polyubiquitinated cargo, p62 polymerizes via the PB1 domain and makes protein aggregates followed by cargo connection to the autophagosome via the LIR motif. Hence, p62 plays a vital role in selective autophagy by recognizing the cytosolic cargo for the lysosomal degradation [145]. With the discoveries of selective autophagy several other receptors that have similar mechanisms of action to p62 have been identified. Since the cargo is recognized in a similar

way via UBA domain these receptors are known as Sequestosome like receptors (SLRs). NBR1, NDP52, /CALCOCO2, OPTN and TAX1BP1 are the additional receptors identified until now that recognize the ubiquitinated substrates, undergo oligomerization, bind to ATG8 family proteins via a LIR interaction and degrade the cargo in the lysosomal compartment and get self-degraded with the substrate [155-159].

1.4 PKA: A potential autophagy modulator in Carney complex

Although the role of PRKAR1A as a tumor-suppressor is well documented as discussed earlier, other studies have also demonstrated that PRKAR1A might be a potential oncogene. Overexpression of PRKAR1A is implicated in varieties of cancers and could contribute to neoplastic transformation and proliferation. In Loilome *et al.* human cholangiocarcinoma (CCA) samples were collected and analyzed [160]. Compared to normal adjacent tissues, CCA had an elevated mRNA expression of PRKAR1A. Western blot analyses on four human CCA cell lines also confirmed the strong mRNA expression of PRKAR1A. In addition, PRKAR1A knockdown of CCA cells led to reduced proliferation rate and elevated apoptosis response. The most important part of this study was that the author identified that knockdown cell lines had reduced phosphorylation of ERK1/2 and Akt when compared to the untreated CCA cell lines. These results indicated that the knockdown of PRKAR1A interfered with PI3K/Akt phosphorylation and subsequent activation in CCA cell lines. Moreover, these results also point to the possibility that the effects of PRKAR1A expression are tissue specific [160].

Mavrakis *et al.* studied the mTOR activity and compared the number of autophagosomes in knock out (*prkar1a* -/-) and wild type PRKAR1A (*prkar1a* +/+) mouse embryonic fibroblasts (MEF) cells. *prkar1a* -/- MEF cells had less number of autophagosomes compared to the wild type cells. PRKAR1A coimmunoprecipitated with mTOR in their experiment. Both knock out cells and reduced PRKAR1A HEK293 cells (using induced siRNA) had high p-mTOR/mTOR ratio. These results indicate that inhibition of PRKAR1A could decrease mTOR activation and induction of autophagy. This explains the molecular basis of reduced autophagy in Carney complex due to PRKAR1A deficiency. They also showed that PRKAR1A colocalized with autophagosome markers LC3 and Rab7 positive late endosomes explaining the role in late steps during autophagosome maturation [161, 162]. However, Day *et al.* 2011 disproved several results from the earlier study of PRKAR1A in autophagy. They did not see colocalization to autophagosomes (LC3) and did not find any significant difference in the number of

autophagosomes between the PRKAR1A knock out and wild type MEF cells. Instead from their electron microscope studies, they conclude that PRKAR1A is localized to the multivesicular bodies (MVBs) via AKAP11 when catalytic PKA is released [163].

1.5 Aim of the study

The aim of the study was to provide more insight into the role of PRKAR1A in autophagy. PRKAR1A has been studied with relation to autophagy only in two papers. Although, it is known that PKA regulates autophagy, very little is known about the role of PRKAR1A and how it reacts under autophagy inducing conditions. Using various analytical techniques, we pursue to identify the subcellular localization of the protein, and its role in autophagy. We aim to identify if PRKAR1A interacts to ATG8 family proteins *in vitro* and in cells. If so, we also aim to determine if the binding is mediated by LIR or not. We also expect to answer the question regarding the degradation pattern of PRKAR1A in cells, degradation via lysosomal pathway (autophagy) or by the proteasome. Using antibodies to endogenous proteins and overexpression of different tagged proteins we seek to learn the colocalization of PRKAR1A with autophagy markers (LC3B, GABARAP and p62) and lysosomal markers (Rab7 and Lamp1). Using LC3B puncta as a read out we aim to identify if PRKAR1A has a regulatory effect in autophagy.

2. Materials and Methods

2.1 Materials

Table 2.1: Plasmids and expression constructs used in this study

Vectors	Description	Source
Gateway cloning vectors		
pDest15	Bacterial GST fusion expression vector, T7 promoter	Invitrogen
pDONR221-PRKAR1A	Mammalian PRKAR1A in Gateway donor vector, DONR221, Kan^R	Harvard Plasmid Repository
pDest-myc	Mammalian myc-tag fusion expression vector, CMV & T7 promoters, AmpR	[164]
pDest-EGFP-C1	Mammalian EGFP fusion expression vector, CMV promoter, AmpR	[164]
pDest-mCherry-C1	Mammalian mCherry fusion expression vector, CMV promoter, AmpR	[145]
pDest-mCherry-EYFP	Mammalian mCherry-EYFP fusion expression vector	[165]
pDest Cerulean-C1	Mammalian Cerulean fusion expression vector, CMV promoter, AmpR	[165]
pDest- 3X Flag	Mammalian triple flag fusion expression vector, CMV promoter, AmpR	[165]
pDest- CatpSR	Mammalian catalytic subunit of PKA expression vector, AmpR	$
cDNA constructs made by site-directed mutagenesis or traditional subcloning and/or Gateway® LR reaction		
pDest-myc-PRKAR1A	Mammalian expression vector for myc-tagged PRKAR1A	This study
pDest-EGFP-PRKAR1A	Mammalian expression vector for EGFP tagged PRKAR1A	This study
pDest-mCherry-EYFP-PRKAR1A	Mammalian expression vector for mCherry-EYFP-tagged PRKAR1A	This study

pDest-Cerulean-PRKAR1A	Mammalian expression vector for Cerulean tagged PRKAR1A	This study
pGEX4T-3	Bacterial GST fusion expression vector,tag	Amersham
pDest 15-LC3A	GST-LC3A fusion protein expression	[145]
pDest 15-LC3B	GST-LC3B fusion protein expression	[145]
pDest 15-LC3C	GST-LC3C fusion protein expression	[145]
pDest 15-GABARAP	GST-GABARAP fusion protein expression	[145]
pDest 15-GABARAPL1	GST-GABARAPL1 fusion protein expression	[145]
pDest 15-GABARAPL2	GST-GABARAPL2 fusion protein expression	[145]
pDest 15-GABARAP Y49A	GABARAP Y49A fusion protein expression	*
pDest 15-GABARAP Y49A/F104A	GABARAP Y49A/F104A fusion protein expression	#
pDest15-LC3B F52A	LC3B F52A fusion protein expression	*
pDest15-LC3B R10A/R11A	LC3B R10A/R11A fusion protein expression	[155]
pDest15-LC3B 30-128	LC3B 30-128fusion protein expression	[145]
pDest15-LC3B 1-18	LC3B 1-18 fusion protein expression	[145]
pDest-3XFlag-LC3A	Flag-tag expression of LC3A	[165]
pDest-3XFlag-LC3B	Flag-tag expression of LC3B	[165]
pDest-3XFlag-LC3C	Flag-tag expression of LC3C	[165]
pDest-3XFlag-GABARAP	Flag-tag expression of GABARAP	[165]
pDest-3XFlag-GABARAPL1	Flag-tag expression of GABARAPL1	[165]
pDest-3XFlag-GABARAPL2	Flag-tag expression of GABARAPL2	[165]
pDest15-mCherry-LC3B	Mammalian expression vector for mCherry tagged LC3B	[164]
pDest15-mCherry-GABARAP	Mammalian expression vector for mCherry tagged GABARAP	[93]
pDest15-mCherry-YFP-p62	Mammalian expression vector for mCherry-YFP tagged p62	[164]

***Unpublised, Grateful to Dr. Jenifer Nunn**

[#] Unpublished, Grateful to Yakubu Princely Abudu
$ Grateful to Professor. Ugo Lionel Moens.
Note: All plasmid constructs made by site-directed mutagenesis or gateway® LR reaction were verified by restriction digestion and/or DNA sequencing

Table 2.2: Primers for site-directed mutagenesis

cDNA clone	Primer Name	Sequence
PRKAR1A stop_ 381	PRKAR1A stop 381_fw	5`-GTGTCACTGTCTGTCTGAGACCCAGCTTTA-3`
	PRKAR1A stop 381_Rev	5`-GAAAGCTGGGTCTCAGACAGACAGTGACAC-3`

Note: All plasmid constructs made by site-directed mutagenesis or gateway® LR reaction were verified by restriction digestion and/or DNA sequencing.

Table 2.3: Sequencing primers

Primer Name	Primer Sequence	Information
M13 Forward `	5`-GTTTTCCCAGTCACGACGTTGTA-3`	Used in this study to investigate inserts in pDONR221
M13 Reverse	5`-GCGGATAACAATTTCACACAGGA-3`	Used in this study to investigate inserts in pDONR221
TOM C1	5'-CGGCATGGACGAGCTGTACA-3'	Used in this study to investigate inserts in pDest15-Cerulean
GFP C1	5'-GATCACATGGTCCTGCTGGA-3'	Used in this study to investigate inserts in pDest15-EGFP and pDest15-mCherry-EFYP

Table 2.4: Restriction enzymes

Enzyme name	**Recognition sequence (5`-3`)**	**Reaction buffer**	**Supplier**
NcoI-High Fidelity (HF)	CCATGG	CutSmart	New England Biolabs
BsrGI	TGTACA	Neb 2.1	New England Biolabs
ScaI	AT/CGAT	Neb 2.1	New England Biolabs

Table 2.5: Antibodies used for Western blotting (WB) and Immune fluorescence (IF)

Primary Antibody		
Antibody	**Manufacturer, Cat. number**	**Dilution (WB/IF)**
Rabbit monoclonal anti-PRKAR1A	Cell Signaling, #D54D9	11000/150
Rabbit anti-LC3B	Novus, #NB100-2220	12000/1200
Mouse anti-LC3B	Nanotools, #0231-100/LC3	-/1200
Mouse anti-GABARAP	MBL, #M135-3	-/1200
Rabbit anti-Actin	Sigma, #A2066	11000
Guinea pig anti-p62	Progen, #Gp62-C	15000/1200
Rabbit anti- GFP	Abcam, #ab-290	15000
Rabbit anti-mTOR(7C10)	Cell Signaling, #2983	-/1200
Rabbit anti-Rab7	Cell Signalling, #D95F2	-/1100
Mouse anti-Lamp1(G1/139/5)	DSHB	-/1200
Mouse anti-Flag M2	Sigma, #F3165	12000
Mouse anti-Myc	Cell Signaling, #9B11	15000
Secondary Antibody		
HRP (Horseradish peroxidase)-conjugated goat anti-Rabbit	BD Bioscience Pharmingen, # 554021	12000
HRP conjugated goat anti-Mouse	BD Bioscience Pharmingen, #554002	18000
HRP-conjugated anti-Biotin	Cell Signaling, #7075	12000
Alexa Fluor® 647 Goat-anti Mouse	Invitrogen	1500
Alexa Fluor® 647 Goat-anti Rabbit	Invitrogen	1500
Alexa Fluor® 555 Goat-anti Rabbit	Invitrogen	15000
Alexa Fluor® 555 Goat-anti mouse	Invitrogen	1500
Alexa Fluor® 555 Goat-anti guinea pig	Invitrogen	1500

- **Not used for WB in this study**

Table 2.6: Bacterial strains used in this study

Strains	**Description**	**Reference**
DH5α	*E. coli* strain used for propagation of plasmids	[166]
SoluBL21 (DE3)	*E. coli* Strain used for protein expression	Novagen

Table 2.7: Growth media for bacteria

Luria Bertani (LB) medium	LB agar plates	2 x TY	Super optimal broth with Catabolite repression (SOC) media
10 g Bacto trypton 5 g Bacto yeast extract 10 g NaCl dH_2O to 1 litre pH adjusted to 7.0 with NaOH Supplemented with appropriate antibiotics	18 g agar 10 g Bacto trypton 5 g Bacto yeast extract 10 g NaCl dH_2O to 1 litre pH adjusted to 7.5 with NaOH Supplemented with appropriate antibiotics	16 g Bacto trypton 5 g Bacto yeast extract 5 g NaCl dH_2O to 1 litre pH adjusted to 7.0 with NaOH 20 mM glucose Supplemented with appropriate antibiotics	20 g Bacto trypton 5 g Bacto yeast extract 5 g $MgCl_2$ 10 ml 250 mM KCl 20mM Glucose dH_2O to 1 litre pH adjusted to 7.5 with NaOH

Table 2.8: Concentration of antibiotics in bacterial growth medium

Antibiotic	Concentration (µg/ml)
Ampicillin (amp)	100
Kanamycin (kan)	50
Chloramphenicol (cam)	25

Table 2.9: Cell lines and growth medium used in this study

Cell line	Description	Growth Medium
HeLa (ATCC® CCL-2™)	Human cervical carcinoma cells	500 ml Minimum Essential Medium Eagle (MEM) (Sigma, M4655) 10% Fetal bovine serum (FBS) (Merck) 1% Penicillin/Streptomycin (SA)
HEK293(ATCC® CRL-1573™)	Human embryonic kidney cells	500 ml Dulbecco's Modified Eagle's Medium (Sigma, D6046)– low glucose 10% Fetal bovine serum (FBS) (Merck) 1% Penicillin/Streptomycin (SA)
U2OS (ATCC® HTB 96™)	Human Bone Osteosarcoma Epithelial Cells	500 ml Dulbecco's Modified Eagle's Medium (Sigma, D6046)– low glucose 10% Fetal bovine serum (FBS) (Merck) 1% Penicillin/Streptomycin (SA)

Table 2.10: Buffers and solutions used in the study

Method	Buffer	Contents
General buffer	Phosphate buffered saline (PBS)	100 ml PBS (10X # 70011-050 pH 7.4, #Gibco /life technologies) dH_20 to 1L
	TE-buffer	10 mM Tris-HCl (pH7.4) 1 mM EDTA (pH 8.0)
Agarose Gel electrophoresis	20x minigel buffer	193.76 g Tris-HCl 27.22 g NaOAc 14.9 g EDTA dH_2O to 2L pH adjusted to 8.0 with acetic acid
	1X gel buffer	250 ml of 20X buffer dH_2O to 5L
	1% Agarose	1 g SeaKem® LE Agarose (Lonza) in 100 ml 1X gel buffer
	6xT gel loading buffer	0.25% Bromophenol blue 60 mM EDTA, pH 8,0 0.6% SDS 40% (w/v) sucrose sterile filtered
	1 kb DNA ladder	1 µl 1kb ladder stock (1.03 µg/µl) 24 µl TE buffer, pH 8.0 5 µl 6xT gel loading buffer
SDS-PAGE gel	4x Concentrating gel buffer	60.55 g Trizma-base 4 g SDS dH_2O to 1L
	4x Separating gel buffer	181.55 g Trizma-base 4g SDS dH_2O to 1L
	10% Separating gel	2.5 ml 40% acrylamide 2.5 ml separating gel buffer 4.9 m dH2O 100 µl 10% APS 10 µl TEMED
	Electrophoresis buffer	15 g Tris-base 75 g glycine 5 g SDS dH_2O to 5 litres
	2x SDS gel loading buffer	100 mM Tris-HCl pH 6.8 200 mM DTT (added fresh) 4 % SDS (w/v)

		0.2 % Bromophenol Blue (w/v) 20% glycerol (w/v)
	16% Separating gel	4 ml 40% acrylamide 2.5 ml separating gel buffer 3.4 ml dH_2O 100 µl 10% APS 10 µl TEMED
Protein production and purification	Lysis buffer (stock)	50 mM Tris-HCl pH 8.0 250 mM NaCl dH_2O to 1L
	Lysis buffer (working)	0.35 mg/ml Lysozyme 1 mM DTT 1 mM EDTA Lysis buffer stock to 10 ml
	NETN buffer	85.3 ml H2O 2 ml 1M Tris-HCl pH 8.0 7.5 ml 2M NaCl 1.25 ml 10% Np-40 200 µl 0.5 M EDTA
Protein production and purification Immunoprecipitation	NETN buffer with inhibitors	10 ml NETN Buffer 1 protease inhibitor cocktail mini tablet (Roche)
	RIPA buffer	1M Tris-Cl (pH7.5) 5ml 2M Nacl (7.5ml) 0.5M EDTA (pH 8) 100 µl 1% NP40 (1ml) 0.25% Triton X100 (250 µl) dH_20 to 100 ml.
	RIPA buffer with inhibitors	10 ml RIPA Buffer 1 protease inhibitor cocktail mini tablet (Roche)
Gel Staining	Fix solution	400 ml MeOH 100 ml Acetic acid 500 ml dH_2O
	Stain stock	2 g Coomassie Brilliant Blue R250 dH_2O to 200 ml
	Staining solution	62.5 ml stain stock 250 ml MeOH 50 ml acetic acid
	Destain I	500 ml MeOH 100 ml Acetic acid dH_2O to 1 L

	Destain II	50 ml MeOH 70 ml Acetic acid dH_2O to 1 L
Immunofluorescence	Fix solution Formaldehyde (FA)	4% FA
	Methanol fix solution	100% methanol
	5% Blocking buffer	5% Goat serum in PBS
	2% Blocking buffer	2% Goat serum in PBS
	DAPI (4',6-diamidino-2-phenylindole)	Thermo Scientific, #62248) 14000 in PBS
	Mowiol mounting media	2.4 g Mowiol 4-88 (CALBIOCHEM, # 475904) Glycerol 6 g dH_20 6 ml 0.2 M Tris pH 8.5 12 ml
Western blot	Lysis buffer (1X SDS)	50 mM Tris-HCl pH 6.8 200 mM DTT (added fresh) 2% SDS (w/v) 0.2 % Bromophenol Blue (w/v) 10% glycerol (w/v)
	TBS-T buffer	75 ml 2 M NaCl 10 ml 1M Tris-HCl pH 7.5 1 ml Tween 20 914 ml dH2O
	5% nonfat dry milk solution	2.5 g dried nonfat dry milk (Magermilch powder) 50mL TBS-T
	1X Transfer buffer (High Ionic Strength)	300 mM Tris 300 mM Glycine 20% Methanol 0.05% SDS dH_2O to 1L
	Ponceau S dye	0.5 g Ponceau in 25 ml acetic acid dH_2O to 500 ml

NB: All buffers are made in dH_2O if nothing else is mentioned. pH values are for room temperature

Table 2.11: Instruments used in different methods.

Method	Instrument	Brand
Cell culturing	LAF cabinet	ScanLaF
Checking induced cells	Leica DM IRB microscope	Leica Microsystems
Concentration measuring	NanoDrop 2000	TFS
Gel electrophoresis	Mini-Sub Cell GT systems	BioRad
	MultiDoc-It Digital Imaging System, transilluminator	UVP (BioDoc-it™)
Immunostaining/Microscopy	ZEISS LSM 780 META	Carl Zeiss AG
Protein measuring	CLARIOSTAR	BMG_LABTECH
Western blot	Trans-Blot® Turbo™	BioRad
	ImageQuant LAS4000	GE Healthcare Life Sciences
Invitro-translation assay	Fujifilm BAS-5000	Fujifilm
	Gel Dryer	BioRad, Model 583

2.1.1 Chemicals and reagents

1. BigDye® Terminator v3.1 Cycle Sequencing Kit, Applied Biosystems, # 4337456
2. PfuTurbo DNA polymerase, Agilent Technologies, # 600254-52
3. QuikChange II XL Site-Directed Mutagenesis Kit, Agilent Technologies, # 200523
4. TNT™ T7 Coupled Reticulocyte Lysate System (RTL), Promega, # L4600
5. Flag® Immunoprecipitation Kit, Sigma-Aldrich, #FLAGIPT1
6. Bafilomycin A1, (200 nM) Sigma-Aldrich, #B1739
7. MG132, Sigma-Aldrich-10 µM, #037M4107V
8. 0.25 Trypsin-EDTA, Sigma-Aldrich, #T4049
9. GenElute™ Plasmid Miniprep Kit, Sigma-Aldrich, #PLN350
10. Pierce™ BCA Protein Assay Kit, Thermo fisher Scientific, #23225
11. Western Blotting Luminol Reagent, Sigma-Aldrich, # SLBP0738V
12. Protein A-Agarose, Santa Cruz Biotechnology Inc. # sc-2001
13. *Trans*IT®-LT1 Transfection Reagent, Mirus Bio LLC, # MIR2300
14. Metafectene Pro, Biontex Laboratories GmbH, #T040
15. Hanks' Balanced Salt Solution, Sigma-Aldrich, # H8264
16. GelRed™ Nucleic Acid Gel stain.
17. Mowiol 4-88, CALBIOCHEM, # 475904

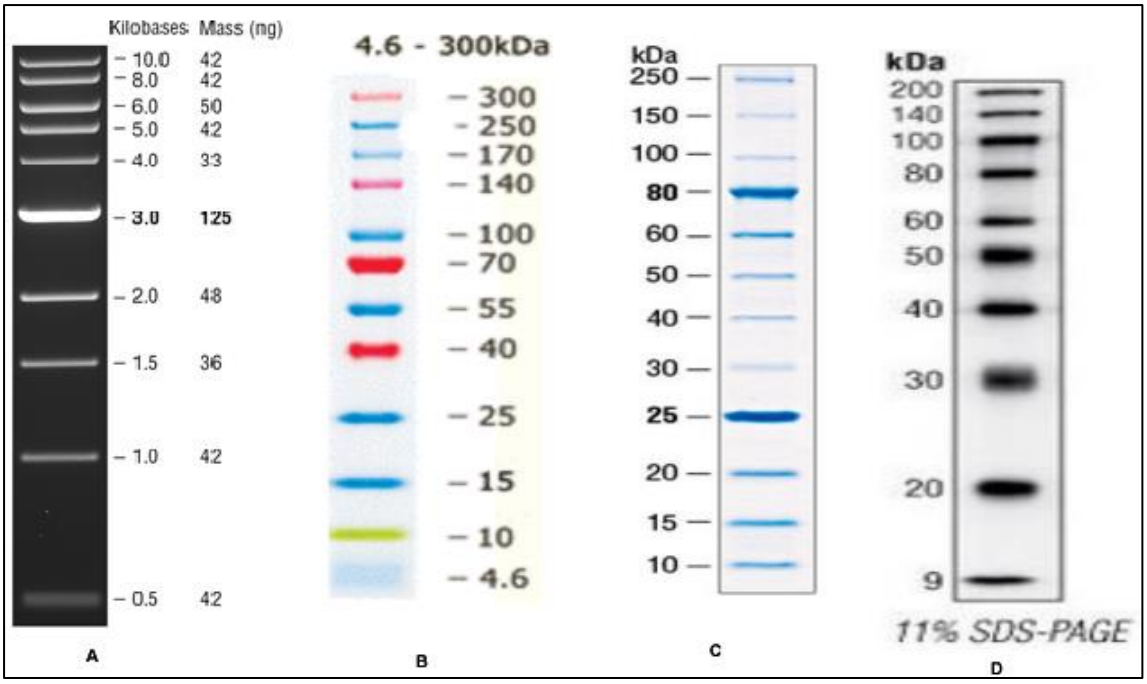

Figure 6: Molecular weight ladders for DNA and proteins. A 1 kb DNA ladder (NEB, #N3232L). **B** ProSieve™ Color Protein Marker for visualizing proteins on SDS-PAGE gel. **C** Unstained protein ladder (10-250 kDa) (NEB, # P7703S) for 10- 20% SDS-PAGE. D Biotin Ladder (Cell Signaling, #7727).

2.2 Methods

2.2.1 Gateway® Cloning technology

Gateway® is a universal cloning system devised by Invitrogen where the gene of interest (GOI) is cloned into a vector based on site-specific recombination. The Gateway® Technology provides a rapid and highly efficient way to move DNA sequences into multiple vectors for functional analysis and protein expression. This technique is based on the site-specific recombinant properties of bacteriophage lambda in *E.coli*, with the properties of switching between a lytic and a lysogenic life cycle which enables fast and in-frame cloning. The vector used in gateway cloning are divided into two categories Entry/Donor and the destination vector. The gene of interest in the entry vector can be transferred to any Destination vector. The gateway method includes two steps. In the first step, the entry vectors are generated by traditional cloning of the GOI between the specific attB1 and attB2 sequences in the vector. The traditional cloning involves restriction enzyme digestion and ligation. In the second step, the gene cassette in the Gateway entry vector can be transferred into a Gateway destination vector (pDest vector with a Gateway attR recombination sequence and other elements such as promoters and/or epitope tags)) by LR Clonase enzyme mix. The resulting expression vector can be transformed to appropriate bacteria host for propagation and used when needed [167, 168].

LR reaction procedure

1. The following components were added to 1.5ml Eppendorf tubes (on ice) and incubated at 25^0C (water bath) for 2-3 hours
    a. 100 ng pENTR cDNA construct
    b. 150 ng pDest vector
    c. 1 µl LR (enzyme) (Invitrogen)
    d. TE buffer (pH8) was added up to a final volume of 10 µl
2. 1µl Proteinase K (Biolabs) was added to the LR mixture to terminate the reaction and vortexed briefly and was incubated at 37^0C for 10 minutes.
3. The mixture was then transformed into DH5α chemically competent *E.coli* cells for plasmid amplification and purification.

All gateway constructs were verified by restriction enzyme digestion/agarose gel electrophoresis and DNA sequencing.

Protocol for restriction digestion

1. The following components of the reaction digestion mixture were mixed in a 1.5 ml Eppendorf tube
    500 ng DNA construct
    1 µl Restriction buffer
    1 µl of each restriction enzyme dH_2O to a final volume of 10 µl
2. The digestion mixture was incubated a 37 ^{0}C for 1 hour in waterbath.
3. The reaction was inactivated by adding 2 µl of 6X loading buffer and run on a 1% agarose gel.
4. Bands were visualized after staining with by GelRed™ Nucleic Acid Gel stain.

2.2.2 Transformation of competent bacterial cells

Transformation is the genetic alteration of bacterial cells where competent bacteria take up naked DNA from the extracellular environment. The term transformation was first proposed in 1944, which was incidentally also the first mention of DNA as the material of inheritance. Transformation can occur naturally (relatively slow) where DNA molecules are transferred between closely related species. However, this process can be provoked by electroporation or heat shock. The quick and efficient transformation can be performed by two commonly used methods,

electroporation or heat shock. Both methods enlarge the pores in the plasma membrane to allow passage of DNA. The host cell DNA polymerases recognize the origin of replication of the foreign DNA and replicate the foreign DNA along with the host cell DNA. Competent bacterial cells can be prepared through calcium chloride ($CaCl_2$) or rubidium chloride (RbCl) treatment. Bacterial cells used in this study were $CaCl_2$ competent and were prepared by laboratory technicians.

Two different *E.coli* strains were used during this study DH5α and SoluBL21 (DE3).

Bacteria transformation procedure

1. Competent bacteria cells were thawed on ice.
2. 50 µl competent bacteria cells were mixed together with the whole LR reaction mixture in 1.5 ml Eppendorf tube. The tubes were flicked 4-5 times to mix (No vortex).
3. The transformation mixture was incubated on ice for 20-30 minutes.
4. The bacterial cells were then heat-shocked by incubating at 37^0C (water bath) for 2 minutes.
5. 350 µl prewarmed catabolite repression (SOC) medium was added to the transformation mixture and incubated at 37^0C for 1 hour with shaking at 150 rpm.
6. LB-agar plates (with required antibiotics) were moved from 4^0C to room temperature.
7. The whole transformation mixtures were plated into the LB-agar plates with appropriate antibiotic using sterile glass beads and grown overnight at 37^0C.
8. The following day, three colonies were transferred into three tubes with 5 ml LB media with appropriate antibiotics and regrown overnight for plasmid purification.

Procedure for freezing down bacterial cells

1. One colony was transferred to 5 ml pre-warmed LB medium with appropriate antibiotics and incubated overnight at 37^0C.
2. 1.2 ml overnight bacteria culture was mixed with 300 µl sterilized 50% Glycerol (Sigma) and stored at -70^0C.

2.2.3 Plasmid Purification using GeneElute Plasmid Miniprep system

GenElute™ Plasmid Miniprep kit was used to purify plasmids from bacterial cells. The method is based on alkaline denaturation of high molecular weight chromosomal DNA followed by adsorption of DNA to silica in high-salt concentration. A spin column featuring a silica based membrane is used to purify the plasmid after the lysate has been cleared. Finally, the bound plasmid DNA is eluted in Tris-EDTA buffer. Miniprep is an expensive system as compared to standard precipitation procedure, however is faster and has higher degree of purification [169].

.

Procedure for GenElute™ Plasmid Miniprep kit (Sigma Aldrich)

1. 5 ml from overnight bacterial culture were pelleted by centrifugation at 13000xg for 1 minute. The supernatant was discarded.
2. Cells were resuspended in 200 µl resuspension Solution by pipetting up and down or vortexing.
3. 200 µl Lysis solution was added and the tubes were inverted gently to mix. The reaction mixtures were incubated for ≤ 5 minutes to obtain complete lysis.
4. 350 µl Neutralization Solution was added to the solution, mixed by inverting the tubes for 4-6 times.
5. The resulting cell debris was pelleted by centrifugation at 13000xg for 10 minutes.
6. Meanwhile,500 µl Column Preparation Solution was added to the binding column in a collection tube and centrifuged at 13000xg for 1 minute. The flow- through was discarded.
7. The cleared lysates were then transferred into the binding column and centrifuged for 1 min at 13000xg. The flow- through was discarded.
8. 750 µl Wash Solution was added to the binding column and Centrifuged for 1 minute at ≥13.000xg followed by another 2 minutes centrifugation at 13000xg to dry the column.
9. The purified plasmid DNA was eluted by transferring the binding column into a new collection tube and eluted by 50-100 µl Elution Solution with 1 min centrifugation at 13000xg.
10. The DNA concentration was measured using a Nanodrop spectrophotometer.

2.2.4 Measurement of DNA concentrations

The concentration of the purified DNA (ng/µl) was measured by *Nanodrop 2000/2000c Spectrophotometer* (Thermo Scientific). Elution buffer was set as blank. The DNA concentration was quantified at 260 nm which is the absorption maximum for double stranded nucleic acids. Since proteins and peptides contaminate the DNA samples because they have absorption at 280 nm and 230 nm; the purity indication of the DNA sample was measured by the 260/280 nm and 260/230 nm ratios. DNA samples were considered pure when the ratio 260/280 nm was between 1.7-1.9 and the ratio of 260/230 was between 2.0-2.2.

2.2.5 Agarose gel electrophoresis

Agarose gel electrophoresis is the most efficient method for separation of DNA fragments ranging from 100 bp to 25 Kb in size. Samples along with the loading buffer (6X) are loaded into pre-cast wells in the agarose gel and subjected to an electric field, causing the negatively charged phosphate backbone of the DNA fragments to move toward the positive electrode. DNA fragments migrate through the agarose gel matrix, composed of a linear polysaccharide extracted from algae that can polymerize to form a porous gel. Shorter DNA fragments will travel more rapidly, whereas the longest fragments will remain closest to the well resulting in separation based on size. The degree of migration depends on the conformation of DNA fragment as well as with the agarose concentration and the voltage. A supercoiled strand, because of its compact conformation will typically migrate faster than the linearized DNA [170]. The DNA fragment can be visualized under UV light with the aid of UVP trans-illuminator after staining with different DNA stains like Gel Red, Ethidium Bromide. In this study, GelRed™ Nucleic Acid Gel stain was used since it is stable, less toxic and is ultra-sensitive. The exact sizes of separated DNA fragments (unknown DNA samples) can be determined by comparing with the bands of a DNA ladder.

Procedure (1 % agarose gel)

1. 1 g agarose was mixed with 100 ml 1X minigel buffer in a 250 ml Erlenmeyer flask.
2. The mixture was heated for 2 minutes in a microwave oven until all agarose was dissolved.
3. The mixture was then cooled down to approximately 60 °C.
4. Appropriate amount of agarose gel was then applied to a casting frame with a comb.

5. The gel was left to solidify for 20 minutes.
6. The comb was removed and the gel was transferred to an electrophoresis chamber filled with minigel buffer.
7. 6xT loading buffer was added to the DNA samples and were loaded into the wells.
8. The gel was run for 50-60 minutes in a 90 V electric field.
9. The gel was incubated in 0.1 M NaCl containing 1 µl Gel Red for 20 minutes to stain DNA.
10. The DNA bands were visualized by exposure in UV-light, and pictures were taken using an UVP trans-illuminator.

2.2.6 Polymerase Chain Reaction

PCR involves the primer mediated enzymatic amplification of a specific DNA fragment. PCR is based on the ability of DNA polymerase to synthesize new strand of DNA complementary to the offered template strand. Primer is an essential component of PCR because DNA polymerase can add a nucleotide only onto a preexisting 3′-OH group to add the first nucleotide. Sequence of the template is needed to synthesize primers which binds to the desired sequence.

Some important steps in primer design

- The primer should be between 20 to 40 bp in length.
- Total GC content should be between 50-60%
- Melting temperature should at least be above 50 °C and the primer pair should not differ more than 5°C in melting temperature.

  Formula for calculating the melting temperature (Tm) of primers;

  Tm = 64.9°C + 41°C x (number of G's and C's in the primer – 16.4)/N

  Where N is the total length of the primer
- Primers with secondary structure should be avoided i.e. primer pairs should not form dimers or hairpin loops
- Multiple thymidine residues should be avoided on 3' and 5'

PCR can be used in arrays of biochemical processes like amplification, real-time quantification of nucleic acids, mutagenesis, DNA sequencing, microRNA analysis, single nucleotide polymorphism (SNP) genotyping and viral quantification. The PCR reaction requires the following components

1. **DNA Template**: The double stranded DNA (dsDNA) of interest.
2. **DNA polymerase:** Usually a thermostable Taq polymerase that does not rapidly denature at high temperatures (98°), and can function at a temperature optimum of about 70°C.
3. **Oligonucleotide primers:** Short pieces of single stranded DNA which are complementary to the 3' ends of the sense and anti-sense strands of the target sequence.
4. **Deoxynucleotide triphosphates:** The donor deoxynucleotide triphosphates dATP, dTTP, dGTP, dCTP provide the energy for polymerization and the building blocks for DNA synthesis.
5. **Buffer system:** Includes magnesium and potassium to provide the optimal conditions for DNA denaturation and renaturation; also, important for polymerase activity, stability and fidelity.

The PCR reaction consists of three different steps

1. **Denaturation (94-98ºC for 15-30 seconds)**

   The double stranded DNA is denatured to single strands due to breakage in weak hydrogen bonds.

2. **Annealing (54-60ºC for 20-40 seconds)**

   This allows annealing of primers to the 5`end of the single stranded DNA (ssDNA) (the temperature is depended on the melting temperature of the primer).

3. **Elongation (70-80ºC)**

   The DNA polymerase binds to the ssDNA and extends the ssDNA through the primers from 5` to 3` and attaches complementary dNTPs to the original DNA strand as a template. Under optimal conditions, DNA polymerase will add about 1000 bp/minute.

Step 1 to 3 are repeated multiple times and the target sequence is amplified at an exponential manner. The temperature is then lowered (4 ^{0}C), as the final step [171].

2.2.6.1 PCR based Site-directed mutagenesis

PCR based site-directed mutagenesis is an *invitro* method for creating a specific mutation in a known sequence by use of PCR. The designed primers containing a specific mutation are used as template for synthesizing the complementary strand with the mutation. In this process, the double stranded DNA molecules are separated and the primers anneal to each single stranded DNA. The whole plasmid is amplified with the help of DNA polymerase so that the double stranded daughter DNA obtained from this process will have the desired mutation [172]. QuickChange® Site-Directed Mutagenesis Kit (Stratagene, #200518) was used to insert the desired mutation throughout this study. As in a normal PCR, the critical step lies in primer design.

Procedure

The following were added in PCR tubes on ice

10 ng template DNA

10 µM mutated forward primer

10 µM mutated reverse primer

2.5 mM dNTP mix (Sigma)

0.5 µl pfu Turbo polymerase

5 µl of 10X cloned pfu reaction buffer

1 µl DMSO (Sigma)

dH_2O to a final volume of 50 µl

The reaction was placed in a PCR cycler (Eppendorf AH diagnostics) with the following PCR program (Table 2.12).

Table 2.12: PCR program for site directed mutagaenesis (4kb target)

Numbers of Cycles	**Temperature (^{0}C)**	**Time**
1	96	30 seconds
18	96	30 seconds
	55 (primer Tm -5^{0}C)	1 minute
	68	2 minutes/kb
Storage	4	∝

2.2.6.2 PCR based DNA Sequencing

DNA sequencing is used to verify the precise order of nucleotides in the DNA. DNA sequencing is used to verify the constructs established by cloning or mutagenesis. PCR based DNA sequencing is a sequencing system based on Sanger's chain terminating method. This requires a single stranded DNA template (obtained from double stranded DNA by denaturation), sequencing primers (designed forward and/or reverse primers), a DNA polymerase, normal deoxynucleotides (dNTPs) and modified 2',3'-dideoxyribonucleotide triphosphates (ddNTPs), and a reaction buffer. The DNA sample is mixed in a sequencing reaction containing four standard deoxynucleotide (dATP, dGTP, dCTP and dTTP), ddNTPs and the DNA polymerase in one tube. The reaction is subjected to cycles of annealing, extension, and denaturation in a PCR machine. DNA synthesis extends from the primer and incorporates either dNTP or ddNTP. Every time a ddNTP is incorporated, the DNA synthesis is terminated because the 3'OH group for extension is lacking. Each dNTPs are coupled to a specific fluorescent dye which are used to identify the sequence. In this study, BigDye®3.1 kit was used for sequencing reactions.

Procedure

1. The following reagents were mixed into PCR tubes and held on ice.

- 200-500 ng Plasmid
- 1 µl BigDye Terminator v3.1 mix
- 4 µl of 5X BigDye sequencing buffer
- 10 µM Sequence primer
- dH_2O to final volume of 20 µl

2. The reagent mix were placed into a PCR cycler and run with following PCR program (Table 2.13).

3. The reactions were then delivered to the core sequencing facility at HelseFak, UiT.

Table 2.13 PCR program for DNA sequencing

Numbers of Cycles	**Temperature (^{0}C)**	**Time**
1	96	1 minute
33	96	30 seconds
	50	15 seconds
	60	4 minutes
Hold	4	∝

2.2.7 Separating proteins by SDS - Polyacrylamide gel electrophoresis (SDS-PAGE)

SDS-PAGE is an analytical method used to separate components of a protein mixture based on their size and charge. SDS is an anionic detergent which breaks the hydrogen bond of the molecules to unfold proteins and break up secondary and tertiary structures thereby denaturating the native protein. Prior to loading the biological samples are boiled with DTT and SDS so that they acquire uniform negative charge after denaturation and then the electrophoretic mobility depends primarily on size. Both the separating and the concentrating gels are made up of acrylamide, bisarcylamide, SDS and Tris-HCl buffer. Ammonium persulfate and Tetramethylethylenediamide (TEMED) are added in the last step inducing polymerization. A low concentration stacking gel is used to concentrate the proteins at the top of the separating gel. The separating gel is longer and has an optimal acrylamide concentration for separating the proteins according to size. 100 kDa proteins can be separated using 6-10% gels, while 10 kDa proteins are best separated on 16% gels. During electrophoresis, an electric field is applied to the gel causing the negatively-charged proteins to migrate towards the positive (+) electrode (anode) across the gel. The gel is run at 20 mA or 30 mA voltage for 1 hour for thin or thick gels respectively.

After the visualization by a staining (protein-specific) technique, the size of a protein can be calculated by comparing its migration distance with that of a known molecular weight ladder (marker) [173, 174].

NB: The stacking gel should not be made until the separating gel is complete and has polymerized.

2.2.7.1 Coomassie blue staining of proteins separated by SDS-PAGE

Coomassie blue (also known as brilliant blue) stain is used to visualize proteins after separation by SDS-PAGE. It creates electrostatic interactions with protonated basic amino acids and hydrophobic associations with aromatic residues inside polyacrylamide gels.

Procedure

1. SDS- PAGE gel was removed out of the electrophoresis apparatus and placed onto a 15-cm plate.

2. Fix solution was added for 10 minutes and the fix solution was discarded.

3. Staining solution (Coomassie Brilliant Blue R-250 (Thermo Scientific™) was added for 1 hour. Coomassie Brilliant Blue R-250 was poured back to its tube.

4. Destaining solution I was added for around 30 minutes. Destaining solution I was collected in a flask.

5. Destaining solution II was added for around 30 minutes/ until adequately destained.
6. The gel was imaged using UVP trans-illuminator but using white light instead of UV light.

2.2.8 GST Pull down assay

The GST pulldown assay is an affinity based method used for the purification of unknown proteins from a pool of proteins. This method can also be used to probe interactions (quantitative or qualitative) between a GST fusion protein and potential interacting proteins in solution. The probing protein is produced as a GST fusion protein and purified using glutathione sepharose beads. The protein-bead complex can then be used to pull target protein(s) from cell lysates out of solution [175, 176]. Potential target proteins can also be *in vitro* translated with ^{35}S-methionine (Met) and incubated with the probing protein. Proteins interacting with the probing protein are separated by SDS-PAGE. The gel is then stained to examine the amount of GST-protein and finally developed to visualize the radiolabeled proteins or subjected to western blot to detect proteins from the lysate. The target proteins can be tested for interaction against GST as a negative control.

2.2.8.1 Recombinant protein production

Proteins used for GST-pulldown assay in this study were produced using a T7 late promoter system in SoluBL21 (DE3) *E.coli.* pDest15 vector was used as a gateway vector for construction of GST fusion proteins containing a GST-tag and T7 promoter. SoluBL21 (DE3) *E.coli* strains are improved strains for producing soluble proteins under control of a T7 promoter. The transcription of the gene is induced upon addition of isopropyl-β-D-thiogalactopyranoside (IPTG) since IPTG inhibits a repressor (Lac repressor), which is bound to the T7 promoter thereby making the T7 promoter available for the T7 RNA polymerase that binds and transcribes the target gene.

IPTG is added to the growth medium in the log phase for approximately 3-4 hours and induces overexpression of the protein of interest.

Procedure

E. coli SoluBL21 (DE3) cells containing the required plasmid were plated out on an agar-plate with specific antibiotic. Each plasmid contains an antibiotic resistant gene, which enables the cells to grow on antibiotic plates

1. One colony was inoculated into 5 ml pre-warmed LB-media with Ampicillin and grown over-night (approximately 16 hours).
2. The over- night bacterial culture was transferred into 100 ml pre-heated 2xYT-media with Ampicillin and grown for 2-3 hours at 37^0C with shaking until it reached an OD_{600nm} between 0.6-0.9.
3. The protein expression was induced by adding 50 µl 1M IPTG (Promega).
4. The culture was incubated for 3-4 hours at room temperature (approximately 25^0C) with shaking.
5. The culture was transferred to 250 ml ultracentrifuge containers and pelleted by centrifugation at 5000 x g for 10 minutes at 4^0C.
6. The supernatant was discarded, and the bacterial pellet was incubated with 4 ml ice-cold lysis buffer containing lysozyme, EDTA and DTT for 20 minutes.
7. The mixture was divided into three cryotubes and 140 µl of 10 % Triton X-100 (Sigma) was added to each tube.
8. The bacterial solution was mixed properly before they were frozen down at -70^0C, to the next day.

Protein harversting procedure

1. The tubes with the lysed bacteria were thawed on ice.
2. The cells were sonicated (Vibra-cell™, Sonics) at 40% amplitude, 4 times for 40 seconds with 10 seconds pause in between.
3. Sonicated lysates were transferred to 2 ml culture tubes and centrifuged at 13000 rpm for 10 min, 4 °C

Protein Purification by GST pull down assay

1. 200 µl of Glutathione Sepharose™ 4 Fast Flow beads (GE healthcare) were transferred to an Eppendorf tube
2. The ethanol was discarded and the beads were washed three times with cold NETN buffer.

3. Protein lysate were added together with the beads and the mixture was incubated at 4^0C for 1hour, rotating. (*NB: - cut pipette tips were always used when pipetting beads)*
4. The beads were spun down and washed three times with NETN buffer.
5. The concentration of beads was adjusted to 50 % with NETN buffer.
6. The beads were stored in NETN buffer with protease inhibitors at 4^0C.
7. 10 µl protein beads were analyzed by SDS-PAGE for estimation of protein concentration.

2.2.8.2 Invitro transcription and translation

In this study, direct protein-protein interaction using TNT™ T7 Coupled Reticulocyte Lysate System (RTL) was used where the *in vitro* transcribed and translated proteins were radioactive labeled with ^{35}S-Met. Here, direct interaction between the *in vitro* translated PRKAR1A and ATG8 proteins bound to GST were tested.

Procedure from the TNT™ T7 Coupled Reticulocyte Lysate System (RTL) kit

The components of the reaction mixture (Promega kit) were mixed in a 1.5µl Eppendorf tube. One reaction mixture was enough for five samples. The reaction mixture was adjusted accordingly based upon number of samples.

Procedure

1. Following components for one reaction mixture were mixed

25 µl reticulocyte lysate

2 µl TNT buffer

1 µl amino acids mix minus methionine

1 µl ^{35}S - Methionine

1 µl TNT polymerase T7

1 µg DNA and dH_2O were added to the total reaction mixture to make the final volume to 50µl

2. The reaction mixtures were incubated at 30^0C for 90 minutes.
3. To verify the translation, 3 µl of the *in vitro* translation were taken out for each sample, mixed with 15 µl 2X SDS- loading buffer with 200 mM DTT, boiled for 3-5 minutes and proteins were separated by SDS-PAGE.

Procedure for GST- pulldown

1. The rest of each *in vitro* translated protein sample were pre-incubated with 15 µl of empty GST-beads (washed with cold NETN buffer) together with 100 µl of cold NETN buffer containing protease inhibitor for 30 minutes at 4 ^{0}C, rotating.
2. 105-110 µl of supernatant was incubated with 15-20 µl 50% GST-protein beads for 1 hour at 4 ^{0}C, rotating.
3. The beads were precipitated by a table centrifuge (2500 g for 1 minute), and washed five times with cold NETN buffer.
4. All of the NETN buffer were discarded and 10 µl of 2X SDS- loading buffer with 200 mM DTT (Sigma) were added. The samples were boiled for 3-5 minutes.
5. 10 µl of the GST-pulldown and 6 µl of the pre-incubation (10 % input) reaction mixture was loaded and run on a 10% SDS-PAGE gel at 20 mA for 50-60 minutes.
6. The gel was fixed, stained and destained as described for Comassie staining and further proceeded for autoradiography

2.2.8.3 Autoradiography Detection of radioactive proteins in polyacrylamide gels

After Coomassie staining the SDS-PAGE gel was transferred on a filter paper, covered with a sheet of plastic foil and dried in a Gel Dryer at 80^{0}C for 30-45 minutes. The dried gel was transferred inside a film cassette with a phosphor imaging plate (Fujifilm Science Lab) on top. The film was scanned the next day with FUJI BAS-5000. All images were detected by Image Gauge V.4.0 (Fujifilm Science Lab).

2.2.9 Pierce Bicinchoninic Acid (BCA) Protein Assay

This protein assay is widely used to measure the protein concentrations of various cell lysates for further experiments. This technique is based on BCA for colorimetric detection of proteins which exhibits a strong absorbance at 562 nm, that is almost linear within 20-2000 µg/ml working range. The unknown samples were then compared with a series of dilutions of known concentrations of Bovine Serum Albumin (BSA).

Procedure

Each well of the micro-plate were loaded with either different BSA standards or a mixture of 10 µl sample and 190 µl working reagent. The working reagent was premixed with 501 dilution of part A and B. The plates were incubated for 30min at 37^{0}C and then colorimetric analyzed

in CLARIOSTAR microplate reader. The results were thereafter analyzed by using Excel to compare the samples with unknown concentrations with a standard curve, made of BSA dilutions.

2.2.10 Western Blot/Immunoblot

Western blot, also known as protein immunoblotting is the most widely used analytical method to detect specific proteins in a given sample. Western blotting usually involves SDS-PAGE, protein transfer to a membrane, and protein blotting by testing against a specific antibody. SDS-PAGE separates various proteins contained in the given sample. The proteins are then transferred from the gel onto a membrane made of nitrocellulose (NC) or polyvinylidene difluoride (PVDF) of mostly 0.45 µm pore size. The transfer process is based on current conduction produced by the transfer buffer. The Gel-Membrane-Filter sandwich is placed into a semi-dry blotting cassette. Proteins are transferred from the gel to the membrane via horizontal transfer because of a high intensity electric field produced. The membrane is blocked using 5% nonfat dry milk to reduce the amount of nonspecific binding of antibodies. The membrane is then stained with antibodies specific to the target protein. The membrane is washed to remove any unbound primary antibody and the membrane is exposed to an enzyme-labelled secondary antibody or conjugated with a fluorescence dye. The secondary antibody binds to the primary antibody which has reacted with the target protein. The intensity of the color or signal produced is directly proportional to the amount of protein present in the sample [177].

Procedure

1. Proteins separated by SDS-PAGE were proceeded for blotting into the membrane. The filter papers and the membrane were suspended into the 1X Transfer buffer prior to making the Gel-Membrane-Filter sandwich.
2. To make the sandwich, one filter paper was placed into a semi-dry blotting cassette. The membrane was placed over the filter paper followed by the gel and another filter paper on top.
3. The protein gel was blotted to the membrane by Trans-Blot® Turbo™.
1. After the blotting, the membrane was blocked with a blocking buffer (5% nonfat dry milk in TBS-T) for 1 hour at room temperature.

2. The membrane was incubated with appropriate primary antibody (diluted in 5% nonfat dry milk) overnight at 4^{o} C on a rotating wheel.
3. The membrane was washed 3 times for 10 minutes each with TBS-T buffer.
4. HRP-conjugated secondary antibody (diluted in 5% nonfat dry milk) was incubated for 1 hour at room temperature and washed 3 times for 10 minutes each time with TBS-T buffer.
5. The membrane was incubated in Luminol reagent for 5 minutes and analyzed with Image Quant LAS 4000 blot analyzer which captures the chemiluminescent image.

2.2.11 Mammalian cell culture

HeLa, HEK293 and U2OS cells were used to study the role of PRKAR1A throughout this study. These cells were kept in their full growth medium (FM), passage every third day (with a confluence between 80%), by dividing them 1/5, 1/10 or 1/20 (depending on the next splitting event) into new flasks. The optimal confluence for transfection, freezing down or before pulldown assay is 70%. New cells were taken up after passage number 10 and 20, according to the cell-type.

Cell passage procedure

1. The full medium (FM) of the cells was discarded.
2. The cells were washed once with room temperature 1X PBS. The PBS was discarded.
3. 0.5-1.5 ml pre-warmed Trypsin-EDTA (Sigma) was added to the cells and incubated at 37^{0}C for 3-5 minutes until they were detached from the surface.
4. 5 ml pre-warmed FM was added to the cells to inactivate the activity of trypsin. The cells were suspended 5-10 times
5. Cells were transferred to a new flask with pre-warmed FM.

2.2.11.1 Cryopreservation of mammalian cells

Cryopreservation is a process where cells get preserved by cooling to very low temperatures that enables the long-term storage and minimizes the genetic changes and contamination.

Procedure

For cryopreservation cells were grown to 70% confluency, detached by Trypsin and frozen in FBS with DMSO. The medium with detached cell cultures were centrifuged for approximately

10-15min at 1000 rpm. The medium was then removed and a mixture of 90% FBS (Merck) and 10% DMSO (Sigma) was added to each tube with pellets, and mixed by pipetting. DMSO can penetrate inside the cells and reduce the formation of ice crystals that could lead to membrane rupture and damage of the cells. The cells were divided into 2 ml cryotubes tubes and frozen at -70°C, then transferred to a liquid nitrogen tank after a week.

2.2.11.2 Starting a cell culture from cryopreserved cells

Cells were taken out from the nitrogen tank and thawed gently. The cells were added into pre-warmed FM in 75cm^2 flask. They were either spun down or incubated between 3-4 hours, before the FM was changed to avoid the toxic effect of DMSO. Cells were incubated at normal condition and splitted when they reach a confluence of around 80%.

2.2.11.3 Mammalian cell lysis

The cells were seeded, harvested and lysed to obtain all proteins for pulldown assays, western blot or immunoprecipitation.

Preparation of cell extracts for western blot

1. Cells were seeded out at a density of around 3×10^5 cells in 6-well culture dish and incubated in a CO_2 incubator overnight.
2. At around 80% confluency, the cells were washed two times with 1X PBS.
3. The cells were lysed with 70-80 µl 1xSDS lysis buffer, scraped and transferred to 1.5 ml Eppendorf tubes.
4. The cell lysates were boiled at 100^{o}C for 10 minutes or until when the lysates were no longer viscous.
5. Protein concentration of lysates were measured using BCA protein measurement assay.
6. Equal amounts of lysate were loaded in each well. Prior to loading on SDS-PAGE gel, 0.2% Bromophenol Blue (BPB) and DTT to a final concentration of 200 mM were added to the lysates.

Preparation of cell extracts for GST- pull down

1. The cells were grown in a 75cm^2 flask and incubated until 80% confluency.
2. The cells were washed two times with 1X PBS.
3. The cells were lysed by adding 3 ml RIPA buffer with protease inhibitor mix) and was incubated on ice shaking (150 rpm) at 4^{o}C for 30 minutes.

4. The cells were scraped and the lysates were transferred to Eppendorf tubes and centrifuged at 16000xg at 4^0C. 20 µl of the supernatant was taken for input (5%).
5. The supernatant was divided into Eppendorf tubes (one for each GST-fusion protein) and the ATG8 proteins fused with GST beads were added on each tube.
6. The binding reaction were allowed to occur by overnight incubation at 4^{o}C on a rotating wheel.
7. The beads were washed 5x with RIPA buffer. After final washing all RIPA buffer was removed and 10 µl of 2X SDS with 200 mM DTT was added to each sample.
8. The sample were boiled for 5 mins at 100^{o}C. 10 µl of sample and input sample (5%) was loaded into wells on a SDS page gel.
9. The bound proteins were detected by western blotting.

2.2.11.4 Transfection of mammalian cells

Transfection is a powerful method of introducing foreign genetic materials into a eukaryotic cell which allows to study the gene/protein function and regulation. Based on the nature of the genetic material (DNA or RNA), the genetic material can exist in a cell either stably or transiently. In transient transfection, the genetic materials are temporarily introduced into the cells and expressed, however the genetic material do not integrate into the host genome. In contrast, for stable transfection the genetic materials usually have a marker (transgene) that are integrated into the host genome and the transgene expression is sustained even after host cell replication. Transfection can be performed by a physical, chemical or biological approach. The ideal method should have high transfection efficiency, low cell toxicity, minimal effects on normal physiology, and be easy to use and reproducible [178].

In this study, two cationic lipid or liposome based regents were used for cell transfections METAFECTENE® (Biontex Laboratories GmbH) and Transit®-LT1 (Mirus Bio LLC). Both are polycationic reagent based on liposome technology where DNA/RNA is captured in a lipid membrane, which then fuses to the plasma membrane of the cell and delivers the DNA/RNA.

Transfection procedure for immunofluorescence

1. The glass coverslips (1.5 mm thickness) were placed into 24 wells cell culture dish. The coverslips were completely covered in 70% ethanol for 30 mins or until the ethanol dries for sterilization.
2. The coverslips were then washed two times with 1X PBS.
3. 50,000 cells were seeded out (500 µl per well) one day before the transfection.
4. The following day, cell media was removed and 450 µl FM with 10% FBS was added.
5. A transfection reagent mix was made by adding 50 µl media without serum and antibiotics to 0.5 µl of Transit®-LT1 reagent in an Eppendorf tube. This mix was then added to a tube containing 100-150 ng of the DNA and was incubated at room temperature for 20-30 minutes.
6. After incubation, the transfection mix was added to the cells in each well drop wise and then incubated in the CO_2 incubator at 37^{o}C overnight. The cells were either fixed or treated post transfection. In this study, if treated, the cells were treated with two inhibitors Bafilomycin A1 (200 nM) and MG132 (10 µM) for 4 hours. If starved, the starvation was always for 4 hours on HBSS.

Transfection procedure for immunoprecipitation and western blot

1. Cells were seeded out in appropriate cell culture dishes and grown overnight to 60-70% confluency.
2. On the next day, fresh cell media was added to the cells.
3. A transfection reagent mix was made by adding 300 µl media without serum and antibiotics to 2 µl of Metafectene® Pro in an Eppendorf tube. This mix was then added to a tube containing 1 µg of the DNA and was incubated at room temperature for 20-30 minutes.
4. The cells were either harvested or treated post-transfection.

2.2.12 Fluorescence and confocal microscopy

A fluorescence microscope is an important instrument to monitor the cell physiology with the use of various fluorescent dyes like fluorescein, Alexa dyes, and rhodamine and fluorescence proteins like green fluorescent protein (GFP), mCherry, Cerulean etc. Fluorescence involves the ability of fluorescent molecules, also known as fluorophores, to absorb the light energy at

a particular wavelength and emit the light energy at longer wavelength that has lower energy. This emitted fluorescence can be used to generate an image [179].

2.2.12.1 Confocal laser scanning microscopy (CLSM)

Confocal microscopes are specialized fluorescence microscope having a specific goal to reject the out-of-focus light from the image, thus providing a sharper image. This phenomenon is achieved with a pinhole aperture ensuring the light reaching the detector is only from a single highly confined sample area, the focal spot where the excitation light was focused. Here, the image can be subsequently gathered pixel by pixel by scanning the confocal excitation and detection point across the specimen by recording the fluorescence intensity at each position. Confocal microscopes are highly sensitive and have a high signal to noise ratio and great specificity in excitation and emission detection [179, 180] .

CLSM employs laser as a light/excitation source which passes through a first pinhole aperture situated in a conjugate plane (confocal) with a scanning point on the specimen and a second pinhole aperture located in front of the detector. A dichromatic mirror now reflects the excited light which is focused by the lens objective before reaching the specimen in a focal lane. The secondary fluorescence emitted from the same focal plane passes back through the mirror and is focused as a confocal point at the detector pinhole aperture and the light is then detected by the photodetector [181, 182]. Due to availability of wide arrays of fluorophores, confocal microscopy has gained an enormous application to study the complex biological processes, cellular localization, co-localization of macromolecules, immunostaining and other cellular studies. In this study, ZEISS LSM 780 META confocal microscope was used.

2.2.12.2 Immunofluorescence

Immunofluorescence is a versatile technique that allows to detect a specific immune reaction/complexes in the tissue/cell by utilizing a fluorophore-labeled antibody. This method is widely used to study protein expression, localization and distribution within individual cells or tissues [183]. Monoclonal and polyclonal antibodies are used in the immunofluorescence technique and the antigen-antibody complexes are visualized using a confocal microscope.

2.2.13 Cell fixation and staining

A good sample preparation is an important part of immunofluorescence/confocal microscopy and various fixation methods are available. The cells are often fixed and washed with PBS

before mounting on an object glass when using fluorescent proteins. However, in immunostaining, the cells must be well fixed and permeabilized to allow access of antibody to the antigen of interest. Many fixation methods like acetone, formaldehyde (FA), methanol, formalin etc. are used. In this study, formaldehyde (FA) and methanol fixation were used.

FA fixation procedure

1. After incubation/treatment, the cell media was removed and the coverslips were fixed with 500 µl 4% formaldehyde (FA) for 8-10 minutes.
2. The coverslips were washed with PBS once, if needed 500 µl of DAPI was added, incubated 5-10 minutes in dark followed by three times washing with 1X PBS.
3. The coverslips were picked up from the wells with a needle and a tweezer. Each coverslip was washed by dipping into dH_2O for 5-6 times to get rid of the salts.
4. Excess wash solutions on the coverslips were removed by touching the edge of a filter paper. The coverslips were then mounted on an object glass. Each coverslip was placed on a 5 µl Mowiol mounting media with the cell side facing the solution.
5. They were then dried over night at RT or for 2 hours at 37°C, before they were analyzed on Zeiss LSM 780 META confocal microscope.

Procedure for Immunofluorescence

1. After incubation/treatment, the cell media was removed and the coverslips were fixed with 500 µl 4% FA for 15-20 minutes.
2. The cells were washed twice with 1X PBS, before they were permeabilized with 500 µl ice cold methanol (stored-20^{o}C) for 5 minutes at RT.
3. The cells were then washed with 1X PBS twice before blocked with 5% fresh made BSA in PBS for 30 minutes.
4. Primary antibodies were diluted in fresh 2% BSA in 1X PBS, and 25 µl were spotted directly on the coverslip followed by 1-hour incubation at RT (without moving).
5. The coverslips were washed two times with 1X PBS.
6. Secondary antibodies were also diluted in fresh 2% BSA in 1X PBS, and 25 µl were spotted directly on the coverslip followed by 1-hour incubation at RT (without moving).
7. The coverslips were again washed two times with 1X PBS, stained with DAPI if needed and mounted in similar manner as in FA fixation.

2.2.14 Immunoprecipitation (IP) using Anti-Flag M2 agarose beads

Immunoprecipitation involves isolation of antigen from a complex mixture of proteins from a cell or tissue homogenate using a specific antibody attached to a solid phase matrix [183]. Immunoprecipitation involves 3 steps Cell lysis, binding of specific antigen to an antibody followed by precipitation of the immune complex, precipitation wash and antigen dissociation from the immune complex. The immunoprecipitated protein can be analyzed using SDS PAGE and western blot.

3X Flag, a 25-amino acid affinity tag is used for highly specific protein purification. The Flag epitope system is based on a small Flag octapeptide (N-Asp-Tyr-Lys-Asp-Asp-Asp-Asp-Lys-C) which allows fusion protein to retain their original confirmation and function. The isolation of Flag tagged protein is one step and is very rapid and simple. FLAG-tagged proteins identified by the anti-FLAG M2 antibody can be efficiently pulled down using M2-conjugated agarose beads. By competition with a 3× FLAG peptide, the pulled-down protein is then eluted from the beads. These antibodies are very specific and can recognize the specific protein present in the lysates with less cross-reactivity with other proteins present in the cells [184]. In this study, Flag IP kit was used which allows rapid and efficient IP and elution of an active Flag fusion protein. IP was done by using Monoclonal ANTI-FLAG M2, a mouse derived, affinity purified IgG1 monoclonal antibody covalently attached to agarose beads.

Procedure for Flag-IP

1. HeLa cells were seeded out with a density of ~300.000 cells/ 6 cm culture dish.
2. The cells were transfected with 4 µl Metafectene® pro ,1 µg of each of Flag-EGFPC1, Flag-(LC3A, LC3B, LC3C, GABARAP, GABARAPL1, GABARAPL2) and 1 µg of pDestEGFP-PRKAR1A together with 300 µl MEM (without FBS and antibiotics) in 7 different Eppendorf tubes. This mixture was incubated at RT for 20-30 minutes
3. The transfection mix was added to the respective cell culture dish with overnight incubation at CO_2 incubator at 37^{o}C.
4. On the next day, the FM was aspirated and the cells were washed with 1X PBS.
5. The cells were lysed by adding 400 µl RIPA buffer (with protease inhibitors). Cells were incubated at 4^{0}C, shaking (150 rpm) for ~30 min.
6. The cells lysates were scraped and pooled into Eppendorf tubes.

7. The lysates were centrifuged at 13,000 g for 10 minutes and the supernatants were transferred to another Eppendorf tubes.
8. The cell lysate supernatants were kept on ice and 20 µl was taken out as input control from each tube.
9. 20 µl of flag beads with antibody was added on each lysate and incubated overnight with rotation at 4^0C.
10. On the next day, bound beads and lysates were centrifuged at 5000 g for 1 minute.
11. The beads were washed 5 times with RIPA buffer.
12. 20 µl of Flag peptide (3 µl flag peptide,4 µl 25X RIPA buffer with inhibitor,93 µl RIPA buffer for 100 µl) was added to each tube with beads and were incubated at 4^0C, shaking (150 rpm) for ~30 min.
13. The beads were centrifuged at 5000 g for 1 minute.
14. The immunoprecipitated fusion proteins on the supernatant were eluted using small pipette tips.
15. 10 µl 2X SDS-loading buffer with 200 mM DTT were added to the eluted samples and boiled for 5 minutes.
16. The samples were loaded onto a SDS- PAGE gel followed by western blot.

Note: All the images shown in this study were made on Canvas X12.

3. Results

3.1 Establishment of various tagged PRKAR1A constructs and validation of PRKAR1A antibody

The aim of this study was to investigate the role of PRKAR1A in autophagy by utilizing fluorescence confocal microscopy and *in vitro* and *in vivo* binding assays. For these purposes, constructs expressing PRKAR1A with the various tags EGFP, Cerulean, mCherry-EFYP and Myc was established by Gateway cloning. All the constructs made were verified by restriction enzyme digestion, DNA sequencing and Western blotting. A Western blot protocol with antibodies specifically detecting PRKAR1A was established. Anti PRKAR1A rabbit monoclonal antibody from Cell Signaling (Cat #D54D9) was tested. Untransfected HeLa cells and HeLa cells transiently transfected with the EGFP-PRKAR1A, Cerulean-PRKAR1A, mCherry-EYFP-PRKAR1A and Myc-PRKAR1A expression constructs were harvested for Western blot and probed with PRKAR1A antibody. PRKAR1A migrates around 48 kDa [185] so EGFP-PRKAR1A, Myc-PRKAR1A, Cerulean-PRKAR1A and mCherry-EYFP-PRKAR1A constructs should migrate around 74, 50, 74 and 100 kDa respectively in the SDS-gel. The expected band sizes were observed in the blot confirming that all the constructs were equally expressed and of correct size. (Figure 3.1.1). Furthermore, the strong bands of correct size validate that anti-PRKAR1A antibody recognizes both the overexpressed and endogenous PRKAR1A. However, the antibody also gives some unspecific bands.

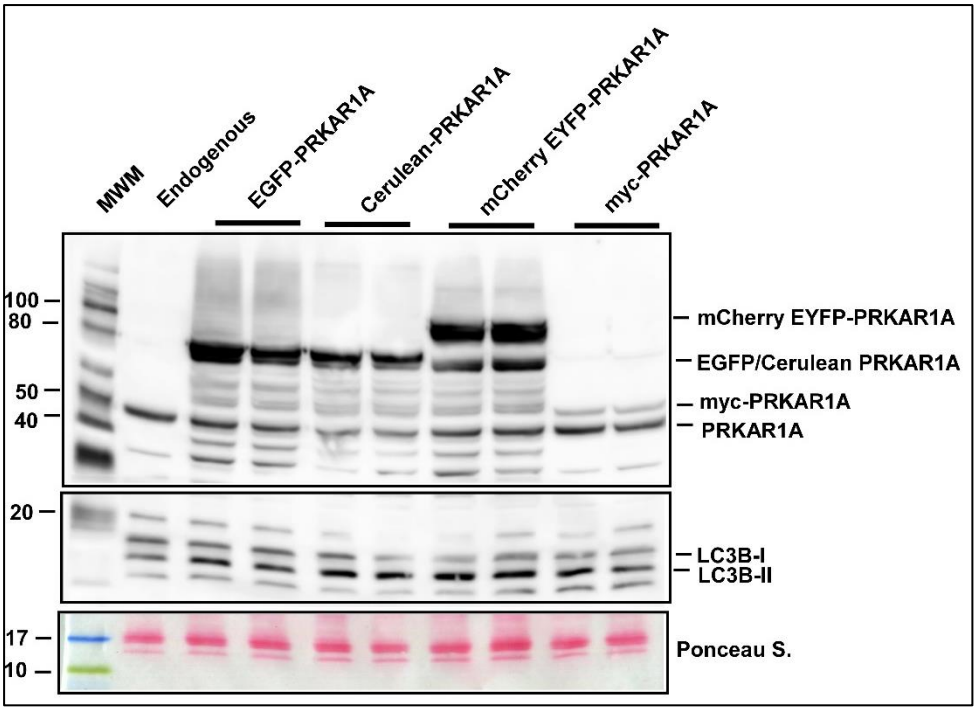

Figure 3.1.1: Western blot of cell extracts from HeLa cells with endogenous and overexpressed PRKAR1A. The cell extracts were separated by SDS-PAGE, blotted to nitrocellulose membrane probed with the PRKAR1A antibody from Cell Signaling. The corresponding lanes are labelled on the top, single lanes for the molecular weight marker and endogenous protein and two parallel lanes for EGFP-PRKAR1A, Cerulean-PRKAR1A, mCherry-EYFP-PRKAR1A and myc-PRKAR1A constructs. LC3B was used as the test control and Ponceau staining was used as a loading control.

To determine the localization pattern of PRKAR1A in cells, mCherry-EYFP-PRKAR1A, EGFP-PRKAR1A and Cerulean-PRKAR1A were overexpressed in HeLa and U2OS cells followed by incubation in full medium (FM) and starved in Hanks Balance Salt Solution (HBSS) conditions (Figure 3.1.2). The protein showed a diffuse cytosolic localization with mCherry-EFYP tag in FM while there were some additional puncta in HBSS, diffused pattern in both FM and HBSS with Cerulean tags (Figure S1 and S2). Surprisingly, bright punctate structures were seen when PRKAR1A was expressed with EGFP tag; with a pronounced perinuclear accumulation (Figure 3.1.3). To determine if the puncta were non-specific aggregates formed by the presence of EGFP, the cells were stained with the anti- PRKAR1A antibody. The strong EGFP puncta were stained very faint by the PRKAR1A antibody in immunofluorescence. The antibody also did not recognize the endogenous PRKAR1A in the cells (data not shown). Hence, the antibody worked very well on western blot but is less specific for immunofluorescence.

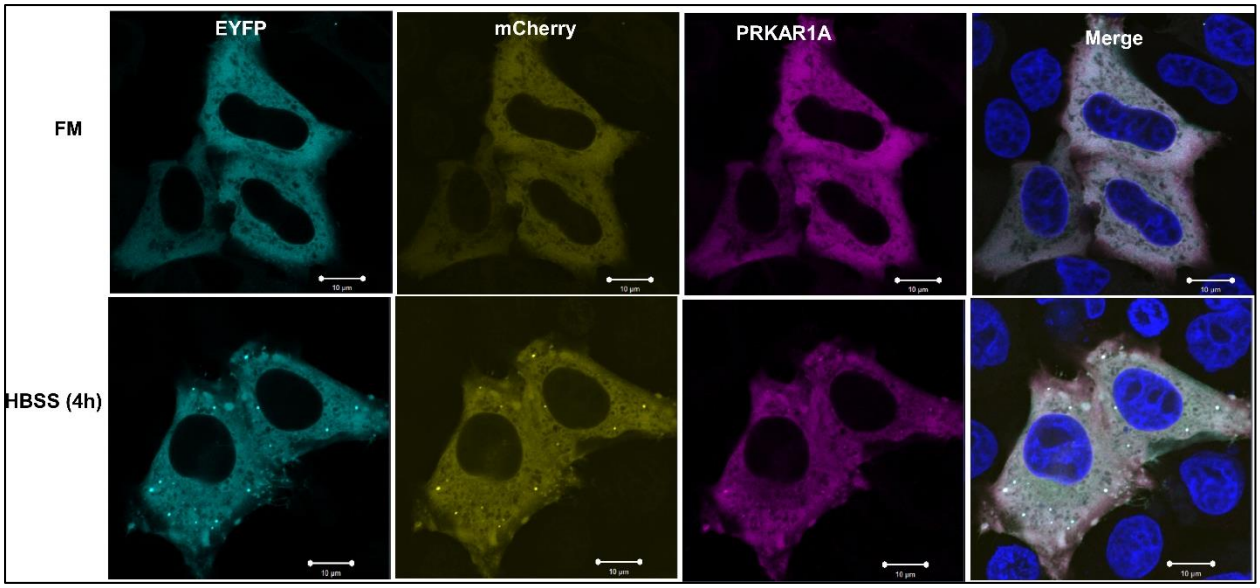

Figure 3.1.2: PRKAR1A is localized to the cytoplasm. HeLa cells were transiently transfected with mCherry-EYFP-PRKAR1A expressing construct and cultured in FM and starved for 4 hours in HBSS, fixed with methanol and subjected to immunofluorescence confocal microscopy using anti-PRKAR1A antibody and anti- Rabbit Alexa 647 secondary antibody. The nuclei were detected using DAPI stain. Scale bar 10 µm.

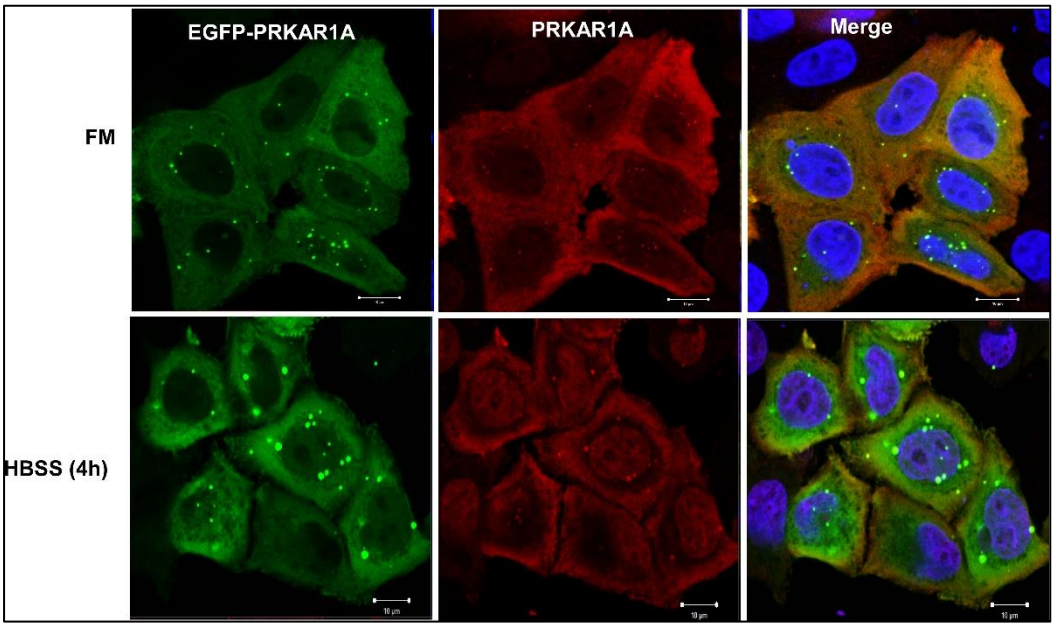

Figure 3.1.3: EGFP-PRKAR1A forms strong puncta when overexpressed. HeLa cells were transiently transfected with EGFP-PRKAR1A expressing construct and cultured in FM and starved for 4 hours in HBSS,fixed with methanol and subjected to immunofluorescence using PRKAR1A antibody and Alexa 555 secondary antibody. The nuclei were detected using DAPI stain. Scale bar 10 µm.

3.2 PRKAR1A interacts with ATG8 family proteins in vitro and in cells

There are only a few studies on the role of PRKAR1A in autophagy. This encouraged us to investigate the role of the protein in autophagy. We started to test if PRKAR1A could interact with ATG8 family proteins using a GST-pulldown assay. GST and GST tagged human ATG8 proteins (LC3A, LC3B, LC3C, GABARAP, GABARAPL1 and GABARAPL2) were expressed and purified from *E. coli* and immobilized on Glutathione Sepharose beads. *In vitro* translated Myc-tagged, full-length PRKAR1A was subjected to pulldown assay together with the GST tagged ATG8 homologues (Figure 3.2.1A). This assay was repeated three times and quantitation of the bound PRKAR1A relative to 10% input is summarized in Figure 3.2.1 B. PRKAR1A bound strongly to GABARAPL2 and GABARAP and with relatively similar affinity to other LC3 and GABARAP proteins analyzed.

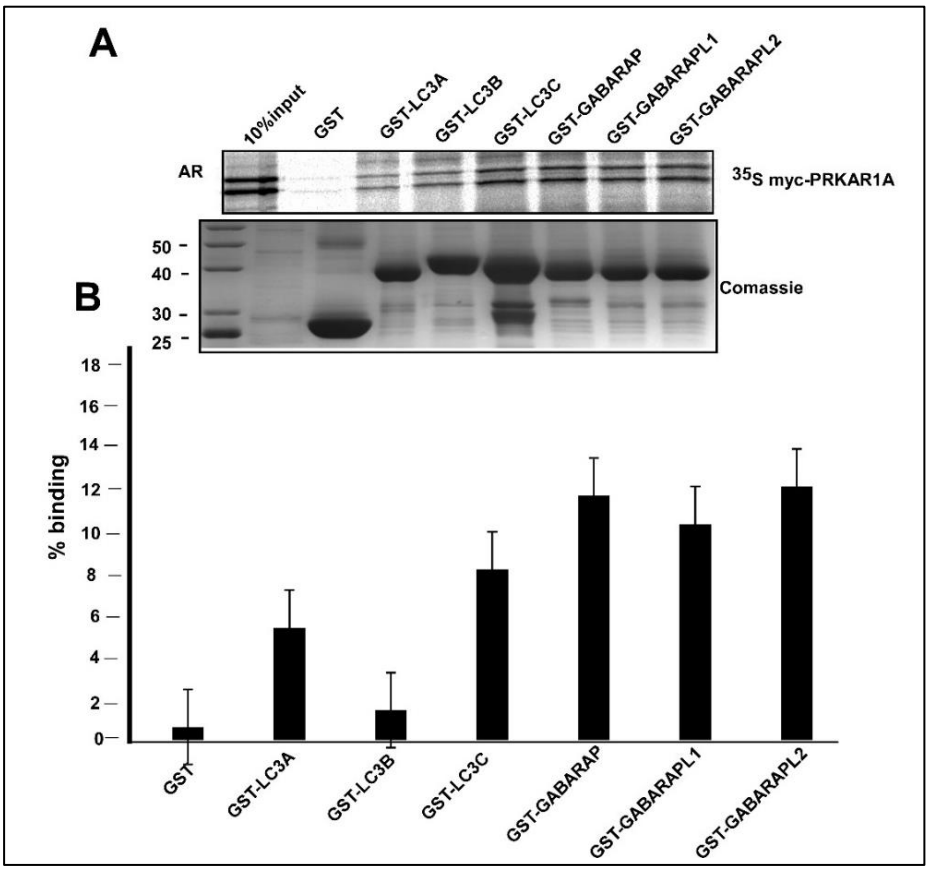

Figure 3.2.1: PRKAR1A interacts with mammalian ATG8s *in vitro*. A GST pull down assay using ^{35}S labelled Myc-PRKAR1A incubated with recombinant GST or GST fused to human ATG8 family proteins. The integrity and relative amounts of immobilized GST and GST-ATG8 family proteins used in the binding assays are shown in the Coomassie Brilliant Blue-stained gel. Bound Myc-PRKAR1A were detected by autoradiography. **B** Quantifications of the binding of Myc-PRKAR1A to the GST-ATG8 proteins presented as percentage binding relative to 10% input. The bars represent the mean values with standard deviation of three independent experiments.

To further investigate whether PRKAR1A expressed in cells interacts with the ATG8 homologues, GST-pulldown assay using extracts from HEK293 cells was performed. The ATG8 family proteins were fused to the GST beads in a similar way as for the *in vitro* translated assay above and incubated with HEK293 cell lysates before PRKAR1A binding was assayed by Western blotting. PRKAR1A bound strongly with GABARAPL2, GABARAP and LC3A, slightly low interactions towards LC3B and intermediate binding towards GABARAPL1 and LC3C. These results correlate with the *in vitro* GST-pull down assay described above. This strongly indicates that PRKAR1A binds to ATG8 proteins in the cell with a preference for GABARAPL2 (Figure 3.2.2).

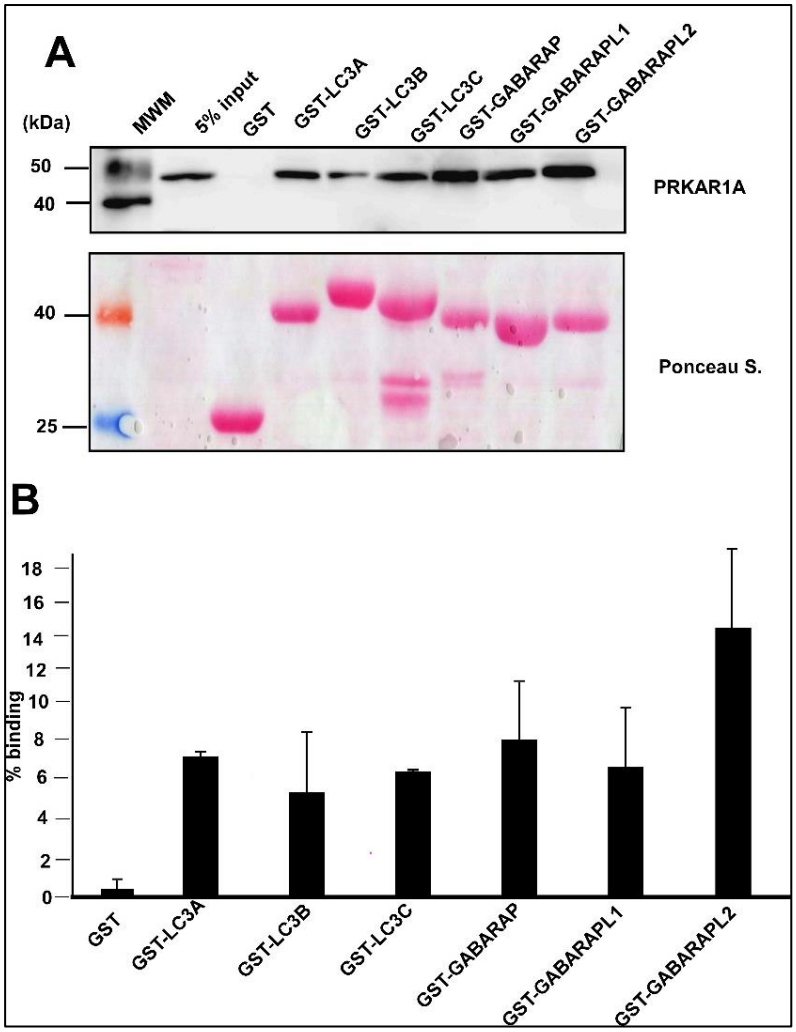

Figure 3.2.2: Endogenous PRKAR1A interacts with ATG8s proteins. A GST pull down assay of endogenous PRKAR1A from a RIPA buffer lysate of human HEK293 cells incubated with recombinant GST or GST fused to human ATG8 family proteins immobilized on Glutathione Sepharose beads. The pulled down PRKAR1A protein and 5% of the input lysate were analyzed by western blotting using anti- PRKAR1A antibody. The amount of GST-ATG8 fusion proteins on Glutathione Sepharose beads were visualized using Ponceau S staining (lower panel). **B** Quantifications of the binding of endogenous PRKAR1A to the GST-ATG8 proteins presented as percentage binding relative to 5% input. The bars represent the mean values with standard deviation of three independent experiments. The intensities of bands were quantified by Image J software.

PRKAR1A interaction with the ATG8 homologs cells was further tested using a Flag based co-immunoprecipitation assay. Flag-tagged ATG8 proteins were co-expressed with GFP-PRKAR1A in HeLa cells, before immunoprecipitations using a Flag antibody was performed. All ATG8 proteins co-precipitated PRKAR1A from the cell lysate (Figure 3.2.3). Interestingly, here the specificity of PRKAR1A seems to be towards the LC3B subfamily and not the GABARAP subfamily. However, this can be due to low expression of at least GABARAP and GABARAPL1. The experiments need to be repeated in the future studies.

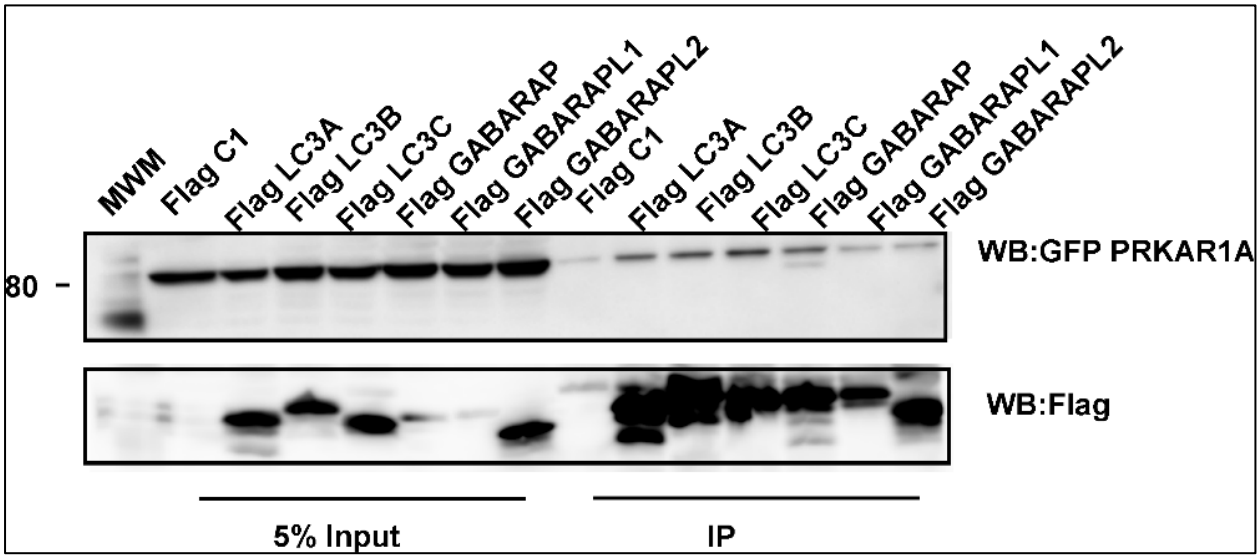

Figure 3.2.3: Co-Immunoprecipitation from HeLa cell lysates. Co-immunoprecipitation experiments performed with Flag antibodies using extracts from HeLa cells transiently transfected with expression construct for Flag tagged ATG8 proteins together with GFP-PRKAR1A. The blots were probed with anti-Flag and anti-PRKAR1A antibodies.

3.3 Binding of PRKAR1A to ATG8 family proteins is LIR independent

The finding that PRKAR1A interacts with the ATG8 family proteins raised the question whether PRKAR1A contains LIR motifs that mediate this interaction. Peptide array was performed to identify putative LIR motifs in PRKAR1A (Gry Evjen and Terje Johansen; unpublished). Using arrays of overlapping 20-mer peptides of PRKAR1A moved by increments of three amino acids to cover the full-length sequence five putative LIRs were identified (Figure 3.3.1).

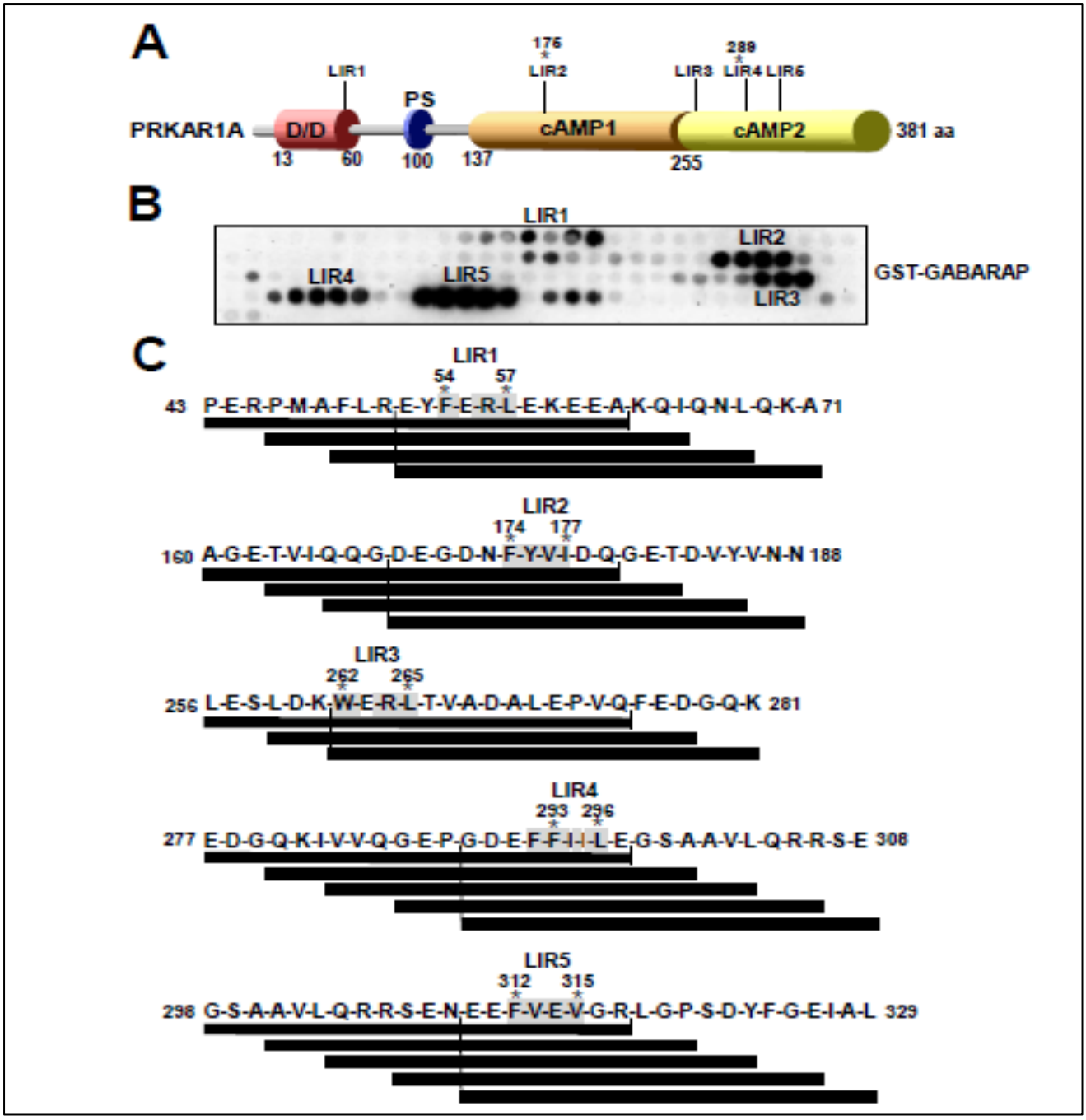

Figure 3.3.1: PRKAR1A contains five putative LIR motifs A Schematic representation of the domain architecture of human PRKAR1A with Dimerizing and Docking domain (pink), two cAMP binding domains 1 (dark yellow) and 2 (light yellow) and one linker region (PS, in blue). **B** Peptide array with 20-mer peptides covering full length PRKAR1A was used for identification of a putative LIR motif in the N terminus of PRKAR1A. Each peptide was shifted three amino acids relative to the pervious peptide. The array was probed for GST-GABARAP for 2h and binding to GST-GABARAP was detected with anti-GST antibody. **C** Five putative LIR motifs were identified. The sequences of the GABARAP interacting protein are shown. Asterisks indicate the conserved aromatic and hydrophobic residues of the LIR motif.

To further investigate whether the binding of PRKAR1A to ATG8 family proteins is dependent on a LIR motif, we performed GST pulldown assay with LC3B and GABARAP that were mutated in their LIR binding pockets, GABARAP (Y49A, Y49A/F104A) and LC3B (F52A). The pull down was also performed with mutated arginine residues in LC3B (R10A/R11A) in N-terminal, an N-terminal deletion (1-28) and a C-terminal deletion (30-125) of LC3B [186]. *In vitro* translated Myc-tagged PRKAR1A was subjected to GST-pull down assay together with the GST tagged wild type (WT) GABARAP and LDS mutants of GABARAP and WT LC3B and LDS mutant of LC3B as well as other mutations mentioned above (Figure 3.3.2 A). Quantitation of the amount of bound PRKAR1A in three independent experiments showed that mutation in LIR binding pocket in GABARAP and LC3B did not affect the binding to a significant degree (Figure 3.3.2 B). These results suggest that interaction of PRKAR1A with the ATG8 family proteins is not mediated via a canonical LIR-LDS binding. Although the interaction of PRKAR1A to LC3B was reduced with both N-terminal and C-terminal deletions and mutated arginine residues of LC3B, the binding was not completely abolished. Furthermore, the weak interaction of PRKAR1A with LC3B makes the validation of the effect of the mutations difficult to measure.

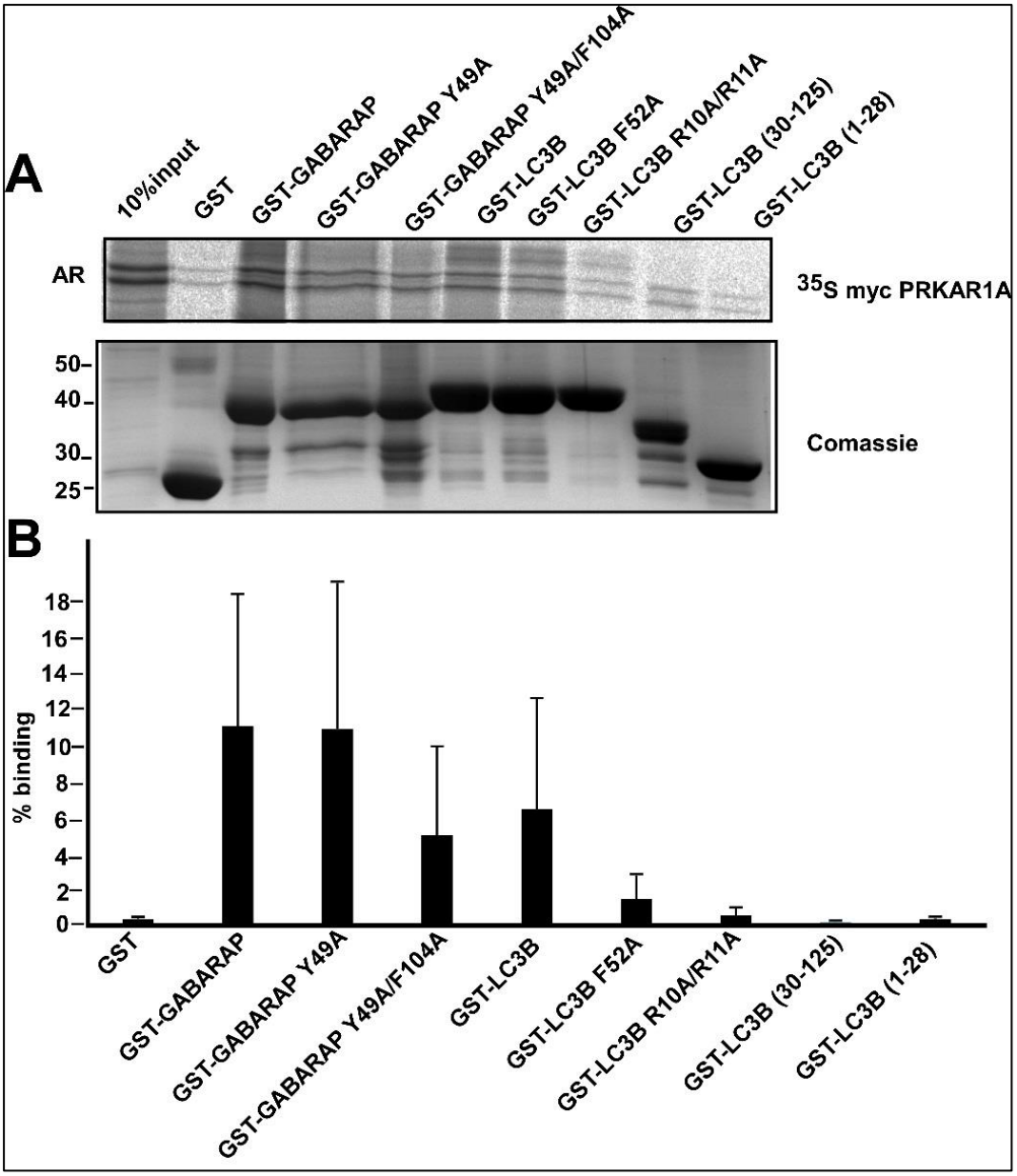

Figure 3.3.2: The PRKAR1A interaction with the ATG8s is LIR independent. A GST pull down assay using ^{35}S labelled Myc-PRKAR1A incubated with recombinant GST or GST fused to WT GABARAP and LDS mutants of GABARAP and WT LC3B and LDS mutants of LC3B. The Coomassie staining represents the amount of GST-ATG8 fusion proteins on Glutathione Sepharose beads used in the assays. Bound Myc-PRKAR1A were detected by autoradiography. **B** Quantifications of the binding of PRKAR1A to GST or GST fused GABARAP and LDS mutants of GABARAP and WT LC3B and LDS mutants of LC3B presented as percentage binding relative to 10% input. The bars represent the mean values with standard deviation of three independent experiments.

3.4 PRKAR1A is not an autophagy substrate

Strong binding to ATG8 family proteins both *in vitro* and in cells led us to determine if the protein was localized to autophagosomes. We also wanted to identify the degradation pathway followed by the protein. To address this, HeLa and U2OS cells were transiently transfected with mCherry-EYFP-PRKAR1A and grown for 24 hours and were further grown in five different conditions, FM, FM in presence of Bafilomycin A1 (BafA1) for 4 hours, starvation medium (HBSS) for 4 hours, starvation medium in presence of BafA1 for 4 hours and FM in presence of proteasome inhibitor (MG132) for 4 hours. The cells were analyzed by fluorescence confocal microscopy. BafA1 is a potent inhibitor of vacuolar H^+-ATPase used at high concentration to block late-phase autophagy [187]. BafA1 acts as an autophagy inhibitor by halting the fusion between autophagosomes and lysosomes and by inhibiting lysosomal degradation [188]. MG132 (carbobenzoxy-Leu-Leu-leucinal) is a proteasomal inhibitor that blocks the proteolytic activity of the 26S proteasome complex [189] [190]. In our study, PRKAR1A was fused to mCherry-EFYP vector that utilizes an advantage of pH sensitive EYFP which is quenched at low pH of the lysosome. The fluorescent protein mCherry is stable at the lysosomal pH. When mCherry-EFYP is expressed in cells induced with autophagy, both EYFP and mCherry are detected and autophagosomes appear as yellow puncta. However, when autolysosome maturates after the autophagososme-lysosome fusion, the EYFP signal is quenched and puncta stains as red only. The tendency of the yellow to red switch is an indication of altered autophagy resulting in matured autophagosomes. However, overexpression of protein in cells also produces a background level of red fluorescence [100, 145, 191]. Figure 3.4.1 shows that the intensity and distribution of PRKAR1A was almost unchanged upon various treatments. No accumulation of aggregates in BafA1 and MG132 was observed within 4 hours of treatment. The protein formed some puncta upon starvation but most of these puncta were not red only (acidified), indicating they were not autophagosomes. However, a few cells displayed around 4-5 red only puncta per cell under starvation conditions. Since the localization of mCherry-EYFP-PRKAR1A to acidic structures was very scarce, localization of a positive control and negative control in parallel was performed for confirmation. The cells were transiently transfected with the autophagy receptor mCherry-EYFP-p62, as a positive control and mCherry-EFYP empty vector as a negative control and grown in the same five conditions as described before. It is well known that p62 is degraded by autophagy [192]. There were around 10 red only puncta per cell in FM with mCherry-EYFP-p62 and more than 20 p62 puncta per cell upon starvation (Figure 3.4.2 and 3.4.7). The negative control formed a few red only puncta in some cells upon starvation (2-3 puncta per cell) (Figure

3.4.2). Hence the number of red only puncta formed by PRKAR1A was similar to the number of red only puncta formed by the negative control. To investigate if the degradation of PRKAR1A could be very slow, the number of red only puncta after 48 hours transfection was analyzed next. For this, HeLa and U2OS cells were transiently transfected with mCherry-EYFP-PRKAR1A grown in full medium for 48 hours before treatments as described above. There were many red only puncta observed 48 hours after transfection as compared to 24 hours after transfection (Figure 3.4.4 and 3.4.9). The number of cells with red only puncta was compared with the negative control 48 hours after transfection (Figure 3.4.5 and 3.4.10). Quantitation of number of red only puncta in more than 100 transfected cells were done manually by inspection. The cells were counted as positive if they had ≥10 red only puncta. The number of cells with red only puncta was similar in the cells transiently transfected with the negative vector control and the cells transfected with mCherry-EYFP-PRKAR1A protein irrespective of hours after transfection and seemed not to be changed upon various type of the cell lines used (Figure 3.4.11). Furthermore, PRKAR1A was mainly diffuse in the cytosol. These results clearly indicate that PRKAR1A is not degraded in acidic compartments and hence not an autophagy substrate.

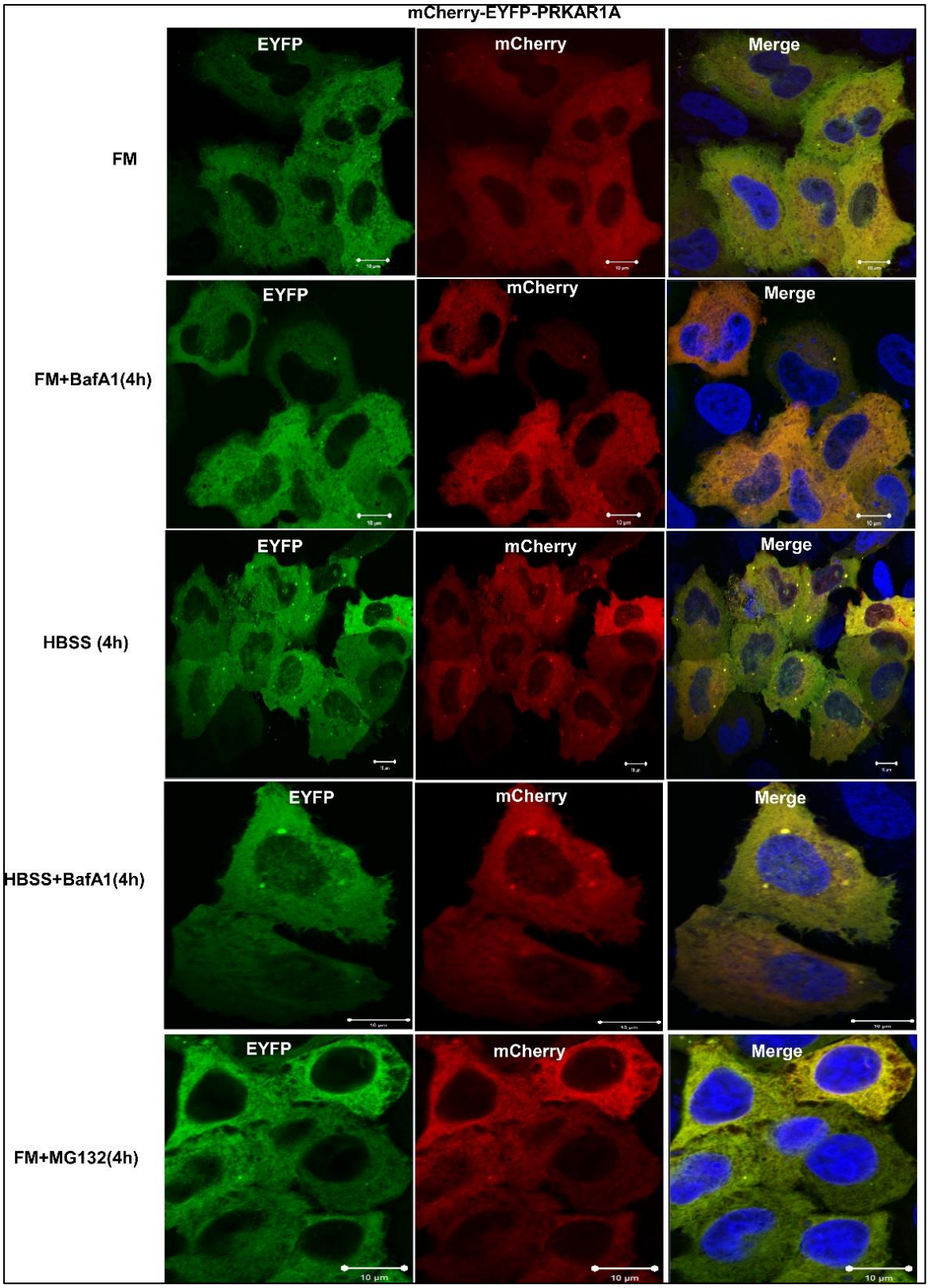

Figure 3.4.1: PRKAR1A puncta does not localize to acidic structures in HeLa cells. HeLa cells transiently transfected with mCherry-EYFP-PRKAR1A expression constructs for 24 hours were cultured either in FM, treatment with BafA1 for 4h, induction of autophagy by starvation (HBSS) for 4 h, starvation and lysosomal blockage (HBSS +BafA1) for 4h and treatment with MG132 for 4h. After treatment the cells were fixed with FA and stained with DAPI and imaged. The figure shows representative images from one independent experiment which was repeated with similar results. Scale bar 10µm.

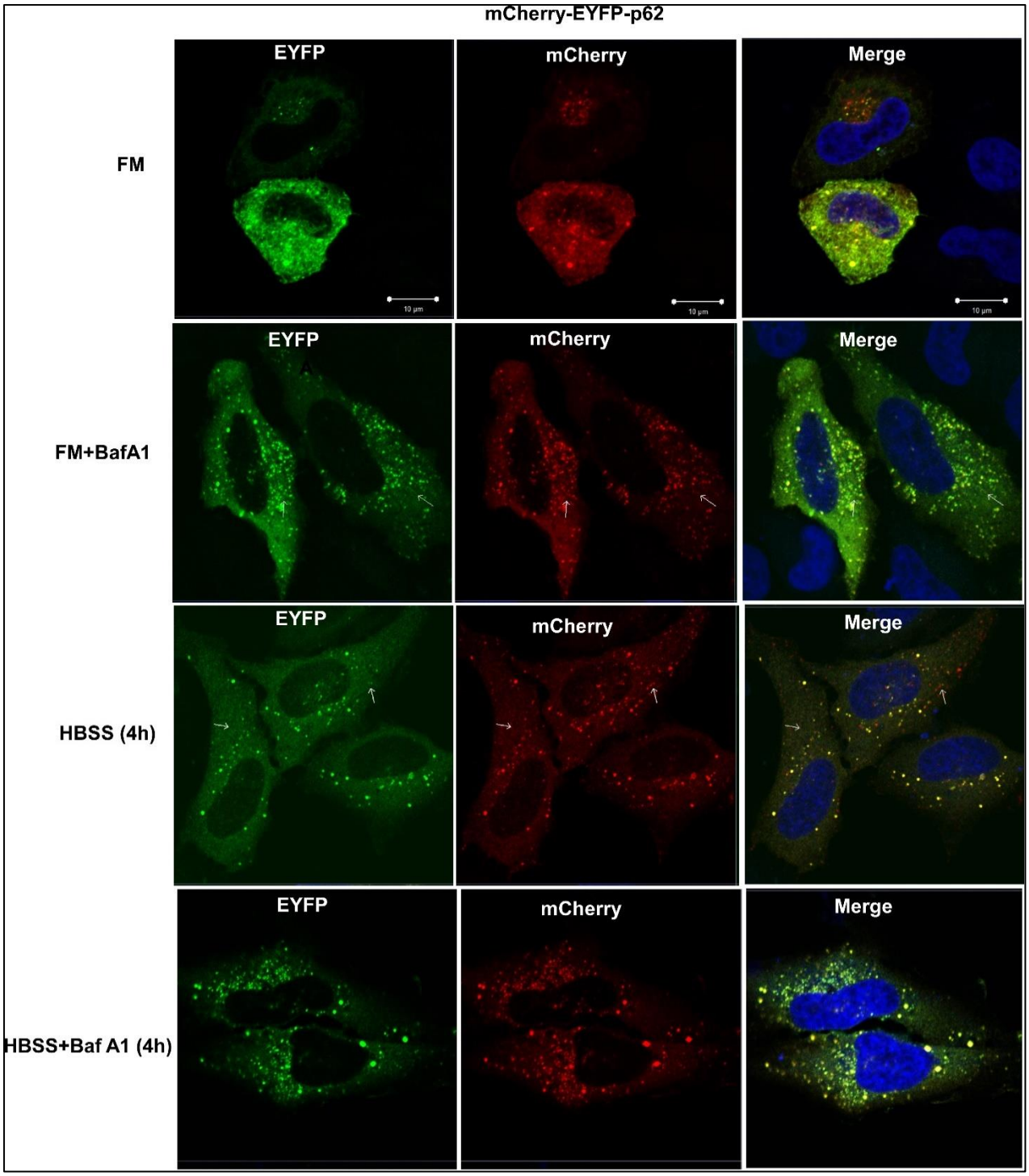

Figure 3.4.2: p62 protein localizes to punctate structures during starvation and is localized with acidic structures. HeLa cells transiently transfected with mCherry-EYFP-p62 expression constructs for 24 hours were cultured either in FM, treatment with BafA1 for 4h, HBSS for 4 h and HBSS +BafA1 for 4h. After treatment the cells were fixed, stained with DAPI for nuclei and imaged. The figure shows representative images from one independent experiment which was repeated with similar results. White arrows indicate in indicate aggregates upon BafA1 treatment and red only puncta upon starvation in HBSS. Scale bar 10 µm.

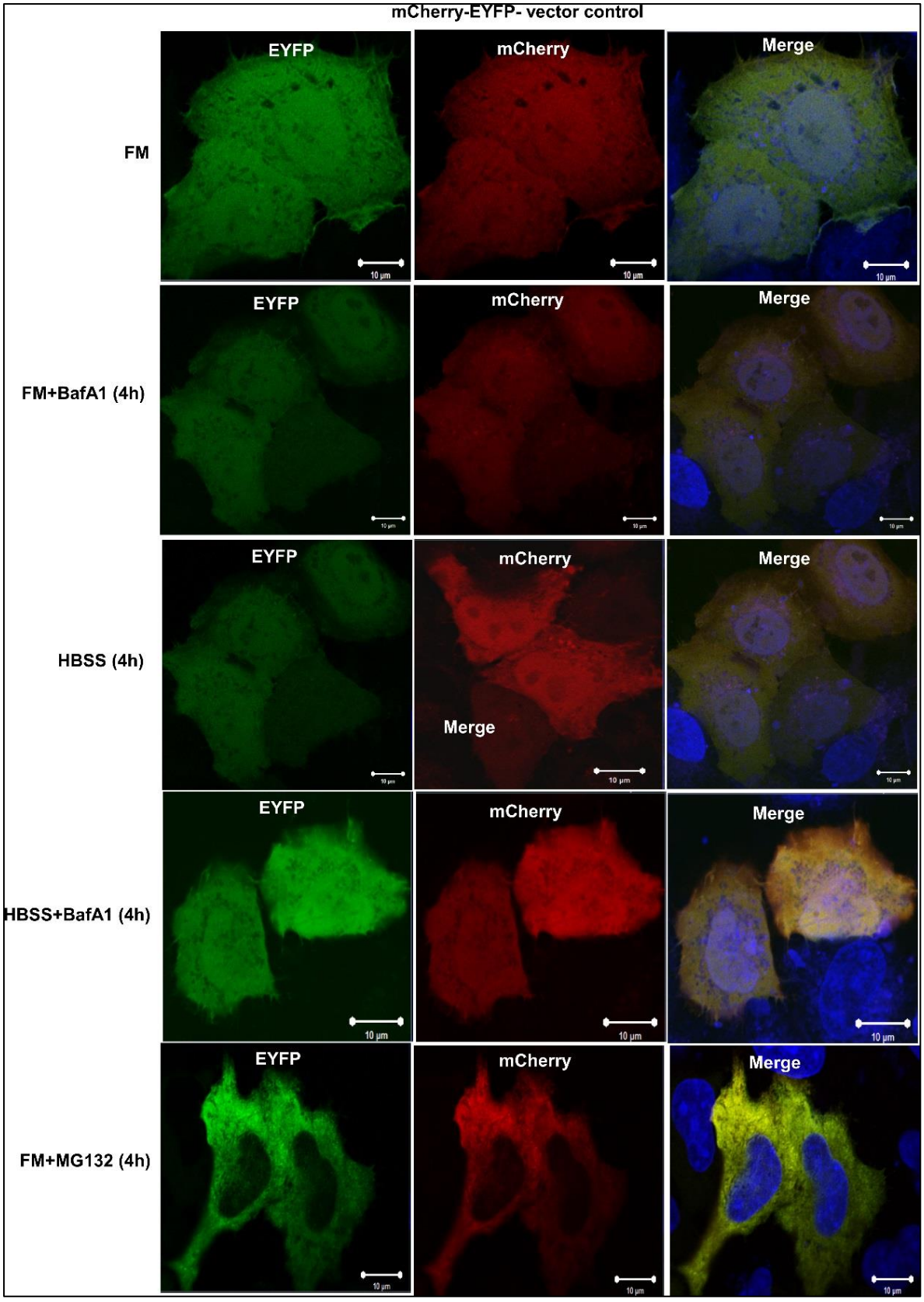

Figure 3.4.3: Vector control is mainly diffuse upon all conditions. HeLa cells transiently transfected with mCherry-EYFP-vector control for 24 hours were cultured either in FM, treatment with BafA1 for 4h, HBSS for 4 h, HBSS +BafA1 for 4h and treatment with MG132 for 4h. After treatment the cells were fixed, stained with DAPI for nuclei and imaged. The figure shows representative images from one independent experiment which was repeated with similar results. Scale bar 10 µm.

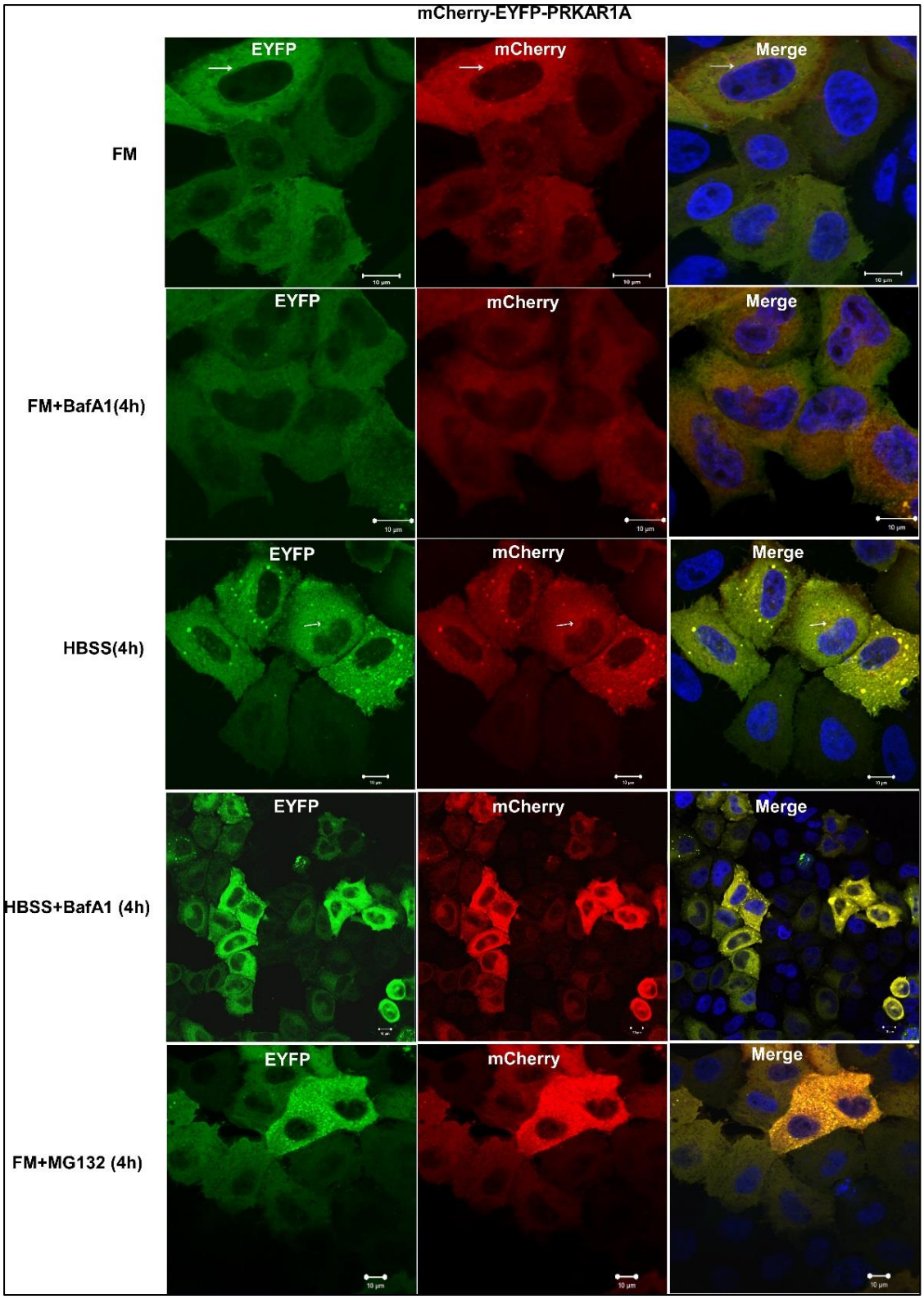

Figure 3.4.4: PRKAR1A does not localize to acidic structures 48 hours after transfection in HeLa cells. HeLa cells transiently transfected with mCherry-EYFP-PRKAR1A expression constructs for 48 hours were cultured in FM, treatment with BafA1 for 4h, HBSS for 4 h, HBSS+BafA1 for 4h and treatment with MG132 for 4h. After treatment the cells were fixed with FA, stained with DAPI for nuclei and imaged. Arrows indicate red only puncta upon starvation in HBSS. The figure shows representative images from one independent experiment which was repeated with similar results. Scale bar 10 µm.

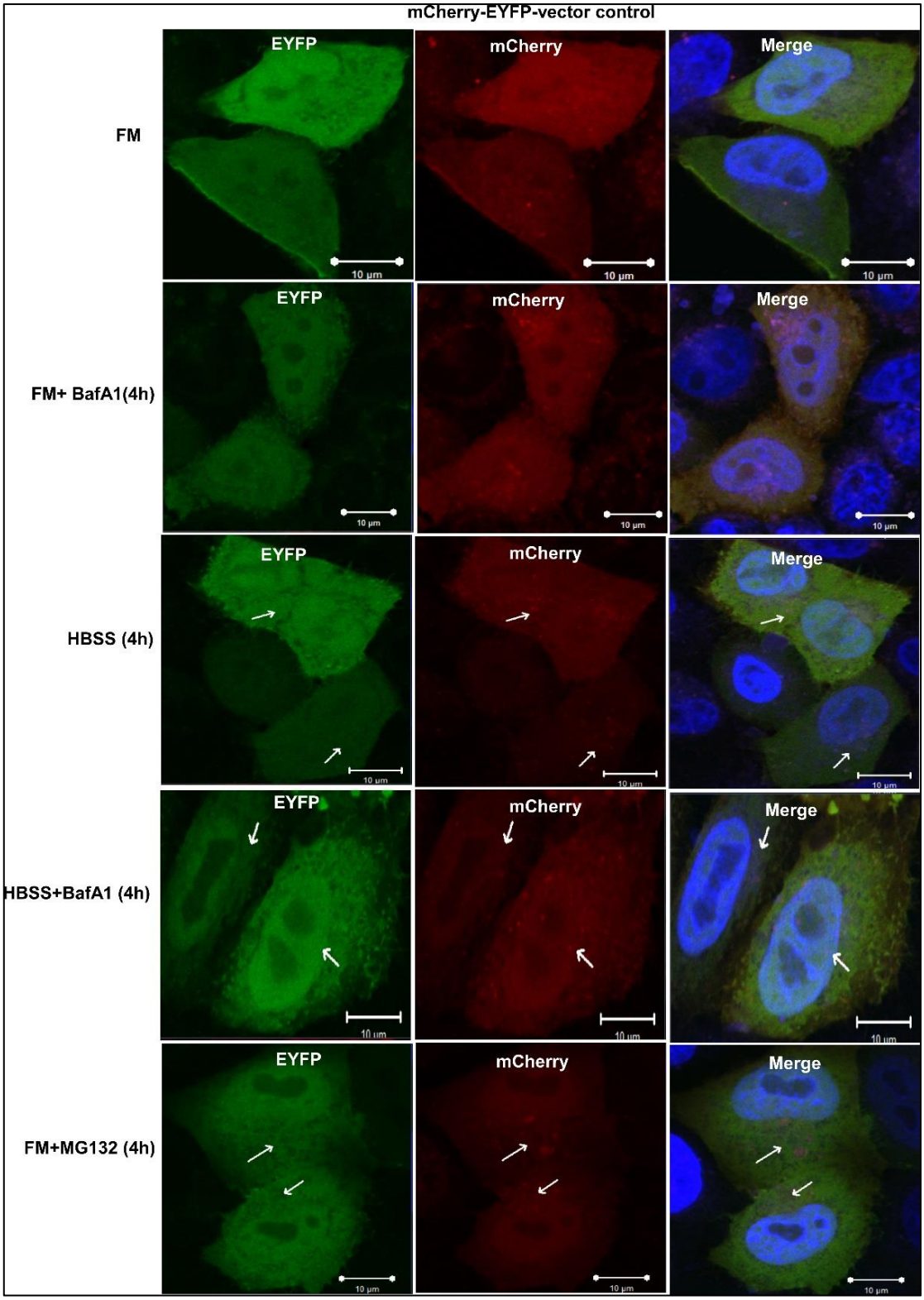

Figure 3.4.5: Red only puncta are formed by vector control after 48 hours transfection in HeLa cells HeLa cells transiently transfected with mCherry-EFYP for 48 hours were cultured in FM, treatment with BafA1 for 4h, HBSS for 4 h, HBSS +BafA1 for 4h and treatment with MG132 for 4h. After treatment the cells were fixed with FA and stained with DAPI for nuclei and imaged. Arrows indicate red only puncta under various treatment and starvation conditions. The figure shows representative images from one independent experiment which was repeated with similar results. Scale bar 10 µm.

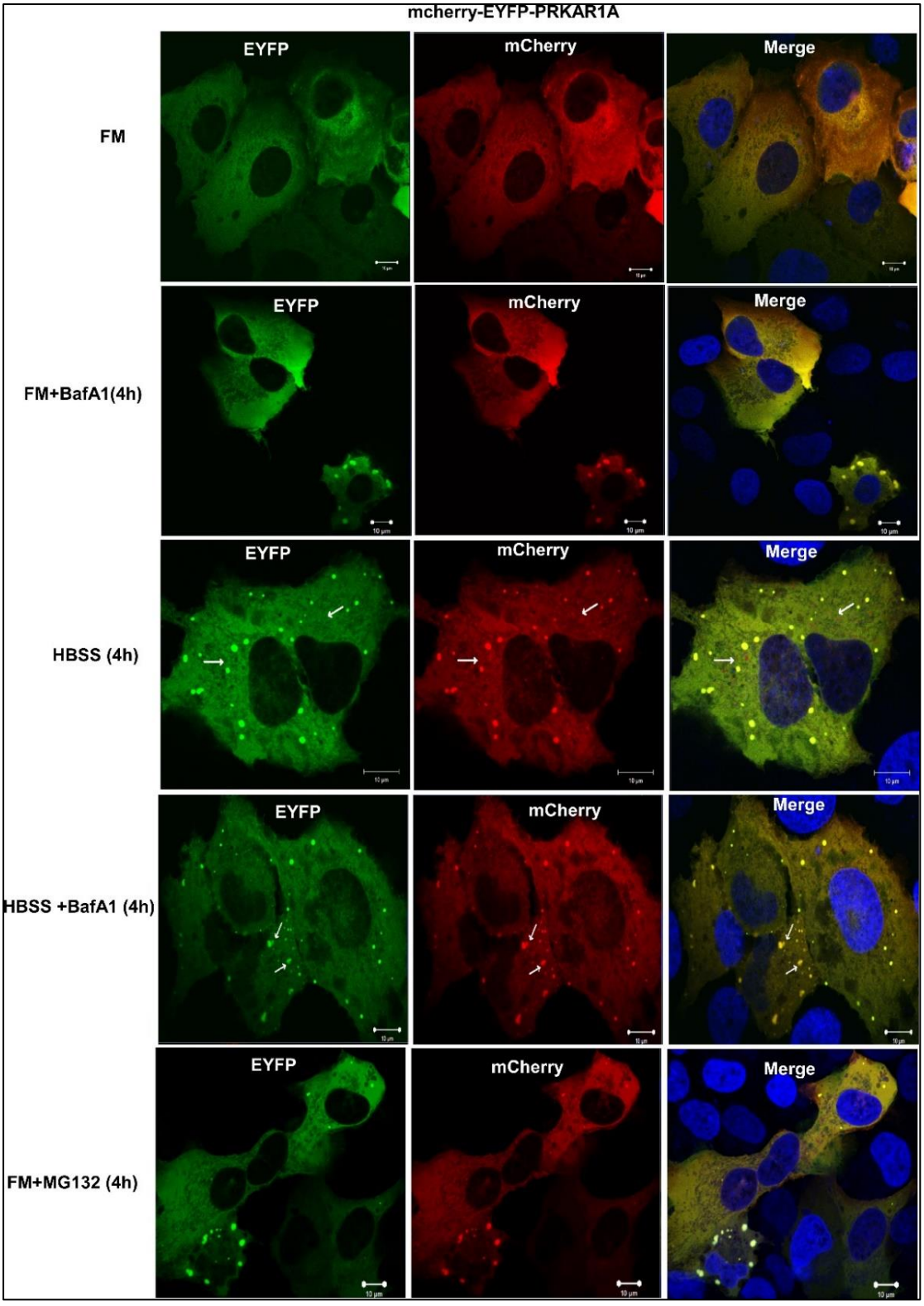

Figure 3.4.6: PRKAR1A puncta does not localize to acidic structures 24 hours after transfection in U2OS cells. U2OS cells transiently transfected with mCherry-EYFP-PRKAR1A expression constructs for 24hours were cultured in FM, treatment with BafA1 for 4h, HBSS for 4 h, HBSS +BafA1 for 4h and treatment with MG132 for 4h. After treatment the cells were fixed with FA, stained with DAPI for nuclei and imaged. Arrows indicate red only puncta upon starvation in HBSS and protein aggregates with BafA1 treatment. The figure shows representative images from one independent experiment which was repeated with similar results. Scale bar 10 μm.

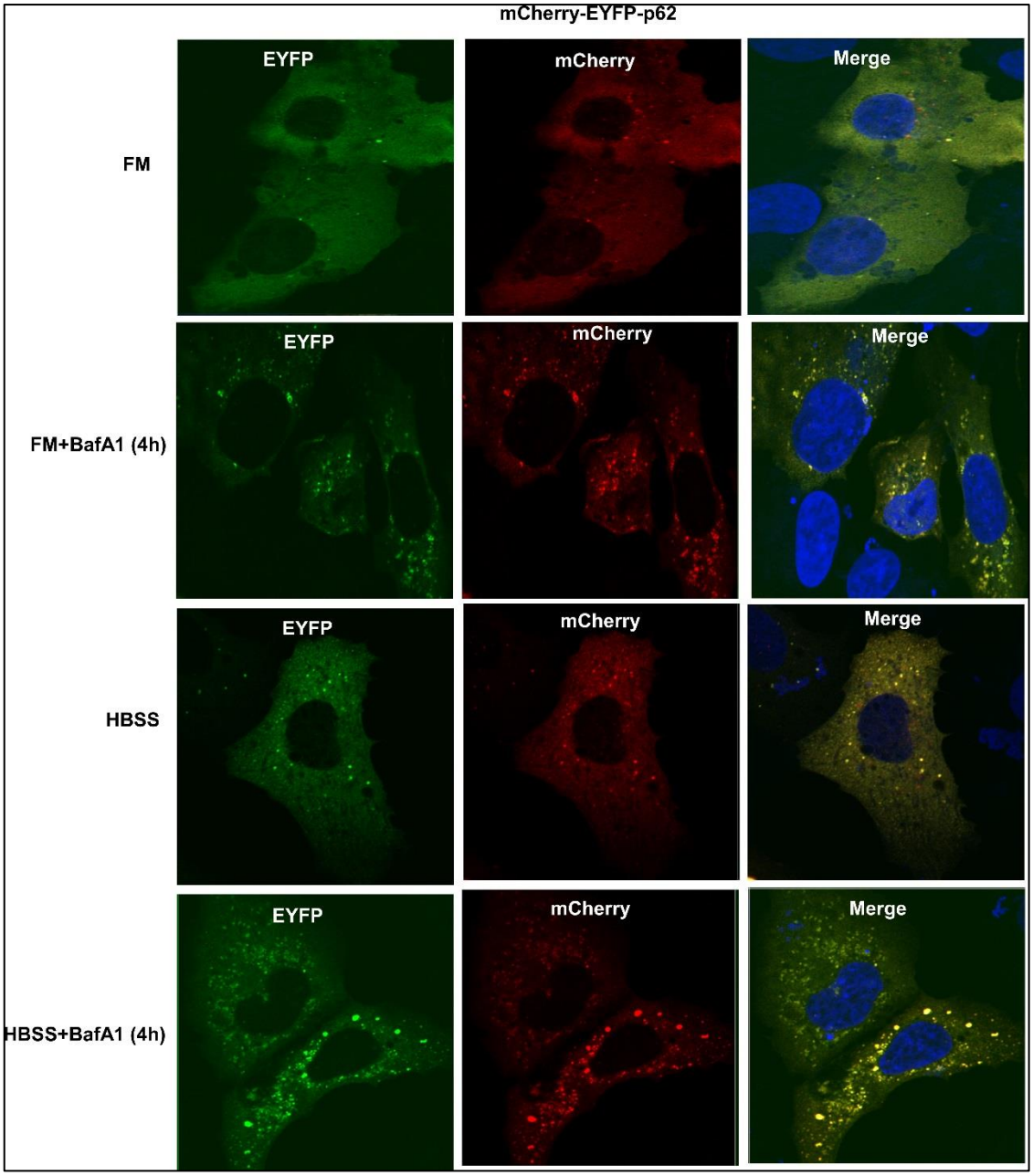

Figure 3.4.7: p62 protein localizes to punctate structures during starvation and is localized to acidic structures in U2OS cells. U2OS cells transiently transfected with mCherry-EYFP-p62 expression constructs for 24 hours were cultured either in FM, treatment with BafA1 for 4h, HBSS for 4 h and HBSS +BafA1 for 4h. After treatment the cells were fixed with FA and stained with DAPI for nuclei and imaged. The figure shows representative images from one independent experiment which was repeated with similar results.

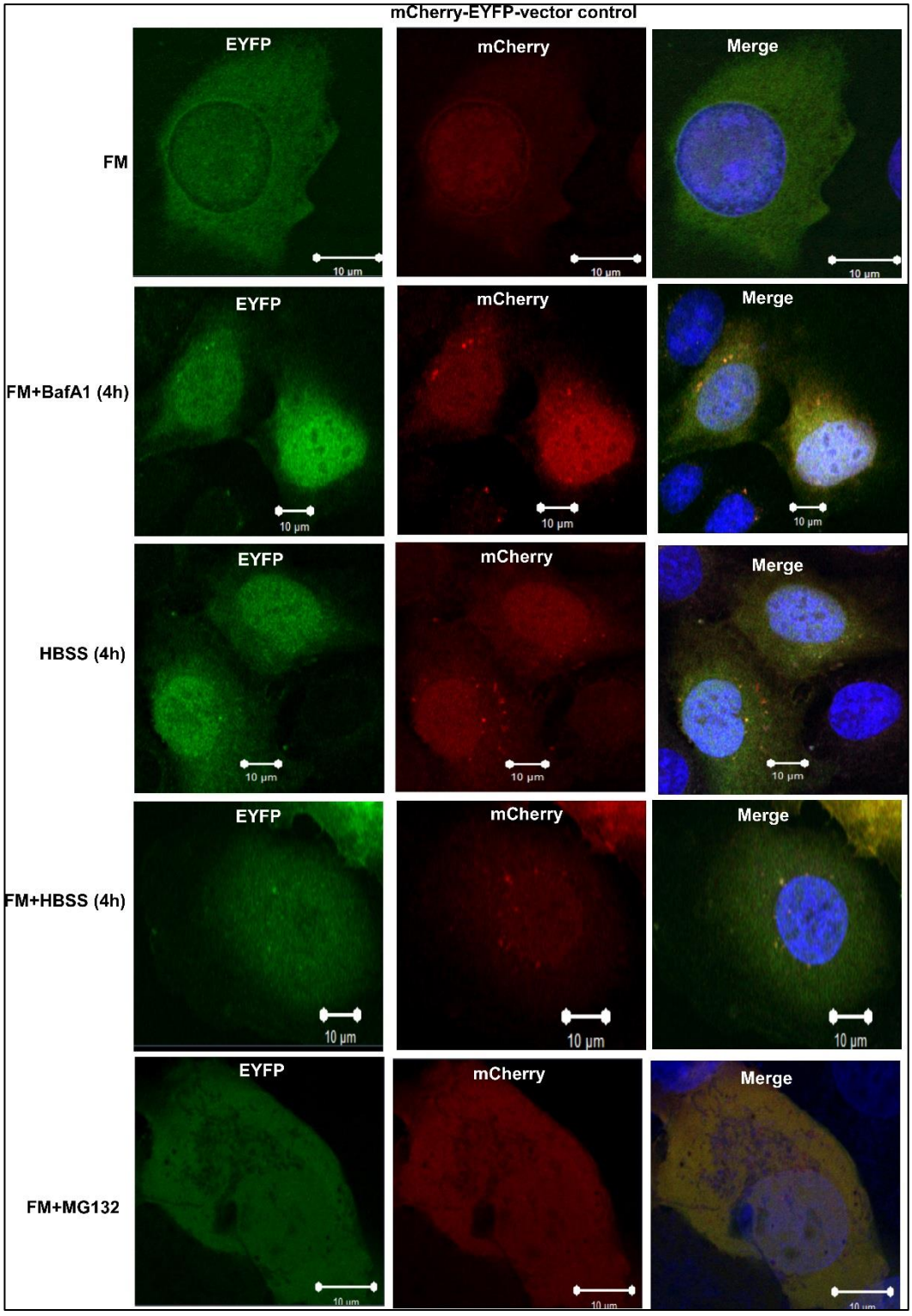

Figure 3.4.8: A few puncta is formed by vector control 24 hours after transfection of U2OS cells. U2OS cells transiently transfected with mCherry-EFYP vector control for 24 hours were cultured in FM, treatment with BafA1 for 4h, HBSS for 4 h, HBSS +BafA1 for 4h and treatment with MG132 for 4h. After treatment the cells were fixed with FA, stained with DAPI for nuclei and imaged. The figure shows representative images from one independent experiment which was repeated with similar results. Scale bar 10µm.

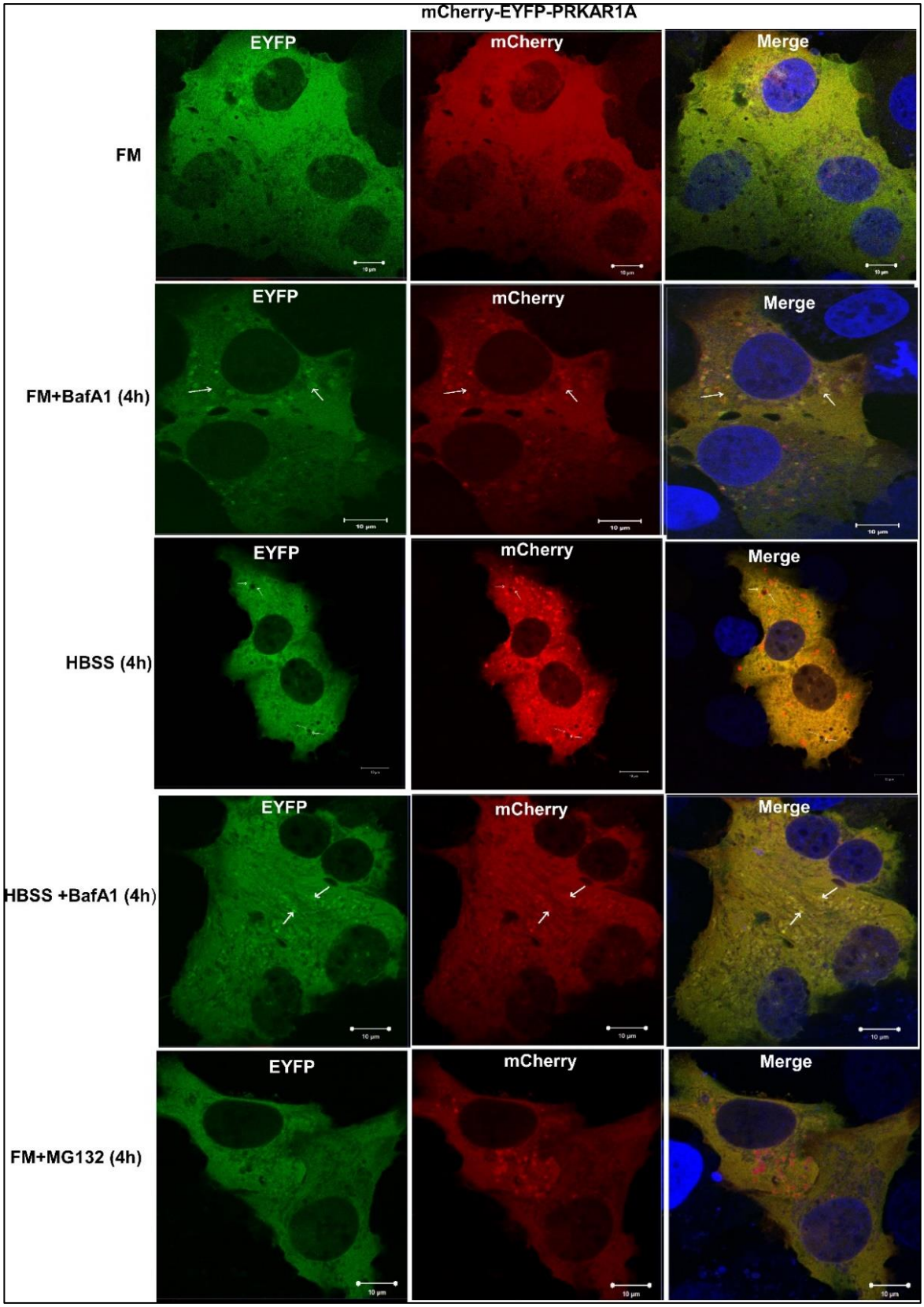

Figure 3.4.9: PRKAR1A puncta does not localize to acidic structures 48 hours transfection of U2OS cells. U2OS cells transiently transfected with mCherry-EYFP-PRKAR1A for 48 hours were cultured in FM, treatment with BafA1 for 4h, HBSS for 4 h, HBSS +BafA1 for 4h and treatment with MG132 for 4h. After treatment the cells were fixed with FA, stained with DAPI and imaged. The figure shows representative images from one independent experiment which was repeated with similar results. Scale bar 10µm. Arrows indicate red only puncta upon starvation in HBSS and background aggregates with BafA1 treatment.

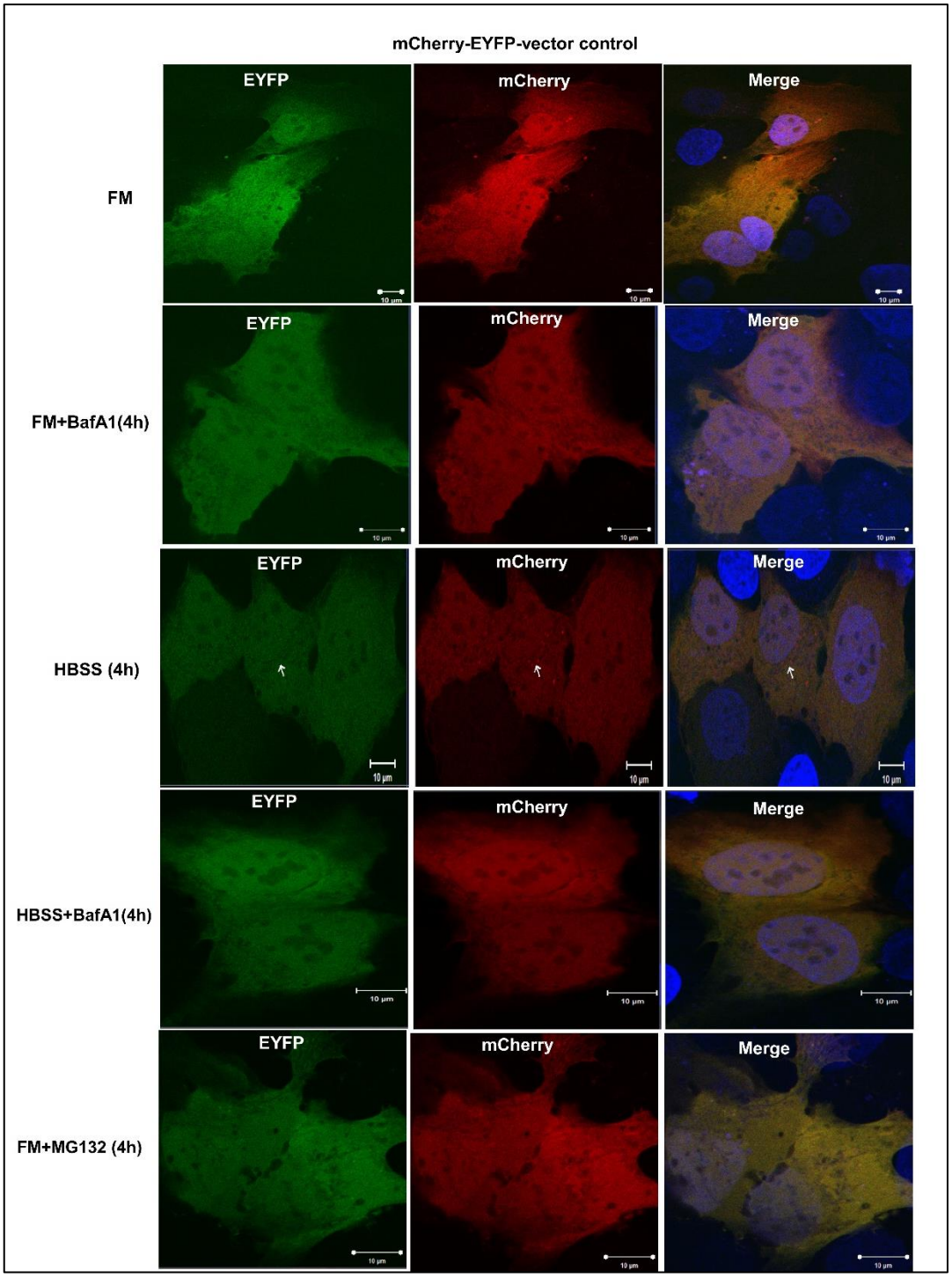

Figure 3.4.10 A few puncta is formed by vector control 48 hours after transfection of U2OS cells. U2OS cells transiently transfected with mCherry-EYFP-vector control for 48 hours were cultured in FM, treatment with BafA1 for 4h, HBSS for 4 h, HBSS +BafA1 for 4h and treatment with MG132 for 4h. After treatment the cells were fixed with FA, stained with DAPI for nuclei and imaged. Arrows indicate red only puncta. The figure shows representative images from one independent experiment which was repeated with similar results. Scale bar 10 µm.

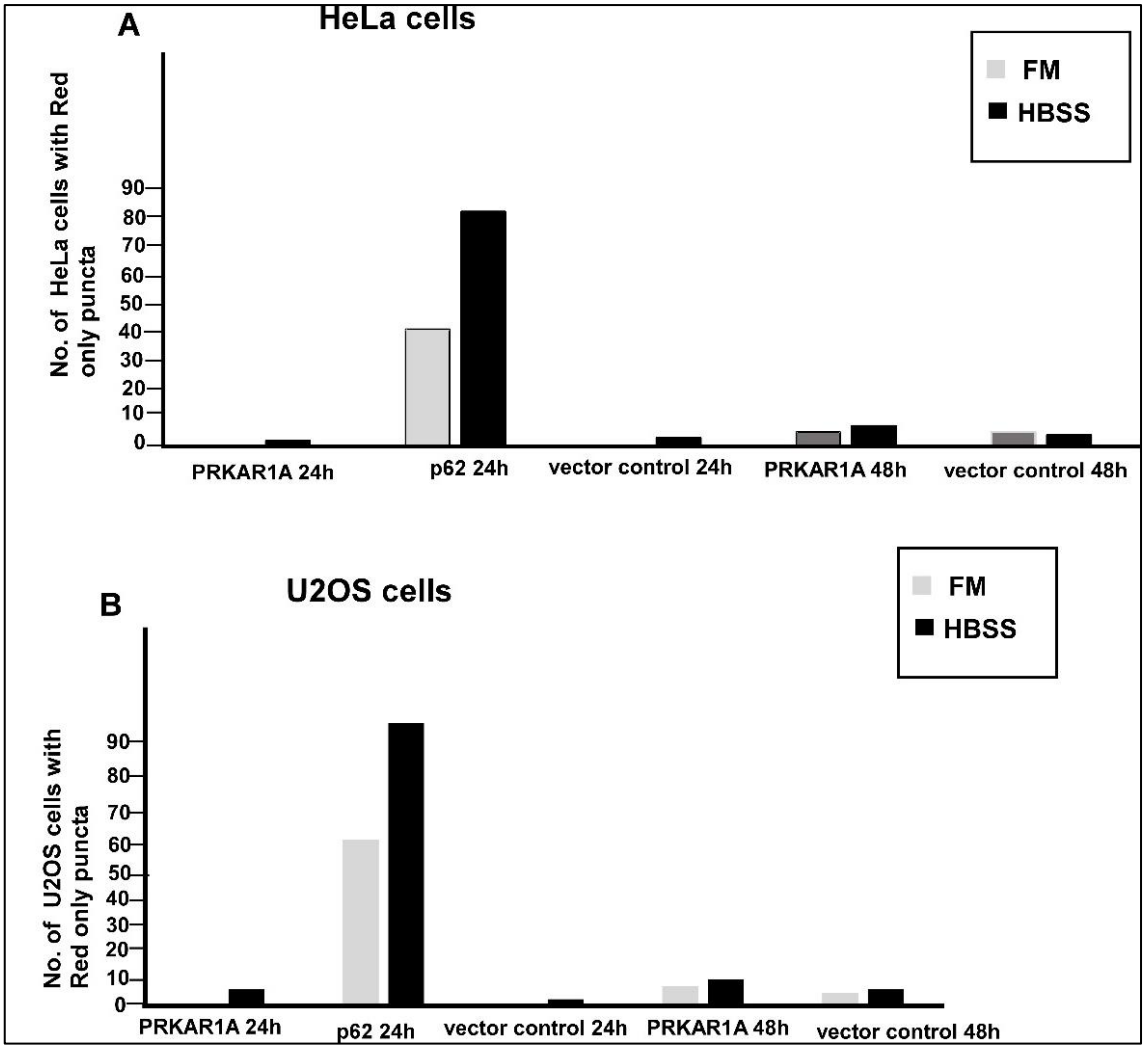

Figure 3.4.11: Quantitation of red only puncta upon starvation of HeLa and U2OS cells. Quantitation was done for the representative experiments based on more than 100 transfected cells. The number of cells with red only puncta were counted with a threshold of ≤10 per cell. The bars were plotted for the cells with red only puncta in FM and HBSS for mCherry-EYFP-PRKAR1A (24 hours post transfection), mCherry-EYFP-p62 (24 hours post transfection), mCherry-EYFP-vector control (24 hours post transfection), mCherry-EYFP-PRKAR1A (48 hours post transfection) and mCherry-EYFP-vector control (48 hours post transfection) for both HeLa and U2OS cells.

To further evaluate if PRKAR1A is degraded by autophagy, western blot analysis of endogenous PRKAR1A was performed during different autophagy inducing and inhibition conditions. HeLa cells were grown in 6 well culture dishes and treated with eight different conditions FM, FM in presence of autophagy inhibitor (BafA1) for 4 hours, starvation medium (HBSS) for 4 hours (autophagy induction), starvation medium in presence of BafA1 for 4 hours and FM in presence of proteasomal inhibitor MG132 for 4 hours, FM in presence of BafA1 for 6 hours, starvation medium (HBSS) for 6 hours, starvation medium in presence of BafA1 for 6 hours and FM in presence of MG132 for 6 hours. The blots were sequentially probed using LC3, p62 and actin antibodies as control. It is well known that p62 degradation in autolysosomes is induced by autophagy [145]. LC3B and p62 are used as markers of

autophagy. LC3B-I is cytosolic however the lipidated form of LC3-II is associated to autophagosomal membranes [193, 194]. Upon BafA1 treatment the lipidated form of LC3B will accumulate since the autophagosomes are not fused with the lysosomes and degraded. Autophagy is induced upon starvation with HBSS, resulting in increased LC3B lipidation and increased degradation of p62 and LC3B. This can be seen by the low intensity bands in lysates treated with HBSS compared to the lysates in the full medium. In our experiments, the levels of p62 and LC3-II changed in the lanes with lysates from starved cells, showing the expected autophagy flux (measure of autophagic degradation activity) [195]. Treatment with autophagy inhibitor BafA1 for 4 hours and 6 hours resulted in no accumulation of PRKAR1A in HeLa cells (Figure 3.4.12 A). Furthermore, the protein was not degraded during HBSS treatment for 4 and 6 hours. There was some accumulation of PRKAR1A upon MG132 treatment for 4 hours and the protein was even more accumulated after 6 hours treatment. Quantitation of various PRKAR1A bands relative to the intensity of FM band indicated that PRKAR1A was unchanged during autophagy induction and inhibiting conditions. Some accumulation upon treatment with the proteasomal inhibitor was observed (Figure 3.4.12B). This suggest that PRKAR1A is mainly degraded by the proteasomal pathway and is a relatively stable protein.

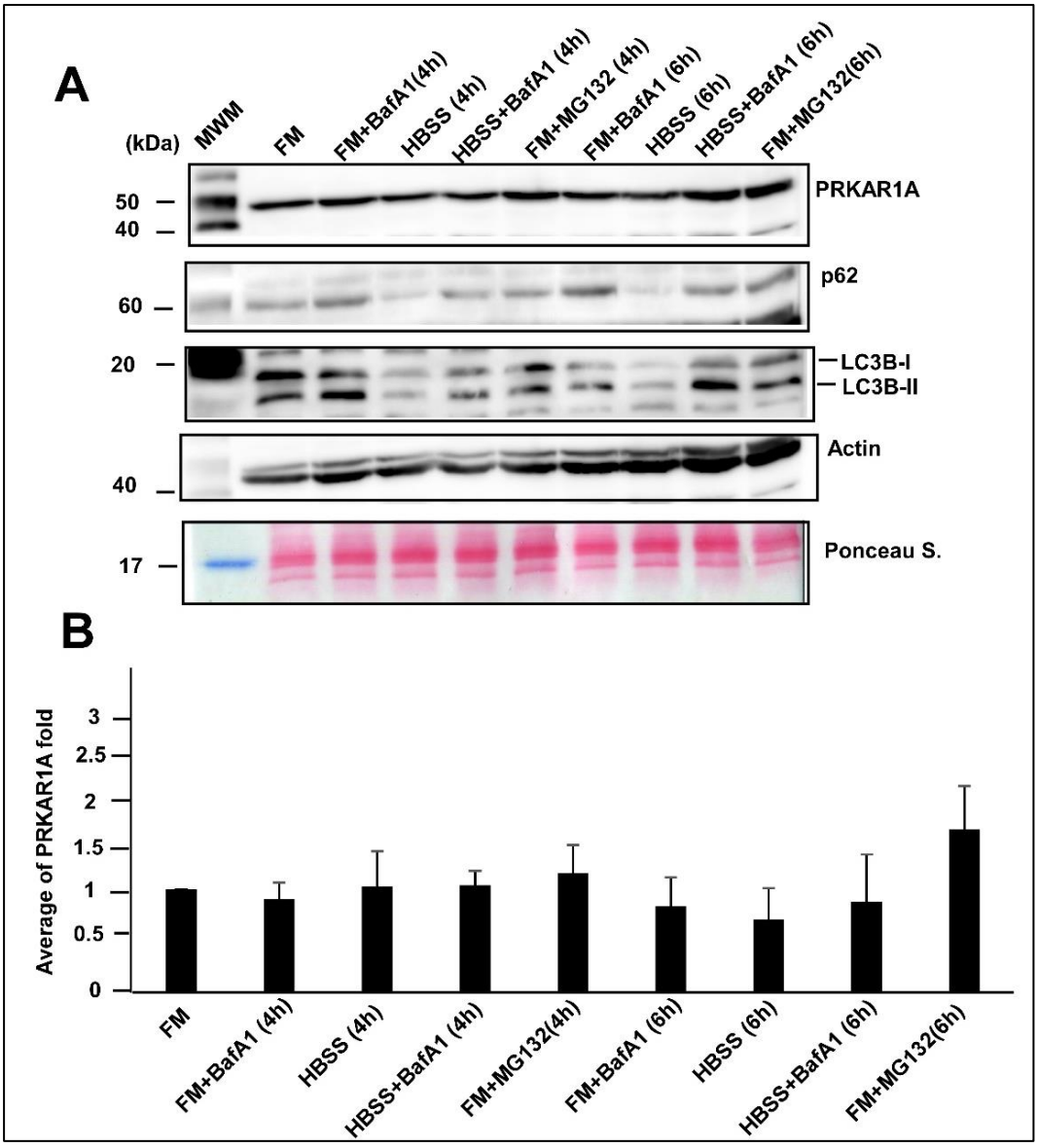

Figure 3.4.12: Endogenous PRKAR1A is mainly degraded by the proteasome. A HeLa cells were grown in FM, FM, FM +BafA1 (4h), HBSS (4h), HBSS+ BAFA1 (4h), FM+MG132 (4h), FM +BafA1 (6h), HBSS (6h), HBSS+ BAFA1 (6h), FM+MG132 (6h). After treatment the cells were lysed and equal amounts of the lysates (20µg) were loaded in each well. The blot was probed for PRKAR1A, LC3B and p62 antibodies. To normalize for protein loading, the membrane was also developed using a β-actin antibody. **B** Quantitation of bands representing PRKAR1A relative to the FM band for all the treatment conditions. Relative band intensities were quantified using Image J Software. The graph represents average of three independent experiments with mean and standard deviations.

3.5 PRKAR1A colocalizes with endogenous LC3B in a few cells upon starvation

Colocalization studies using various markers may provide better knowledge regarding the function of a protein. PRKAR1A is reported to associate with the autophagy marker protein LC3B [184]. To further investigate if PRKAR1A has a role in autophagy, confocal microscopy was applied on HeLa and U2OS cells. This approach was used to determine whether PRKAR1A colocalizes with the endogenous LC3B. The cells were transiently transfected with mCherry-EYFP-PRKAR1A expressing constructs. After 24 hours of transfection, the cells were treated with FM+ BafA1, HBSS, HBSS+BafA1 and FM+MG132 for 4 hours and stained for endogenous LC3B.

Under most conditions, PRKAR1A displays a diffuse localization pattern while LC3B is enriched in clear dots, both in HeLa and U2OS cells (Figure 3.5.1 and 3.5.2). Hence, colocalization was difficult to determine. However, upon starvation (HBSS 4 hours) PRKAR1A formed distinct puncta, and some of these puncta were colocalized with LC3B puncta. LC3B have been used to identify autophagosomes [196]. Hence this suggests that PRKAR1A may be transiently associated with autophagosomes upon starvation conditions.

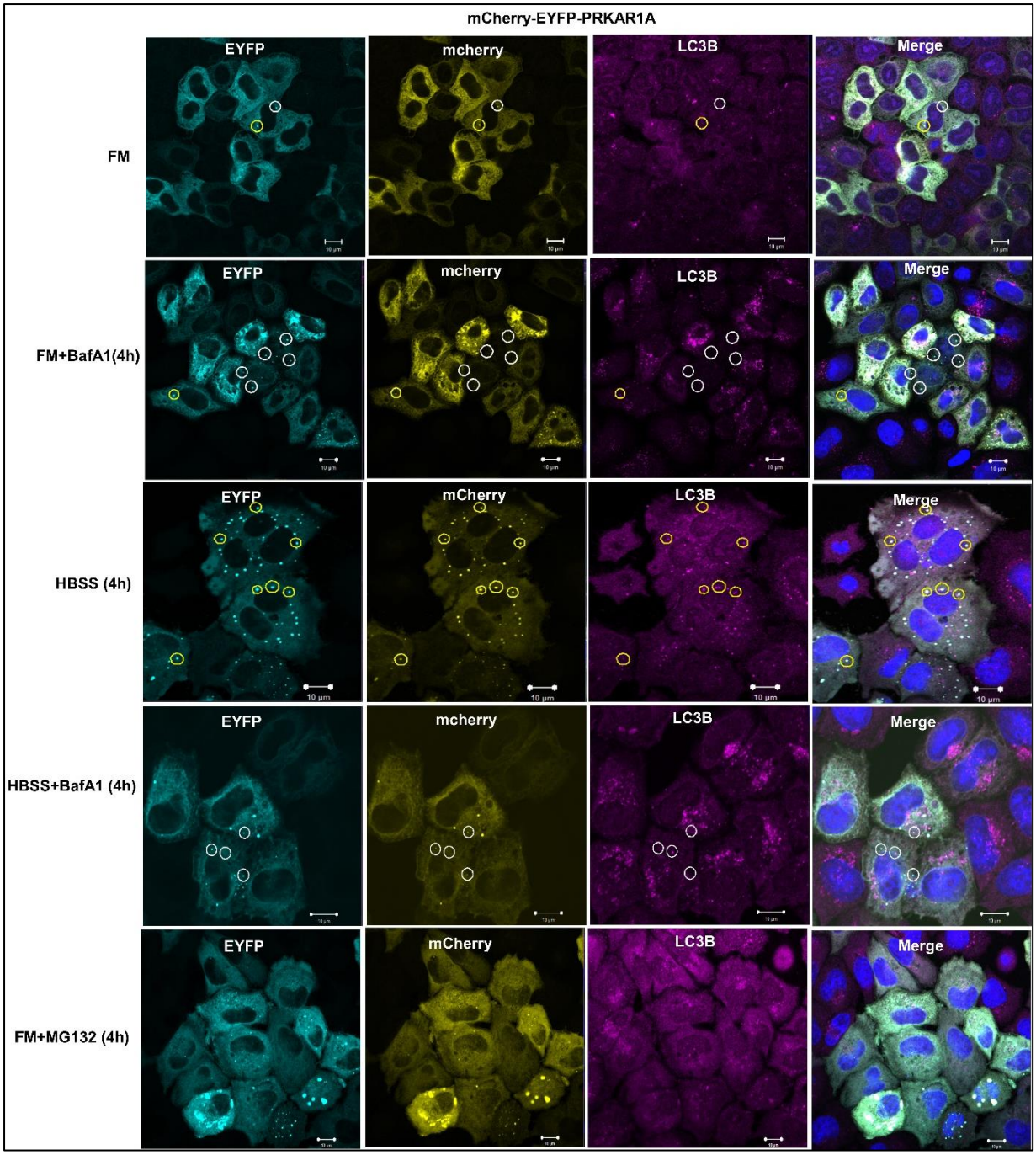

Figure 3.5.1: PRKAR1A is colocalized with endogenous LC3B upon starvation in HeLa cells. HeLa cells transiently transfected with mCherry-EYFP-PRKAR1A expression constructs were grown in FM, M+BafA1 (4h), HBSS (4h), HBSS+BafA1 (4h) and FM +MG132 (4h). After treatment the cells were fixed and endogenous LC3B was stained using an anti-LC3B antibody and secondary antibody AlexaFluor647. The nuclei were visualized by DAPI staining. White circles indicate no colocalization and yellow circles indicate PRKAR1A puncta colocalizing with LC3B. Scale bar 10 µm.

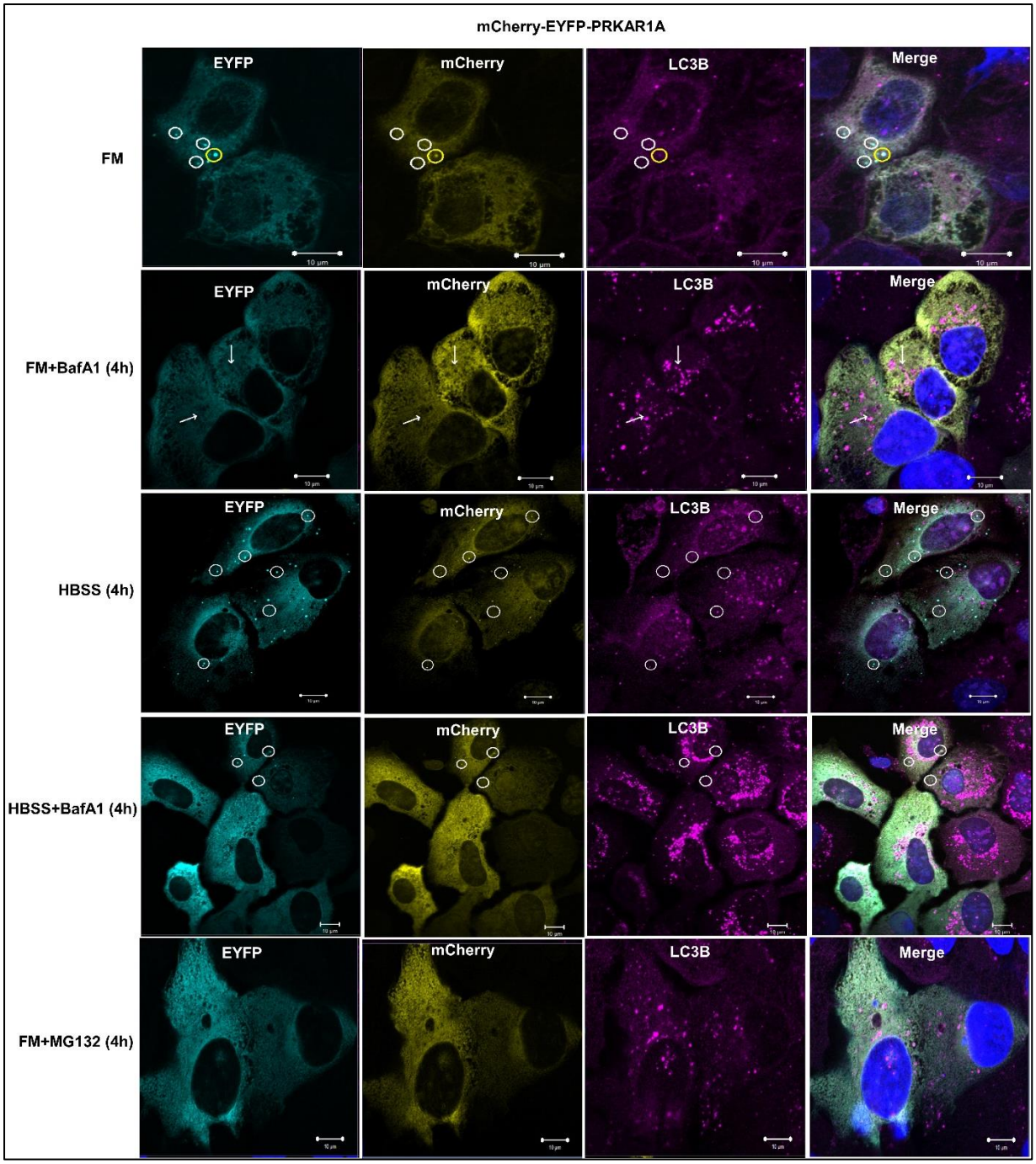

Figure 3.5.2: PRKAR1A colocalizes with LC3B upon starvation in U2OS cells. U2OS cells transiently transfected with mCherry-EYFP-PRKAR1A expression constructs were grown in FM, FM+BafA1 (4h), HBSS (4h), HBSS+BafA1 (4h) and FM +MG132 (4h). After treatment the cells were fixed and endogenous LC3B were stained using LC3B antibodies and secondary antibody AlexaFluor647. The nuclei were visualized with DAPI staining. White circles indicate no colocalization and yellow circles indicate PRKAR1A puncta colocalizing with LC3B. Arrows indicate typical LC3B puncta. Scale bar 10 µm.

3.6 PRKAR1A does not colocalize with endogenous p62

p62 is the most studied autophagy receptor and it is degraded by autophagy [192]. To study if PRKAR1A colocalizes with p62, HeLa cells were transiently transfected with mCherry-EYFP-PRKAR1A expression construct and grown in FM and HBSS (4h) conditions. The cells were fixed and stained with p62 antibody. Figure 3.6 shows that p62 forms distinct cytoplasmic puncta in FM and the number of puncta increases by HBSS treatment. However, no colocalization or enrichment of PRKAR1A was observed in the p62 puncta. This suggests PRKAR1A is not a p62 substrate.

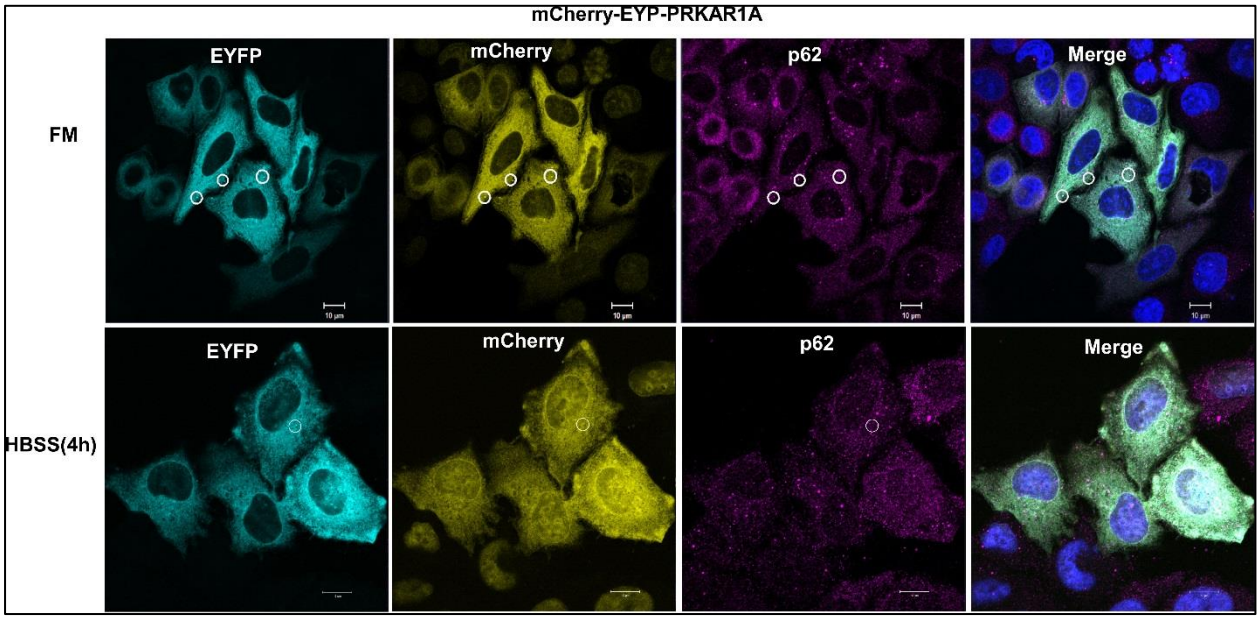

Figure 3.6: PRKAR1A is not colocalized with p62. HeLa cells transiently transfected with mCherry-EYFP-PRKAR1A expression constructs were grown in FM and HBSS (4h). After treatment the cells were fixed and stained with p62 and secondary antibody AlexaFluor647. There was no colocalization of the cytoplasmic PRKAR1A with p62 bodies. White circles indicate PRKAR1A not colocalizing with p62. The nuclei were visualized with DAPI staining. Scale bar 10 µm.

3.7 PRKAR1A does colocalize with over expressed LC3B and GABARAP in a few puncta

Since PRKAR1A did not show pronounced colocalization with endogenous LC3B, we tried similar experiment by overexpressing the autophagy marker proteins LC3B and GABARAP. HeLa cells were transiently co-transfected with EGFP-PRKAR1A and either mCherry-LC3B or mCherry-GABARAP. After 24 hours the cells were subjected to FM or starvation and fixed for confocal microscopy. EGFP-PRKAR1A formed bright puncta both in FM and under starved conditions. However, very few of these puncta colocalized with the LC3B puncta (Figure 3.7.1).

Similar result was obtained in cells with overexpressed GABARAP (Figure 3.7.2). This further suggests that PRKAR1A only transiently colocalizes with autophagosomes.

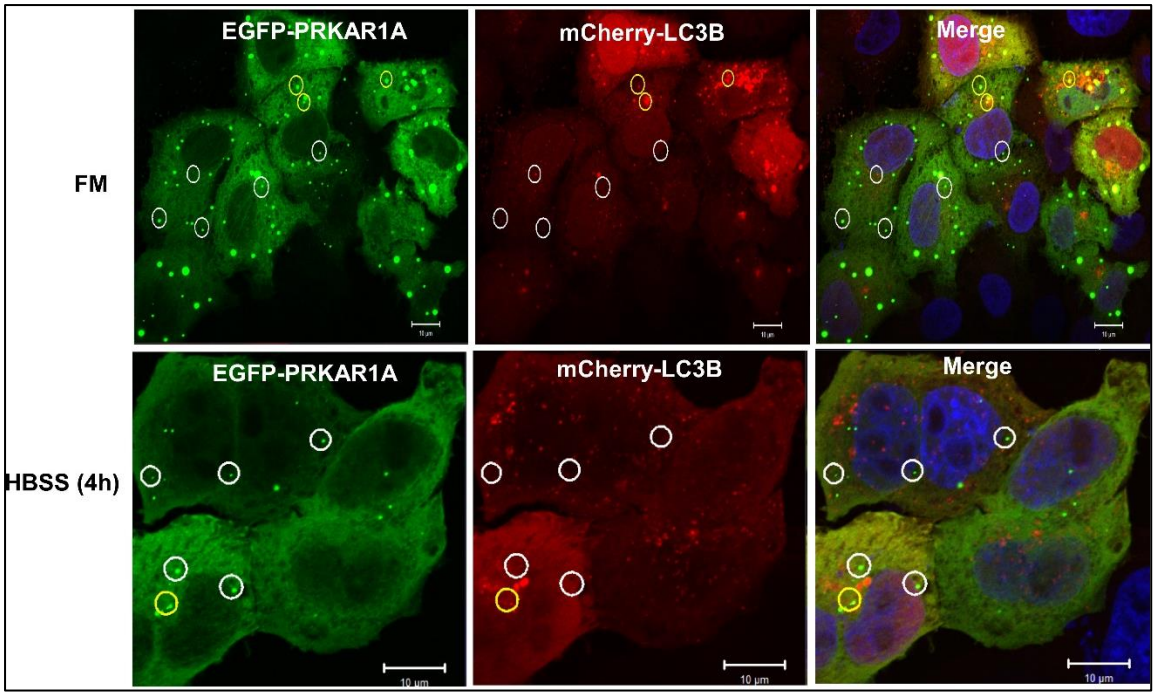

Figure 3.7.1: EGFP-PRKAR1A colocalizes in certain puncta with overexpressed LC3B in HeLa cells. HeLa cells transiently co-transfected with EGFP-PRKAR1A and mCherry-LC3B were grown in FM and HBSS (4h). After treatment the cells were fixed and subjected to imaging. The nuclei were visualized with DAPI staining. White circles indicate no colocalization and yellow circles indicate EGFP-PRKAR1A puncta colocalizing with mCherry-LC3B.
Scale bar 10 µm.

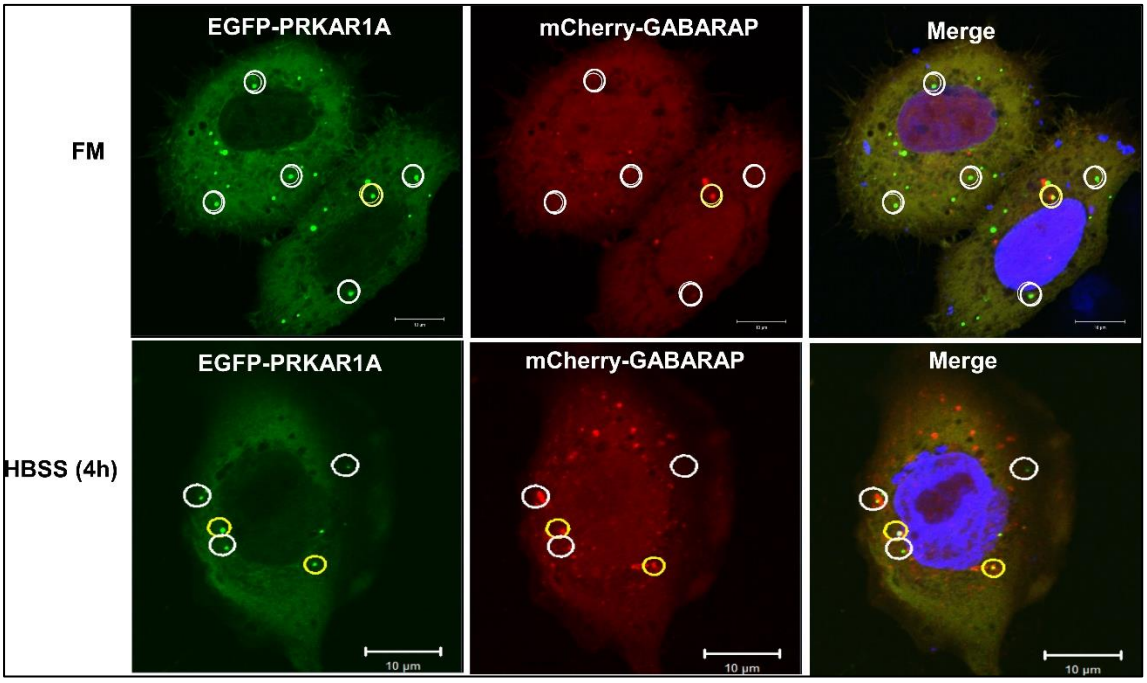

Figure 3.7.2: EGFP-PRKAR1A colocalizes with overexpressed GABARAP in few puncta in HeLa cells. HeLa cells transiently co-transfected with EGFP-PRKAR1A and mCherry-GABARAP were grown in FM and HBSS (4h). After treatment the cells were fixed and subjected to imaging. The nuclei were visualized with DAPI staining. White circles indicate no colocalization and yellow circles indicate EGFP-PRKAR1A puncta colocalizing with mCherry-GABARAP. White arrows in indicate typical GABARAP puncta upon starvation. Scale bar 10 µm.

3.8. PRKAR1A colocalization with GABARAP is induced by the catalytic subunit of PKA

Colocalization of PRKAR1A with the autophagy proteins tested so far has suggested only a very transient interaction. This finding led us to investigate if the catalytic subunit of PKA could affect the interactions. To address this, HeLa cells were co-transfected with the expression constructs for the catalytic subunit of PKA along with EGFP-PRKAR1A and mCherry-GABARAP or mCherry-LC3B and colocalization with the autophagy markers were studied by confocal microscopy. Interestingly, colocalization of overexpressed PRKAR1A with overexpressed GABARAP under both FM and starved conditions was clearly enhanced by the presence of the catalytic subunit of PKA (Figure 3.8.1). However, the catalytic subunit did not enhance the colocalization with LC3B (Figure 3.8.2).

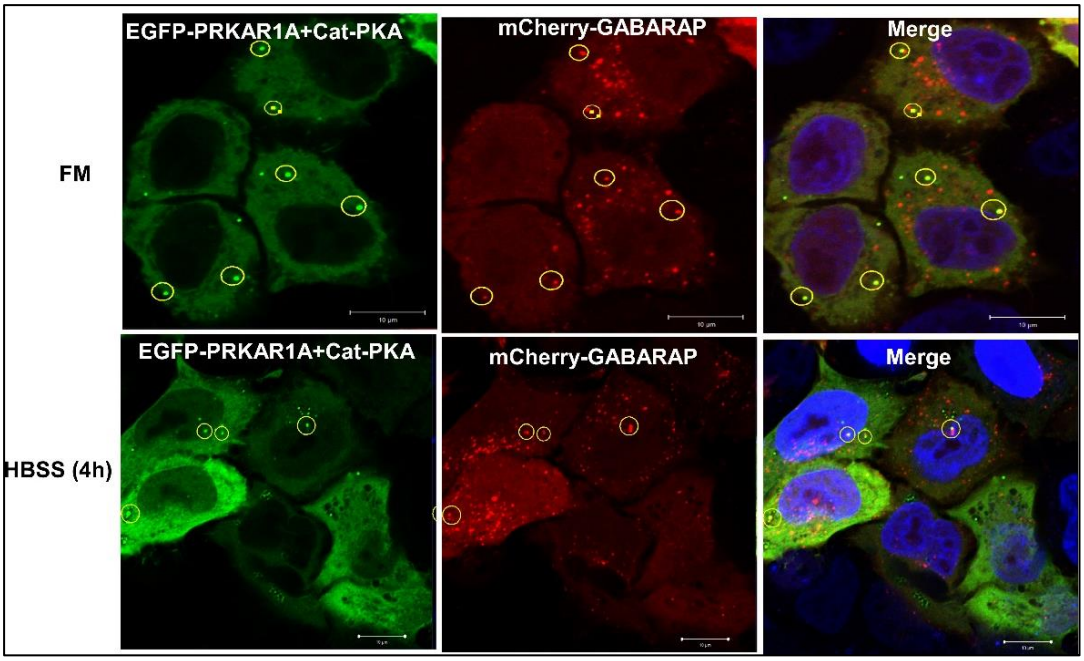

Figure 3.8.1: PRKAR1A colocalization with GABARAP is enhanced by catalytic PKA subunit. HeLa cells transiently co-transfected with expression constructs for EGFP-PRKAR1A, mCherry-GABARAP and catalytic subunit of PKA and grown in FM and HBSS (4h). After treatment, the cells were fixed and subjected to confocal microscopy. The nuclei were visualized by DAPI. Yellow circles indicate EGFP-PRKAR1A+Cat-PKA puncta colocalized with mCherry-GABARAP. Scale bar 10 µm.

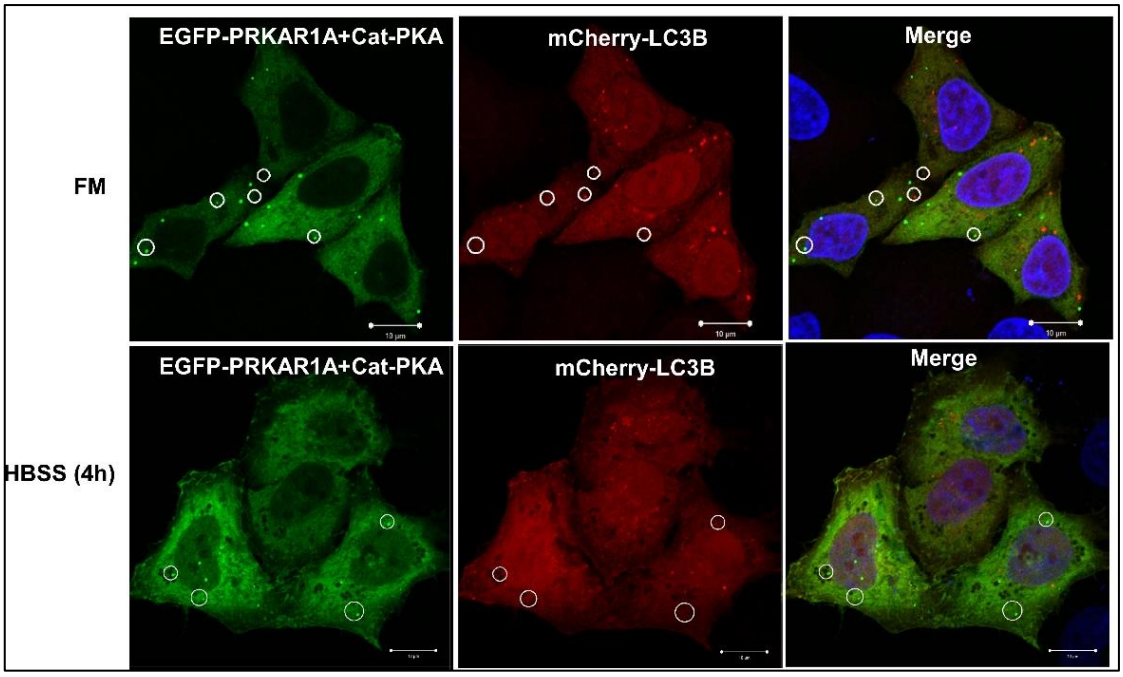

Figure 3.8.2: Co-expression of catalytic PKA does not enhance PRKAR1A colocalization with LC3B. HeLa cells transiently co-transfected with EGFP-PRKAR1A, mCherry-LC3B and catalytic subunit of PKA and grown in FM and HBSS (4h). After treatment, the cells were fixed and subjected to confocal microscopy. The nuclei were visualized by DAPI. White circles indicate EGFP-PRKAR1A puncta not colocalized with LC3B and vice versa. Scale bar 10 µm.

3.9 PRKAR1A inhibits LC3B puncta formation upon starvation

Studies have shown that PKA signaling have regulatory functions in various cellular pathways as well as in autophagy [129]. In an attempt to investigate if PRKAR1A alone or together with the catalytic subunit exhibit some regulatory functions on autophagy, HeLa cells were transiently co-transfected with EGFP-PRKAR1A with or without the catalytic PKA in two different sets of experiments. The cells were further stained with an antibody against LC3B and the number of LC3B puncta was used as a read out for the autophagy activity. The number of LC3B puncta were also counted in cells transfected with EGFP empty vector. Quantitation was done in a total of 50 cells per condition and the average number of LC3B puncta per cell was calculated. Interestingly, there was a significant reduction in the average number of LC3B puncta in the cells expressing EGFP-PRKAR1A compared to vector control (Figure 3.9.3). The inhibitory effect was strongest upon starvation, where the number of LC3B puncta was reduced compared to the FM in the EGFP-PRKAR1A overexpressing cells while the puncta increased as expected in the control cells (Figure 3.9.2). Co-expression of the catalytic subunit did not lead to an additional inhibition suggesting that this inhibitory effect on LC3B puncta formation is mediated by PRKAR1A alone.

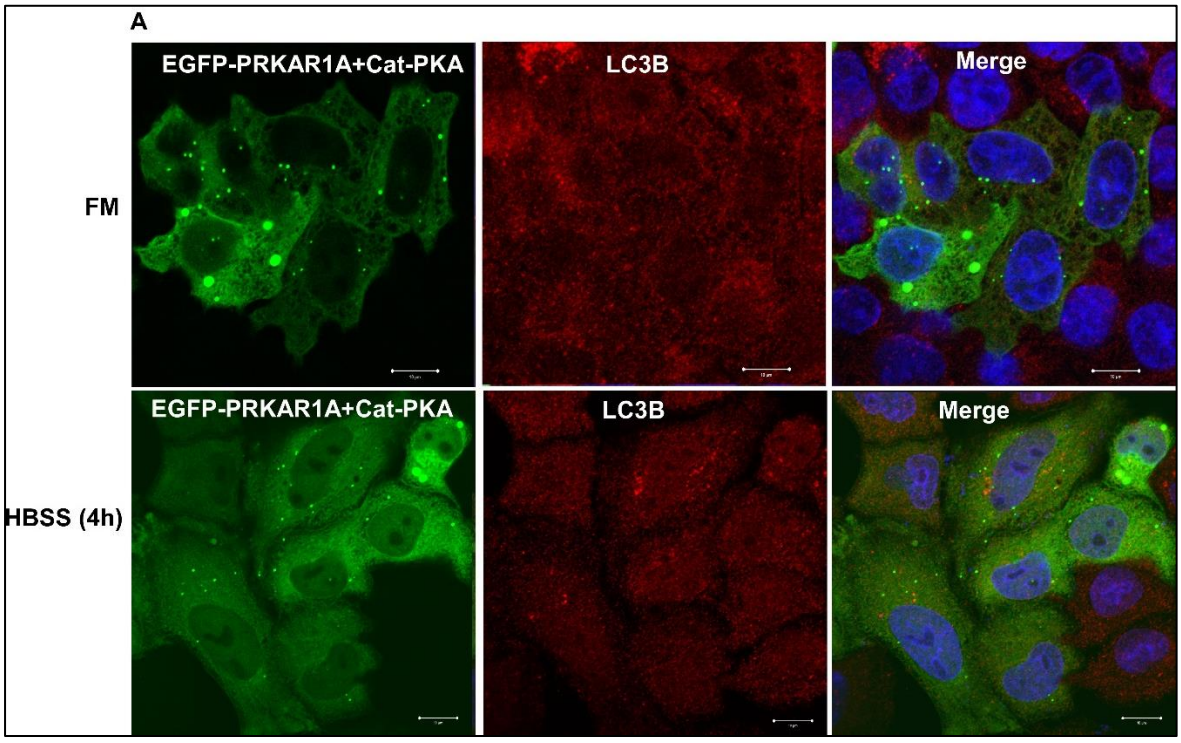

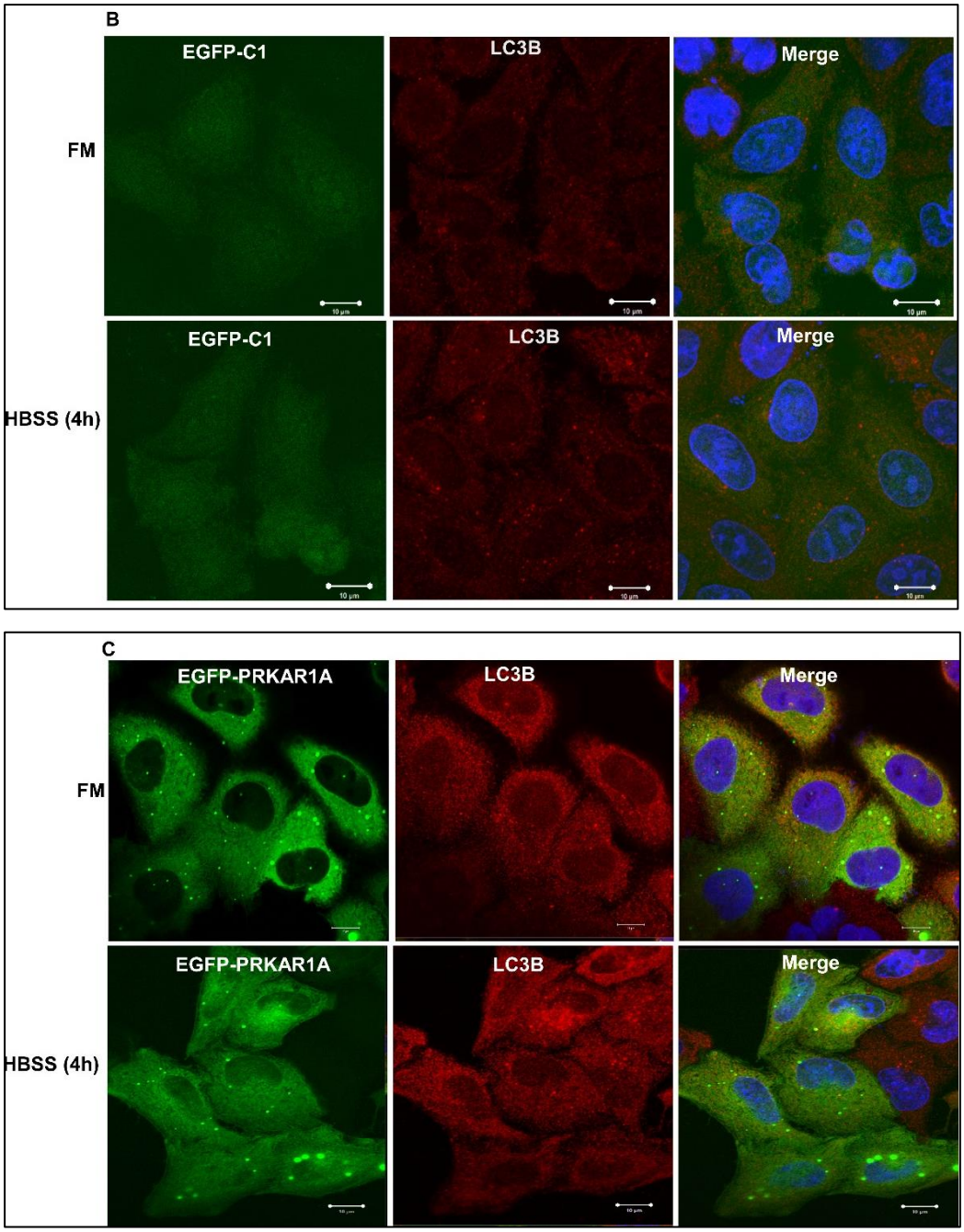

Figure 3.9.1: PRKAR1A inhibits LC3B puncta formation both in FM and upon starvation. HeLa cells transiently transfected with the expression constructs **A** EGFP-PRKAR1A co-expressed with the catalytic subunit of PKA, **B** EGFP-vector control and **C** EGFP-PRKAR1A. All the cells were grown in both FM and HBSS. After treatment the cells were fixed in methanol and stained for endogenous LC3B antibody and secondary antibody Alexa555 and subjected to confocal microscopy. The number of LC3B puncta in FM and HBSS in **A** and **C** were compared with the vector control in B. Scale bar 10 µm.

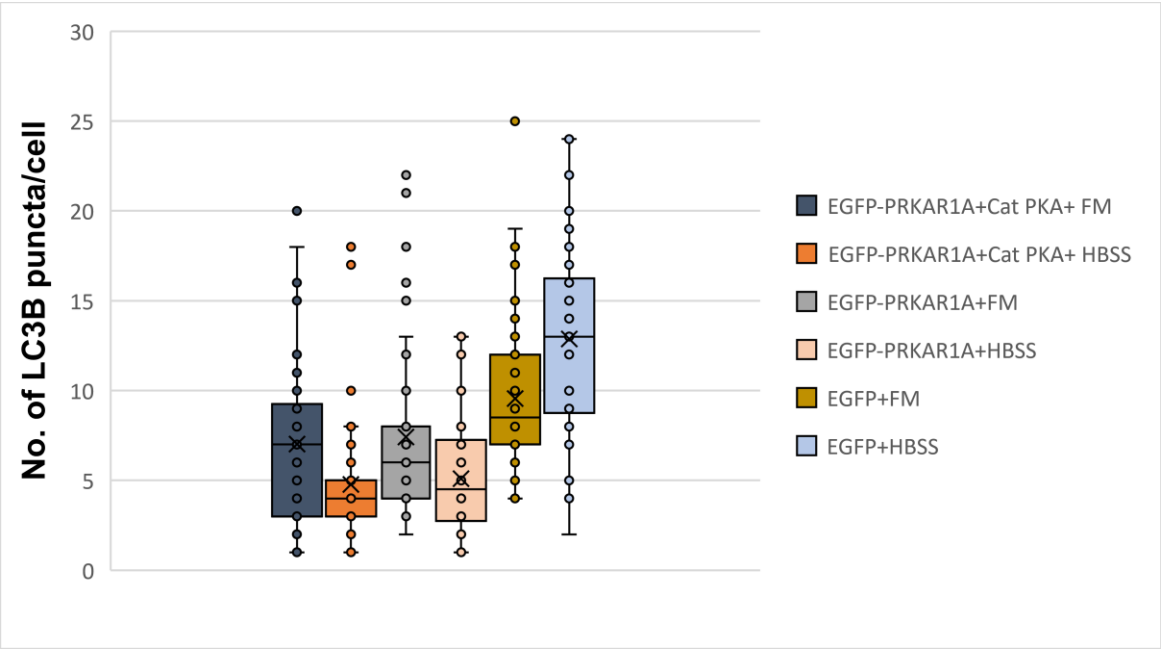

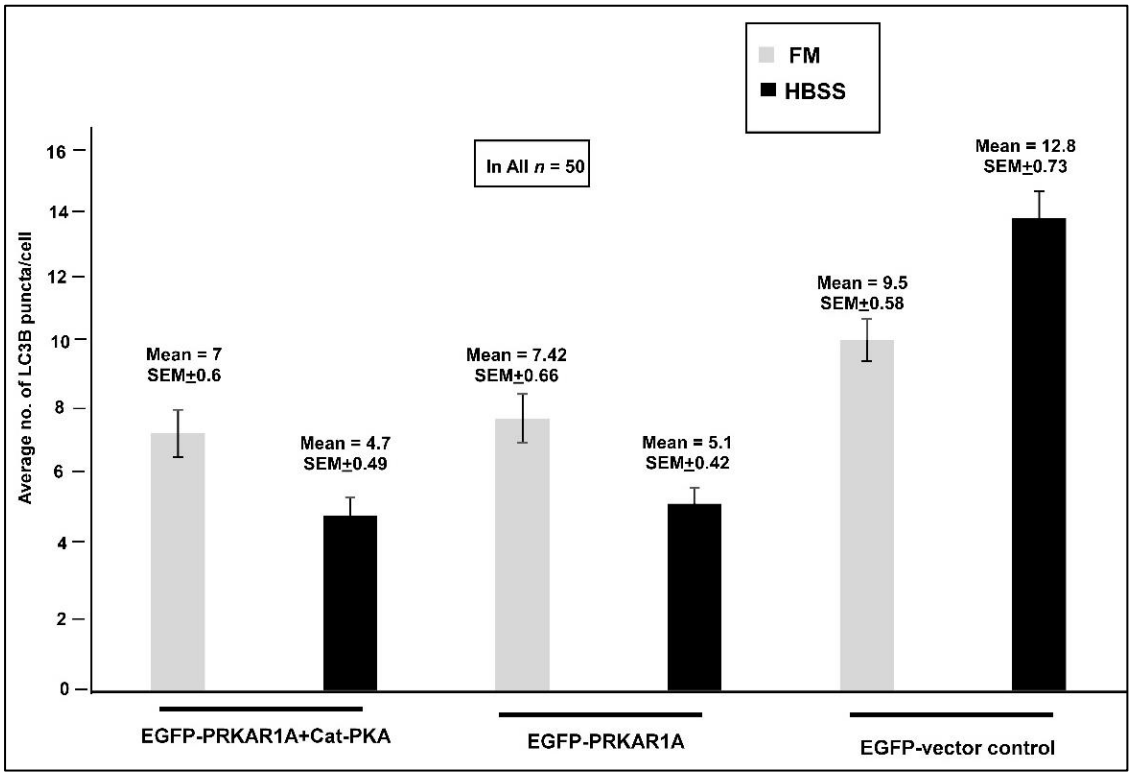

3.9.2: No. of LC3B puncta is reduced when PRKAR1A is overexpressed. Quantitation of LC3B puncta in HeLa cells transiently transfected with expression constructs for EGFP-PRKAR1A alone or together with the catalytic subunit of PKA under FM and starved conditions (HBSS-4h). Fifty transfected cells were counted manually for each experiment. The number of LC3B puncta per cell is plotted in Y axis. The puncta in the upper chart indicate the range of LC3B puncta in each cell and the lines in each bar indicate the average number of LC3B puncta per cell. The error bars on the upper chart indicate mean and standard deviation. The error bars on the lower graph indicate standard error of mean in total of 50 cells.

3.10 PRKAR1A does not colocalize with the late endosomal markers upon starvation

To further analyze whether PRKAR1A may co-localize with the late endosome/lysosomal compartments, we took advantage of the known localization of Rab7 and Lamp1 at the late endosomal/lysosomal compartments. Previous studies have shown that PRKAR1A colocalize to Rab7 and are located to subcellular structures like multivesicular bodies (MVBs) [161, 163]. We studied the colocalization in HeLa cells in FM and starved conditions both in presence or absence of overexpressed catalytic subunit of PKA. HeLa cells transiently transfected with Cerulean-PRKAR1A were co transfected with and without the catalytic subunit. The cells were subjected to immunofluorescence after staining with Lamp1 and Rab7 antibodies. Since PRKAR1A is mainly diffuse in the cytosol, it was difficult to observe any clear colocalization pattern displayed by Cerulean -PRKAR1A in absence of the catalytic PKA subunit (Figure 3.10A). However, with co-expression of the catalytic PKA subunit, PRKAR1A formed dots. However, these did not colocalize with the lysosomal compartments (Figure 3.10B). The Rab7 antibody used in this study was very weak and detected only few endogenous Rab7 positive cells. We also observed PRKAR1A structures in some cells that looked like vesicle clusters/aggregates. These clusters were only seen when PRKAR1A was co-expressed with the catalytic PKA subunit and can be an artefact due to high overexpression of the catalytic subunit. However, this must be analyzed more in the future studies with specific markers and a good antibody (Figure 3.10C).

To conclude, these results did not come to the same conclusion as previous published data showing that PRKAR1A partly colocalizes with the late endosomal/lysosomal structures in the cells.

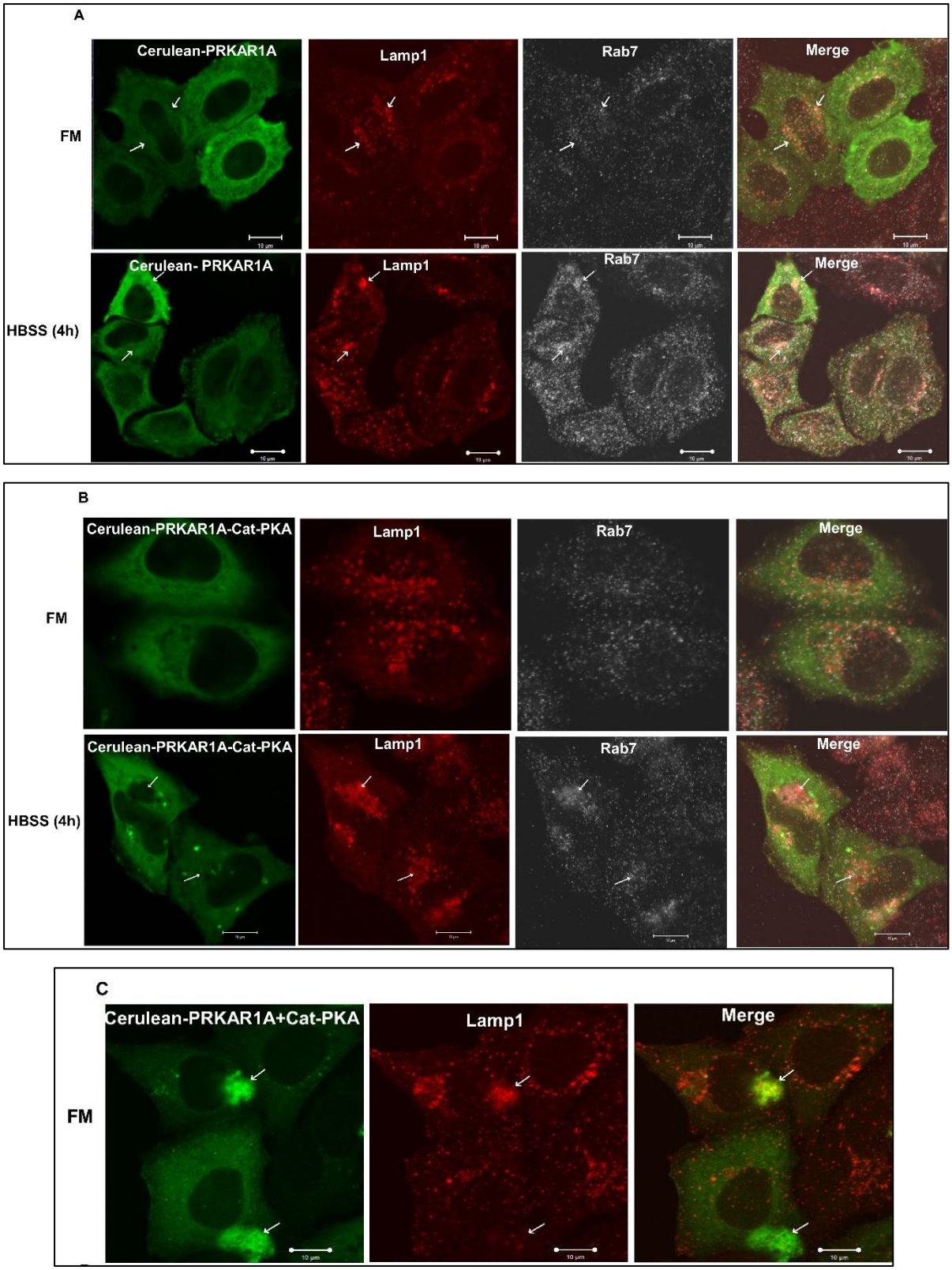

Figure 3.10: PRKAR1a does not colocalize with Lamp1 and Rab7 positive structures. HeLa cells transiently transfected with Cerulean-PRKAR1A expression constructs co-expressed with (B) and without (A) the catalytic PKA were grown in FM and HBSS (4h). After treatment the cells were fixed with methanol and stained with Lamp1 and Rab7 antibodies, secondary antibodies Alexa647 and Alexa555 respectively. C Arrows in **A** and **B** indicate Lamp1 staining that colocalize with Rab7 and arrows in **C** indicate vesicles like clusters. Scale bar 10 µm.

4. Discussion

Although PKA has been broadly studied for years, the independent roles of the regulatory subunits have not been well characterized; the focus has been mainly into its catalytic subunits. The roles of PRKAR1A has only been a subject for extensive studies in phenotypes like the Carney Complex and PPNAD. The first study of PRKAR1A in autophagy showed colocalization with the autophagy marker LC3 and the late endosomal and lysosomal marker Rab7 and a reduced number of autophagosomes in PRKAR1A knock out MEF cells [161, 162]. However, a more recent study disproved many findings from the earlier one. Here they found that PRKAR1A is localized to MVBs via AKAP11 when the regulatory subunit is free from the catalytic subunit [163]. These contradictory finding in addition to very limited studies of PRKAR1A in relation to autophagy encouraged us to investigate if PRKAR1A is associated with autophagy proteins and if it has a regulatory role on autophagy activity. In this study we show strong binding of PRKAR1A to the ATG8 family proteins both *in vitro* and in cell extracts. PRKAR1A itself seems not to be an autophagy substrate, and it seems to be very transiently associated with autophagosomes. However, when it is co-expressed with its catalytic subunit, PRKAR1A clearly colocalizes with GABARAP in cells. Interestingly, over-expression of PRKAR1A significantly reduces the formation of autophagosomes, and this inhibition is independent of the catalytic subunit.

4.1 PRKAR1A is mainly cytosolic but forms strong puncta when expressed as EGFP fusion

The aim was to investigate the localization of PRKAR1A by utilizing fluorescence confocal microscopy. We expressed PRKAR1A with the double tag mCherry-EFYP and two different single tags; Cerulean and EGFP in HeLa and U2OS cells. The protein exhibited a diffuse cytosolic localization in full medium. A few cells had some additional spot like structures (puncta) scattered in the cytosol upon starvation in both cell lines when PRKAR1A was expressed with the mCherry-EFYP and Cerulean tags. However, when expressed with the EGFP tag, PRKAR1A formed multiple strong puncta in both FM and starved conditions. These puncta were quite big and looked like round aggregates. Staining with the PRKAR1A antibody did not clearly identify these puncta as PRKAR1A aggregates due to less specificity of the antibody in immunofluorescence. As previously shown by Day ME and colleagues [163], both endogenous and overexpressed PRKAR1A forms puncta only when it is free from the PKA holoenzyme. They found that when PRKAR1A is dissociated from the catalytic subunit upon

cAMP binding, it is recruited to MVBs via AKAP11 [163]. In the paper Mavrakis M *et al.* used EGFP, Hemagglutinin (HA) and Venus tagged PRKAR1A. The HA and EGFP tagged constructs showed similar punctate structures as our EGFP-PRKAR1A construct, while images in the paper display quite less number of puncta for the Venus tagged construct [161]. This may indicate that PRKAR1A exhibits varying ability to form puncta dependent on which tag it is fused to. This can be due to conformational differences of the protein induced by the tag, which may influence its binding to the catalytic subunit. However, in our study, we did not manage to test if these puncta formation was a result of cAMP stimulation. We also speculate EGFP may impose a stronger ability for aggregation because EGFP has a tendency to form dimers. This pending question urgently needs to be addressed in future studies.

4.2 PRKAR1A interacts with ATG8 family proteins and this is not mediated via a canonical LIR-LDS binding

This is the first study that identify strong interaction of PRKAR1A with the ATG8 family proteins both *in vitro* and in cells. GST pull down assays showed that PRKAR1A interacts with all the ATG8 family proteins, preferably with GABARAPL2 followed by GABARAP and LC3A. Among the six ATG8 tested, LC3B was found to bind very weakly to PRKAR1A. Binding to ATG8 family proteins was also shown via Flag based immunoprecipitation. This was the first hint towards PRKAR1A involvement in autophagy. GABARAP family proteins have a significant role in maturation of autophagosomes and LC3 proteins are essential for elongation of the phagophore membrane. The strong binding to GABARAPL2 suggests that PRKAR1A might have a role in the later stage of the autophagy process; the autophagosome maturation [197, 198].

To answer the question if PRKAR1A interacts with the ATG8 family proteins via a LIR motif, we performed peptide array to find putative LIR motifs in PRKAR1A. Many proteins like p62, FKBP8, Syntaxin 17 have been identified to have functional LIR motifs essential for LDS dependent binding with the ATG8 homologues [165, 199-201]. We identified five putative LIRs in PRKAR1A which could mediate the interaction with ATG8 homologues. For this, we tested binding of PRKAR1A to the LDS mutants of LC3B and GABARAP. Since mutations in LDS or LIR motifs prevent binding of LIR containing cargo proteins with ATG8s, LDS mutants (LC3B F52A) and (GABARAP Y49A)) have been used to test LIR mediated binding to ATG8 family proteins. Apart from LDS mutants, deletion of the C-terminal (LC3B 1-28), the N-terminal (LC3B 30-125) and mutation of two arginine residues (R10A and R11A)

in the N- terminal of LC3B have also been used in binding studies [186, 202]. Both the C-terminal and the N-terminal domains of LC3B are required for the binding of proteins like p62, NBR1 and FYCO1 [144, 145, 155]. In this study, we found that mutations in the LIR binding pockets of LC3B and GABARAP did not affect the binding of PRKAR1A to a significant degree. Furthermore, we found that binding of PRKAR1A to LC3B might require both N and C-terminal domains of LC3B and the N-terminal arginine residues R10A and R11A. Even though the binding was reduced with the deletions and mutated arginine residues, the binding was not completely abolished. Hence, we conclude that the PRKAR1A interaction with ATG8 family proteins is not mediated via a canonical LIR-LDS binding. Further mapping and structural studies are needed for better understanding about the mechanisms involved in PRKAR1A interaction with ATG8 family proteins.

4.3 PRKAR1A is mainly degraded by the proteasome

In eukaryotic cells, proteins are degraded by two major pathways. Long lived proteins are degraded by autophagy and short-lived proteins by the proteasome [203]. This study measured the degradation pattern of PRKAR1A via confocal microscopy and Western blot. To explore the relationship between autophagy/proteasome and PRKAR1A degradation, cells were treated with lysosomal inhibitor BafA1 and proteasomal inhibitor MG132. BafA1 is an inhibitor of vacuolar ATPase that blocks the autophagosome -lysosome fusion thereby inhibiting lysosomal degradation [188]. MG132 blocks the proteolytic activity of the 26S proteasome complex and acts as a proteasomal inhibitor [189]. Treatment with BafA1 for 4h did not result in any accumulation of PRKAR1A puncta/aggregates or band intensity as measured by confocal microscopy and Western blot, respectively. Pronounced accumulation of endogenous PRKAR1A was observed in the Western blot after 6 hours of MG132 treatment in HeLa cells. Consistent with the Western blot results in HeLa cells, the confocal microscopy revealed no acidified mCherry-EYFP-PRKAR1A proteins under FM and starved conditions. This strongly suggest that PRKAR1A is not degraded by autophagy. Western blot with antibodies against LC3B and p62 showed a strong induction of the autophagy under starvation and accumulation of LC3B and p62 upon treatment with lysosomal and proteasomal inhibitors. The lipidated form of LC3B have been used as an important marker of autophagy [193]. From our data, we conclude PRKAR1A is mainly degraded by the proteasomal pathway.

4.4 PRKAR1A is not associated with autophagosomes

Amino acid starvation leads to induction of autophagy resulting in an increase of the number of autophagosomes [190]. PRKAR1A was fused to mCherry-EFYP vector that uses as an advantage of pH sensitive EYFP which is quenched at low pH of the lysosome. After maturation of the autophagosome mCherry-EFYP tagged proteins stain as red only if they are present in acidic compartments. However, overexpression of protein in cells also produces a background level of red fluorescenct dots [100, 191]. In this study, amino acid starvation did not lead to a clear increase of the number of PRKAR1A puncta in cells. The initially diffusely appearing cytosolic pool of mCherry-EYFP-PRKAR1A became localized to very few punctate structures that mainly displayed both red and green color. These punctate structures were quite clear and pronounced in U2OS cells as compared to HeLa cells because of their big and flat size. However, quantitation of 100 cells 24 and 48 hours after transfection showed that mCherry-EYFP-PRKAR1A formed a similar number of acidified puncta as the empty vector control under starvation. Although, the number of red only puncta were increased in the cells 48 hours after transfection compared to 24 hours post transfection, the increase was also observed in the negative vector control. The positive control p62 showed red only puncta even in full medium and red only puncta been increased upon starvation. p62 is the best studied autophagy receptor and has shown to be degraded in autolysosomes [204, 205]. Again, to mention PRKAR1A was mainly diffuse and seemed not to change upon various starvation and treatment conditions. These findings clearly indicate that PRKAR1A is not degraded in the acidic compartments and hence is not an autophagy substrate. This was also supported by the results from the Western blot.

4.5 PRKAR1A does not colocalize with the autophagy markers

We were interested to see if PRKAR1A colocalized with the autophagy marker proteins LC3B, GABARAP and p62. LC3B is used as a marker of autophagosomes as lipidated LC3B is associated with the autophagosomal membrane. GABARAP is important for autophagosome maturation [206]. p62 is known to be associated with autophagosomes and is degraded by autophagy [205]. To examine this, we performed localization studies by applying fluorescence confocal microcopy. First, we considered the colocalization with endogenous LC3B in HeLa and U2OS cells. Unfortunately, colocalization was difficult to determine because PRKAR1A mainly displayed a diffuse localization pattern in HeLa and U2OS cells. However, upon starvation PRKAR1A formed some puncta, and some of these colocalized with LC3B puncta. When we observed more than 50 cells under similar conditions, very few cells (approximately

4-5) showed a few puncta that colocalized with LC3B. Similar experiment with p62 showed no colocalization with endogenous p62. To conclude, these results confirm previous published data showing PRKAR1A is not colocalized with autophagosomes [163].

4.5 PRKAR1A colocalization with GABARAP is induced by the catalytic PKA subunit

The strong interaction with the GABARAP proteins both *in vitro* and in cells triggered us to investigate if the catalytic PKA subunit could affect the interaction between PRKAR1A and the ATG8 proteins. For this purpose, we co-expressed the catalytic subunit together with PRKAR1A and GABARAP/LC3B. We observed a significant colocalization of PRKAR1A with GABARAP whereas no colocalization was seen with LC3B. Colocalization with GABARAP suggests that PRKAR1A could have a role in regulation of autophagosome formation and/or maturation with the help of the catalytic subunit of PKA.

4.6. PRKAR1A impairs autophagosome formation

Cherra *et al.* 2010 have shown that a PKA phosphorylation site (Serine 12) in LC3B is involved in regulation of autophagy [129]. PKA has been shown to regulate autophagy in yeast [131, 207]. With the hypothesis that PKA regulates autophagy, we investigated if PRKAR1A overexpression would affect autophagosome formation. Since lipidated LC3B is associated with the autophagosome membrane, it can be used as a biomarker for autophagosomes [196, 208]. In this study, we overexpressed EGFP-PRKAR1A with and without the catalytic PKA subunit and stained for endogenous LC3B. The number of LC3B puncta in each cell was counted in 50 transfected cells and compared with the empty vector control upon FM and starved conditions. Interestingly, the average number of LC3B puncta per cell was significantly reduced under starvation in cells expressing EGFP-PRKAR1A with and without the catalytic subunit compared to the normal condition. The average number of LC3B puncta in the negative vector control were increased under starvation as expected. This suggests that PRKAR1A has an independent role in regulation of autophagosome formation, since the number of LC3B puncta was similar in cells where the catalytic subunit of PKA was co-expressed. This could suggest that PRKAR1A has a regulatory function in autophagy. This will be an interesting question to address in further studies.

4.5 PRKAR1A is not localized to late endosomes and lysosomes

To investigate if PRKAR1A may be associated with late stages of the autophagy process, we took advantage of staining with the late endosomal and lysosomal markers Rab7 and Lamp1. Mavrakis *et al.* 2006 showed that PRKAR1A localized to Rab7 and Rab9 positive endosomes. Rab7 is a small GTPase involved in the transport of autophagosomes and endosomes for lysosomal degradation [101]. Lamp proteins are involved in the late endosomal lysosomal fusion to autophagosomes [99, 115]. Rab7 and Lamp1 are colocalized in the endosomal-lysosomal compartments [209]. In this study, Cerulean-PRKAR1A was co-transfected with and without the catalytic PKA subunit and the cells stained with Rab7 and Lamp1 antibodies. Because of the highly diffuse localization of PRKAR1A it was difficult to observe colocalization with the marker proteins. However, Rab7 and Lamp1 colocalized with each other. Day *et al.* 2011 showed that PRKAR1A localization to MVBs is mediated by AKAP11 by using Correlative light electron microscopy (CLEM). However, we did not perform experiments using CLEM in this study. The Rab7 antibody used in our study gave very weak staining pattern. Hence, further studies using a recently published Rab7 antibody [210] could provide a clear result. However, MVBs can be identified only at the ultrastructural level , which was not within the scope of this study [211]. MVBs can create endosomal compartments where the autophagosome does not fuse to the lysosome. This compartment can act as a storage house of proteins without degradation of the cargo [163]. This might be the explanation why PRKAR1A is associated with MVBs but not being degraded by autophagy.

5. Conclusion and future perspectives

The focus of this study was to identify the functional role of PRKAR1A in mechanistic steps of autophagy. We found that PRKAR1A interacts with ATG8 family proteins in a LIR independent manner. However, PRKAR1A seems not to be degraded by autophagy in full medium or upon cellular stresses. Interestingly, PRKAR1A over-expression leads to a significant decrease of autophagosome formation during starvation. Furthermore, co-overexpression of PRKAR1A with the catalytic PKA subunit induces colocalization of PRKAR1A with GABARAP. This suggests a role for PRKAR1A during autophagosome maturation. The function of the strong binding of PRKAR1A to GABARAPL2 would be an important topic in future studies.

In this study, transient over-expression of PRKAR1A was used for most cell studies. Transient over-expression may result in high amounts of the protein overwhelming the regulatory mechanisms in the cell. For further studies of the roles of PRKAR1A in autophagy, it will be necessary to established knock-out cell lines and stable cell lines expressing near to endogenous levels of PRKAR1A. This will probably give a clear basis for understanding its role in autophagy.

6. References

1. Wang, Z. and P.A. Cole, *Catalytic mechanisms and regulation of protein kinases.* Methods Enzymol, 2014. **548**: p. 1-21.
2. Manning, G., et al., *The protein kinase complement of the human genome.* Science, 2002. **298**(5600): p. 1912-34.
3. Fabbro, D., S.W. Cowan-Jacob, and H. Moebitz, *Ten things you should know about protein kinases: IUPHAR Review 14.* Br J Pharmacol, 2015. **172**(11): p. 2675-700.
4. Formosa, R. and J. Vassallo, *cAMP signalling in the normal and tumorigenic pituitary gland.* Mol Cell Endocrinol, 2014. **392**(1-2): p. 37-50.
5. Shibasaki, T., et al., *Cooperation between cAMP signalling and sulfonylurea in insulin secretion.* Diabetes Obes Metab, 2014. **16 Suppl 1**: p. 118-25.
6. Vilardaga, J.P., F.G. Jean-Alphonse, and T.J. Gardella, *Endosomal generation of cAMP in GPCR signaling.* Nat Chem Biol, 2014. **10**(9): p. 700-6.
7. Roskoski, R., Jr., *A historical overview of protein kinases and their targeted small molecule inhibitors.* Pharmacol Res, 2015. **100**: p. 1-23.
8. Almeida, M.Q. and C.A. Stratakis, *How does cAMP/protein kinase A signaling lead to tumors in the adrenal cortex and other tissues?* Mol Cell Endocrinol, 2011. **336**(1-2): p. 162-8.
9. Zhang, P., et al., *Structure and allostery of the PKA RIIbeta tetrameric holoenzyme.* Science, 2012. **335**(6069): p. 712-6.
10. Espiard, S., B. Ragazzon, and J. Bertherat, *Protein kinase A alterations in adrenocortical tumors.* Horm Metab Res, 2014. **46**(12): p. 869-75.
11. Wilkes, D., K. Charitakis, and C.T. Basson, *Inherited disposition to cardiac myxoma development.* Nat Rev Cancer, 2006. **6**(2): p. 157-65.
12. Correa, R., P. Salpea, and C.A. Stratakis, *Carney complex: an update.* Eur J Endocrinol, 2015. **173**(4): p. M85-97.
13. Murray, A.J., *Pharmacological PKA inhibition: all may not be what it seems.* Sci Signal, 2008. **1**(22): p. re4.
14. Das, A., et al., *Protein Kinase A Catalytic Subunit Primed for Action: Time-Lapse Crystallography of Michaelis Complex Formation.* Structure, 2015. **23**(12): p. 2331-2340.
15. Rababa'h, A., et al., *Compartmentalization role of A-kinase anchoring proteins (AKAPs) in mediating protein kinase A (PKA) signaling and cardiomyocyte hypertrophy.* Int J Mol Sci, 2014. **16**(1): p. 218-29.
16. Taylor, S.S., et al., *Assembly of allosteric macromolecular switches: lessons from PKA.* Nat Rev Mol Cell Biol, 2012. **13**(10): p. 646-58.
17. Bossis, I. and C.A. Stratakis, *Minireview: PRKAR1A: Normal and Abnormal Functions.* Endocrinology, 2004. **145**(12): p. 5452-5458.
18. Di Benedetto, G., et al., *Protein kinase A type I and type II define distinct intracellular signaling compartments.* Circ Res, 2008. **103**(8): p. 836-44.
19. Veugelers, M., et al., *Comparative PRKAR1A genotype-phenotype analyses in humans with Carney complex and prkar1a haploinsufficient mice.* Proc Natl Acad Sci U S A, 2004. **101**(39): p. 14222-7.
20. Berthon, A.S., E. Szarek, and C.A. Stratakis, *PRKACA: the catalytic subunit of protein kinase A and adrenocortical tumors.* Front Cell Dev Biol, 2015. **3**: p. 26.
21. Espiard, S. and J. Bertherat, *Carney complex.* Front Horm Res, 2013. **41**: p. 50-62.
22. Carney, J.A., et al., *The complex of myxomas, spotty pigmentation, and endocrine overactivity.* Medicine (Baltimore), 1985. **64**(4): p. 270-83.
23. Stratakis, C.A., L.S. Kirschner, and J.A. Carney, *Clinical and molecular features of the Carney complex: diagnostic criteria and recommendations for patient evaluation.* J Clin Endocrinol Metab, 2001. **86**(9): p. 4041-6.

24. Kirschner, L.S., et al., *Genetic heterogeneity and spectrum of mutations of the PRKAR1A gene in patients with the carney complex.* Hum Mol Genet, 2000. **9**(20): p. 3037-46.
25. Kirschner, L.S., et al., *Mutations of the gene encoding the protein kinase A type I-α regulatory subunit in patients with the Carney complex.* Nature Genetics, 2000. **26**: p. 89.
26. Yu, S., et al., *The N-terminal capping propensities of the D-helix modulate the allosteric activation of the Escherichia coli cAMP receptor protein.* J Biol Chem, 2012. **287**(47): p. 39402-11.
27. Nadella, K.S. and L.S. Kirschner, *Disruption of protein kinase a regulation causes immortalization and dysregulation of D-type cyclins.* Cancer Res, 2005. **65**(22): p. 10307-15.
28. Kirschner, L.S., *Use of mouse models to understand the molecular basis of tissue-specific tumorigenesis in the Carney complex.* J Intern Med, 2009. **266**(1): p. 60-8.
29. Kirschner, L.S., et al., *A mouse model for the Carney complex tumor syndrome develops neoplasia in cyclic AMP-responsive tissues.* Cancer Res, 2005. **65**(11): p. 4506-14.
30. Griffin, K.J., et al., *A transgenic mouse bearing an antisense construct of regulatory subunit type 1A of protein kinase A develops endocrine and other tumours: comparison with Carney complex and other PRKAR1A induced lesions.* J Med Genet, 2004. **41**(12): p. 923-31.
31. Griffin, K.J., et al., *Down-regulation of regulatory subunit type 1A of protein kinase A leads to endocrine and other tumors.* Cancer Res, 2004. **64**(24): p. 8811-5.
32. Yin, Z. and L.S. Kirschner, *The Carney complex gene PRKAR1A plays an essential role in cardiac development and myxomagenesis.* Trends Cardiovasc Med, 2009. **19**(2): p. 44-9.
33. Sahut-Barnola, I., et al., *Cushing's syndrome and fetal features resurgence in adrenal cortex-specific Prkar1a knockout mice.* PLoS Genet, 2010. **6**(6): p. e1000980.
34. Parkhitko, A.A., O.O. Favorova, and E.P. Henske, *Autophagy: mechanisms, regulation, and its role in tumorigenesis.* Biochemistry (Mosc), 2013. **78**(4): p. 355-67.
35. Wu, S., et al., *Inhibition of macrophage autophagy induced by Salmonella enterica serovar typhi plasmid.* Front Biosci (Landmark Ed), 2014. **19**: p. 490-503.
36. Ghavami, S., et al., *Autophagy and apoptosis dysfunction in neurodegenerative disorders.* Prog Neurobiol, 2014. **112**: p. 24-49.
37. Ciechanover, A., *The unravelling of the ubiquitin system.* Nat Rev Mol Cell Biol, 2015. **16**(5): p. 322-4.
38. Mizushima, N., et al., *Autophagy fights disease through cellular self-digestion.* Nature, 2008. **451**(7182): p. 1069-75.
39. Lee, D.H. and A.L. Goldberg, *Proteasome inhibitors: valuable new tools for cell biologists.* Trends Cell Biol, 1998. **8**(10): p. 397-403.
40. Shen, M., et al., *Targeting the ubiquitin-proteasome system for cancer therapy.* Expert Opin Ther Targets, 2013. **17**(9): p. 1091-108.
41. Glickman, M.H. and A. Ciechanover, *The ubiquitin-proteasome proteolytic pathway: destruction for the sake of construction.* Physiol Rev, 2002. **82**(2): p. 373-428.
42. Goldberg, A.L., et al., *New insights into the mechanisms and importance of the proteasome in intracellular protein degradation.* Biol Chem, 1997. **378**(3-4): p. 131-40.
43. Gallastegui, N. and M. Groll, *The 26S proteasome: assembly and function of a destructive machine.* Trends Biochem Sci, 2010. **35**(11): p. 634-42.
44. Tanaka, K., *The proteasome: overview of structure and functions.* Proc Jpn Acad Ser B Phys Biol Sci, 2009. **85**(1): p. 12-36.
45. Glick, D., S. Barth, and K.F. Macleod, *Autophagy: cellular and molecular mechanisms.* J Pathol, 2010. **221**(1): p. 3-12.
46. Amaya, C., C.M. Fader, and M.I. Colombo, *Autophagy and proteins involved in vesicular trafficking.* FEBS Lett, 2015. **589**(22): p. 3343-53.
47. Ma, K.G., et al., *Autophagy is activated in compression-induced cell degeneration and is mediated by reactive oxygen species in nucleus pulposus cells exposed to compression.* Osteoarthritis Cartilage, 2013. **21**(12): p. 2030-8.

48. Sato, K., et al., *Autophagy is activated in colorectal cancer cells and contributes to the tolerance to nutrient deprivation.* Cancer Res, 2007. **67**(20): p. 9677-84.
49. Ogata, M., et al., *Autophagy is activated for cell survival after endoplasmic reticulum stress.* Mol Cell Biol, 2006. **26**(24): p. 9220-31.
50. Patel, A.S., D. Morse, and A.M. Choi, *Regulation and functional significance of autophagy in respiratory cell biology and disease.* Am J Respir Cell Mol Biol, 2013. **48**(1): p. 1-9.
51. Patel, A.S., et al., *Autophagy in idiopathic pulmonary fibrosis.* PLoS One, 2012. **7**(7): p. e41394.
52. Li, W.W., J. Li, and J.K. Bao, *Microautophagy: lesser-known self-eating.* Cell Mol Life Sci, 2012. **69**(7): p. 1125-36.
53. Cuervo, A.M. and E. Wong, *Chaperone-mediated autophagy: roles in disease and aging.* Cell Res, 2014. **24**(1): p. 92-104.
54. De Duve, C., et al., *Tissue fractionation studies. 6. Intracellular distribution patterns of enzymes in rat-liver tissue.* Biochem J, 1955. **60**(4): p. 604-17.
55. Ohsumi, Y., *Historical landmarks of autophagy research.* Cell Res, 2014. **24**(1): p. 9-23.
56. Takeshige, K., et al., *Autophagy in yeast demonstrated with proteinase-deficient mutants and conditions for its induction.* J Cell Biol, 1992. **119**(2): p. 301-11.
57. Baba, M., et al., *Ultrastructural analysis of the autophagic process in yeast: detection of autophagosomes and their characterization.* J Cell Biol, 1994. **124**(6): p. 903-13.
58. Yao, Z., et al., *Atg41/Icy2 regulates autophagosome formation.* Autophagy, 2015. **11**(12): p. 2288-99.
59. Ohsumi, Y., *Historical landmarks of autophagy research.* Cell Research, 2014. **24**(1): p. 9-23.
60. Tsukada, M. and Y. Ohsumi, *Isolation and characterization of autophagy-defective mutants of Saccharomyces cerevisiae.* FEBS Lett, 1993. **333**(1-2): p. 169-74.
61. Jiang, P. and N. Mizushima, *Autophagy and human diseases.* Cell Res, 2014. **24**(1): p. 69-79.
62. Abada, A. and Z. Elazar, *Getting ready for building: signaling and autophagosome biogenesis.* EMBO Rep, 2014. **15**(8): p. 839-52.
63. Mizushima, N., Y. Ohsumi, and T. Yoshimori, *Autophagosome formation in mammalian cells.* Cell Struct Funct, 2002. **27**(6): p. 421-9.
64. Xie, Z. and D.J. Klionsky, *Autophagosome formation: core machinery and adaptations.* Nat Cell Biol, 2007. **9**(10): p. 1102-9.
65. Feng, Y., et al., *The machinery of macroautophagy.* Cell Res, 2014. **24**(1): p. 24-41.
66. Birgisdottir, A.B., T. Lamark, and T. Johansen, *The LIR motif - crucial for selective autophagy.* J Cell Sci, 2013. **126**(Pt 15): p. 3237-47.
67. Mizushima, N., *Autophagy: process and function.* Genes Dev, 2007. **21**(22): p. 2861-73.
68. Hayashi-Nishino, M., et al., *A subdomain of the endoplasmic reticulum forms a cradle for autophagosome formation.* Nat Cell Biol, 2009. **11**(12): p. 1433-7.
69. van der Vaart, A. and F. Reggiori, *The Golgi complex as a source for yeast autophagosomal membranes.* Autophagy, 2010. **6**(6): p. 800-1.
70. Hailey, D.W., et al., *Mitochondria supply membranes for autophagosome biogenesis during starvation.* Cell, 2010. **141**(4): p. 656-67.
71. Ravikumar, B., et al., *Plasma membrane contributes to the formation of pre-autophagosomal structures.* Nat Cell Biol, 2010. **12**(8): p. 747-57.
72. Alers, S., et al., *Role of AMPK-mTOR-Ulk1/2 in the regulation of autophagy: cross talk, shortcuts, and feedbacks.* Mol Cell Biol, 2012. **32**(1): p. 2-11.
73. Mizushima, N., *The role of the Atg1/ULK1 complex in autophagy regulation.* Curr Opin Cell Biol, 2010. **22**(2): p. 132-9.
74. Jung, C.H., et al., *ULK-Atg13-FIP200 complexes mediate mTOR signaling to the autophagy machinery.* Mol Biol Cell, 2009. **20**(7): p. 1992-2003.

75. Sarkar, S., et al., *Rapamycin and mTOR-independent autophagy inducers ameliorate toxicity of polyglutamine-expanded huntingtin and related proteinopathies.* Cell Death Differ, 2009. **16**(1): p. 46-56.
76. Mehrpour, M., et al., *Overview of macroautophagy regulation in mammalian cells.* Cell Res, 2010. **20**(7): p. 748-62.
77. Suzuki, K., et al., *The pre-autophagosomal structure organized by concerted functions of APG genes is essential for autophagosome formation.* Embo j, 2001. **20**(21): p. 5971-81.
78. Kim, J., et al., *Convergence of multiple autophagy and cytoplasm to vacuole targeting components to a perivacuolar membrane compartment prior to de novo vesicle formation.* J Biol Chem, 2002. **277**(1): p. 763-73.
79. Burman, C. and N.T. Ktistakis, *Regulation of autophagy by phosphatidylinositol 3-phosphate.* FEBS Lett, 2010. **584**(7): p. 1302-12.
80. Hale, A.N., et al., *Autophagy: regulation and role in development.* Autophagy, 2013. **9**(7): p. 951-72.
81. Proikas-Cezanne, T., et al., *WIPI-1alpha (WIPI49), a member of the novel 7-bladed WIPI protein family, is aberrantly expressed in human cancer and is linked to starvation-induced autophagy.* Oncogene, 2004. **23**(58): p. 9314-25.
82. Polson, H.E., et al., *Mammalian Atg18 (WIPI2) localizes to omegasome-anchored phagophores and positively regulates LC3 lipidation.* Autophagy, 2010. **6**(4): p. 506-22.
83. Kihara, A., et al., *Two distinct Vps34 phosphatidylinositol 3-kinase complexes function in autophagy and carboxypeptidase Y sorting in Saccharomyces cerevisiae.* J Cell Biol, 2001. **152**(3): p. 519-30.
84. Fimia, G.M., et al., *Ambra1 regulates autophagy and development of the nervous system.* Nature, 2007. **447**(7148): p. 1121-5.
85. Liang, C., et al., *Beclin1-binding UVRAG targets the class C Vps complex to coordinate autophagosome maturation and endocytic trafficking.* Nat Cell Biol, 2008. **10**(7): p. 776-87.
86. He, C. and D.J. Klionsky, *Regulation mechanisms and signaling pathways of autophagy.* Annu Rev Genet, 2009. **43**: p. 67-93.
87. Simonsen, A. and S.A. Tooze, *Coordination of membrane events during autophagy by multiple class III PI3-kinase complexes.* J Cell Biol, 2009. **186**(6): p. 773-82.
88. Kaiser, S.E., et al., *Noncanonical E2 recruitment by the autophagy E1 revealed by Atg7-Atg3 and Atg7-Atg10 structures.* Nat Struct Mol Biol, 2012. **19**(12): p. 1242-9.
89. Mizushima, N., et al., *A protein conjugation system essential for autophagy.* Nature, 1998. **395**(6700): p. 395-8.
90. Kuma, A., et al., *Formation of the approximately 350-kDa Apg12-Apg5.Apg16 multimeric complex, mediated by Apg16 oligomerization, is essential for autophagy in yeast.* J Biol Chem, 2002. **277**(21): p. 18619-25.
91. Mizushima, N., et al., *Mouse Apg16L, a novel WD-repeat protein, targets to the autophagic isolation membrane with the Apg12-Apg5 conjugate.* J Cell Sci, 2003. **116**(Pt 9): p. 1679-88.
92. Shpilka, T., et al., *Atg8: an autophagy-related ubiquitin-like protein family.* Genome Biol, 2011. **12**(7): p. 226.
93. Alemu, E.A., et al., *ATG8 family proteins act as scaffolds for assembly of the ULK complex: sequence requirements for LC3-interacting region (LIR) motifs.* J Biol Chem, 2012. **287**(47): p. 39275-90.
94. Marino, G., et al., *Human autophagins, a family of cysteine proteinases potentially implicated in cell degradation by autophagy.* J Biol Chem, 2003. **278**(6): p. 3671-8.
95. Mizushima, N., et al., *Dissection of autophagosome formation using Apg5-deficient mouse embryonic stem cells.* J Cell Biol, 2001. **152**(4): p. 657-68.
96. Fujita, N., et al., *The Atg16L complex specifies the site of LC3 lipidation for membrane biogenesis in autophagy.* Mol Biol Cell, 2008. **19**(5): p. 2092-100.

97. Eskelinen, E.L., *Maturation of autophagic vacuoles in Mammalian cells.* Autophagy, 2005. **1**(1): p. 1-10.
98. Noda, T., N. Fujita, and T. Yoshimori, *The late stages of autophagy: how does the end begin?* Cell Death Differ, 2009. **16**(7): p. 984-90.
99. Jager, S., et al., *Role for Rab7 in maturation of late autophagic vacuoles.* J Cell Sci, 2004. **117**(Pt 20): p. 4837-48.
100. Kimura, S., T. Noda, and T. Yoshimori, *Dissection of the autophagosome maturation process by a novel reporter protein, tandem fluorescent-tagged LC3.* Autophagy, 2007. **3**(5): p. 452-60.
101. Hyttinen, J.M., et al., *Maturation of autophagosomes and endosomes: a key role for Rab7.* Biochim Biophys Acta, 2013. **1833**(3): p. 503-10.
102. Guerra, F. and C. Bucci, *Multiple Roles of the Small GTPase Rab7.* Cells, 2016. **5**(3).
103. Pereira-Leal, J.B. and M.C. Seabra, *Evolution of the Rab family of small GTP-binding proteins.* J Mol Biol, 2001. **313**(4): p. 889-901.
104. Bucci, C., et al., *Rab7: a key to lysosome biogenesis.* Mol Biol Cell, 2000. **11**(2): p. 467-80.
105. Pereira-Leal, J.B. and M.C. Seabra, *The mammalian Rab family of small GTPases: definition of family and subfamily sequence motifs suggests a mechanism for functional specificity in the Ras superfamily.* J Mol Biol, 2000. **301**(4): p. 1077-87.
106. Progida, C., et al., *Dynamics of Rab7b-dependent transport of sorting receptors.* Traffic, 2012. **13**(9): p. 1273-85.
107. McGough, I.J. and P.J. Cullen, *Recent advances in retromer biology.* Traffic, 2011. **12**(8): p. 963-71.
108. Liu, T.T., et al., *Rab GTPase regulation of retromer-mediated cargo export during endosome maturation.* Mol Biol Cell, 2012. **23**(13): p. 2505-15.
109. Mizuno, K., A. Kitamura, and T. Sasaki, *Rabring7, a novel Rab7 target protein with a RING finger motif.* Mol Biol Cell, 2003. **14**(9): p. 3741-52.
110. Alessandrini, F., L. Pezze, and Y. Ciribilli, *LAMPs: Shedding light on cancer biology.* Semin Oncol, 2017. **44**(4): p. 239-253.
111. Wilke, S., J. Krausze, and K. Bussow, *Crystal structure of the conserved domain of the DC lysosomal associated membrane protein: implications for the lysosomal glycocalyx.* BMC Biol, 2012. **10**: p. 62.
112. Eskelinen, E.L., *Roles of LAMP-1 and LAMP-2 in lysosome biogenesis and autophagy.* Mol Aspects Med, 2006. **27**(5-6): p. 495-502.
113. Murphy, K.E., et al., *Lysosomal-associated membrane protein 2 isoforms are differentially affected in early Parkinson's disease.* Mov Disord, 2015. **30**(12): p. 1639-47.
114. Eskelinen, E.L., et al., *Disturbed cholesterol traffic but normal proteolytic function in LAMP-1/LAMP-2 double-deficient fibroblasts.* Mol Biol Cell, 2004. **15**(7): p. 3132-45.
115. Eskelinen, E.-L., *Roles of LAMP-1 and LAMP-2 in lysosome biogenesis and autophagy.* Molecular Aspects of Medicine, 2006. **27**(5): p. 495-502.
116. Mizushima, N., T. Yoshimori, and Y. Ohsumi, *The role of Atg proteins in autophagosome formation.* Annu Rev Cell Dev Biol, 2011. **27**: p. 107-32.
117. Reggiori, F. and D.J. Klionsky, *Autophagic processes in yeast: mechanism, machinery and regulation.* Genetics, 2013. **194**(2): p. 341-61.
118. Parzych, K.R. and D.J. Klionsky, *An overview of autophagy: morphology, mechanism, and regulation.* Antioxid Redox Signal, 2014. **20**(3): p. 460-73.
119. Noda, T. and Y. Ohsumi, *Tor, a phosphatidylinositol kinase homologue, controls autophagy in yeast.* J Biol Chem, 1998. **273**(7): p. 3963-6.
120. Zoncu, R., A. Efeyan, and D.M. Sabatini, *mTOR: from growth signal integration to cancer, diabetes and ageing.* Nat Rev Mol Cell Biol, 2011. **12**(1): p. 21-35.
121. Rabanal-Ruiz, Y. and V.I. Korolchuk, *mTORC1 and Nutrient Homeostasis: The Central Role of the Lysosome.* Int J Mol Sci, 2018. **19**(3).

122. Jiang, Y. and J.R. Broach, *Tor proteins and protein phosphatase 2A reciprocally regulate Tap42 in controlling cell growth in yeast.* Embo j, 1999. **18**(10): p. 2782-92.
123. Rohde, J., J. Heitman, and M.E. Cardenas, *The TOR kinases link nutrient sensing to cell growth.* J Biol Chem, 2001. **276**(13): p. 9583-6.
124. Beck, T. and M.N. Hall, *The TOR signalling pathway controls nuclear localization of nutrient-regulated transcription factors.* Nature, 1999. **402**(6762): p. 689-92.
125. Pattingre, S., et al., *Bcl-2 antiapoptotic proteins inhibit Beclin 1-dependent autophagy.* Cell, 2005. **122**(6): p. 927-39.
126. Yang, Y.P., et al., *Molecular mechanism and regulation of autophagy.* Acta Pharmacol Sin, 2005. **26**(12): p. 1421-34.
127. Tee, A.R., *The Target of Rapamycin and Mechanisms of Cell Growth.* Int J Mol Sci, 2018. **19**(3).
128. Stephan, J.S., et al., *The Tor and cAMP-dependent protein kinase signaling pathways coordinately control autophagy in Saccharomyces cerevisiae.* Autophagy, 2010. **6**(2): p. 294-5.
129. Cherra, S.J., 3rd, et al., *Regulation of the autophagy protein LC3 by phosphorylation.* J Cell Biol, 2010. **190**(4): p. 533-9.
130. Budovskaya, Y.V., et al., *The Ras/cAMP-dependent protein kinase signaling pathway regulates an early step of the autophagy process in Saccharomyces cerevisiae.* J Biol Chem, 2004. **279**(20): p. 20663-71.
131. Torres-Quiroz, F., M. Filteau, and C.R. Landry, *Feedback regulation between autophagy and PKA.* Autophagy, 2015. **11**(7): p. 1181-3.
132. Yorimitsu, T., et al., *Protein kinase A and Sch9 cooperatively regulate induction of autophagy in Saccharomyces cerevisiae.* Mol Biol Cell, 2007. **18**(10): p. 4180-9.
133. Cebollero, E. and F. Reggiori, *Regulation of autophagy in yeast Saccharomyces cerevisiae.* Biochim Biophys Acta, 2009. **1793**(9): p. 1413-21.
134. Budovskaya, Y.V., et al., *An evolutionary proteomics approach identifies substrates of the cAMP-dependent protein kinase.* Proc Natl Acad Sci U S A, 2005. **102**(39): p. 13933-8.
135. McEwan, D.G. and I. Dikic, *The Three Musketeers of Autophagy: phosphorylation, ubiquitylation and acetylation.* Trends Cell Biol, 2011. **21**(4): p. 195-201.
136. Klionsky, D.J. and S.D. Emr, *Autophagy as a regulated pathway of cellular degradation.* Science, 2000. **290**(5497): p. 1717-21.
137. Weidberg, H., E. Shvets, and Z. Elazar, *Biogenesis and cargo selectivity of autophagosomes.* Annu Rev Biochem, 2011. **80**: p. 125-56.
138. Wood, V., et al., *The genome sequence of Schizosaccharomyces pombe.* Nature, 2002. **415**(6874): p. 871-80.
139. Weidberg, H., et al., *LC3 and GATE-16/GABARAP subfamilies are both essential yet act differently in autophagosome biogenesis.* Embo j, 2010. **29**(11): p. 1792-802.
140. Xie, Z., U. Nair, and D.J. Klionsky, *Atg8 controls phagophore expansion during autophagosome formation.* Mol Biol Cell, 2008. **19**(8): p. 3290-8.
141. Lynch-Day, M.A. and D.J. Klionsky, *The Cvt pathway as a model for selective autophagy.* FEBS Lett, 2010. **584**(7): p. 1359-66.
142. Suzuki, K., et al., *Selective transport of alpha-mannosidase by autophagic pathways: identification of a novel receptor, Atg34p.* J Biol Chem, 2010. **285**(39): p. 30019-25.
143. Rogov, V., et al., *Interactions between autophagy receptors and ubiquitin-like proteins form the molecular basis for selective autophagy.* Mol Cell, 2014. **53**(2): p. 167-78.
144. Ichimura, Y., et al., *Structural basis for sorting mechanism of p62 in selective autophagy.* J Biol Chem, 2008. **283**(33): p. 22847-57.
145. Pankiv, S., et al., *p62/SQSTM1 binds directly to Atg8/LC3 to facilitate degradation of ubiquitinated protein aggregates by autophagy.* J Biol Chem, 2007. **282**(33): p. 24131-45.

146. Johansen, T. and T. Lamark, *Selective autophagy mediated by autophagic adapter proteins.* Autophagy, 2011. **7**(3): p. 279-96.
147. Behrends, C., et al., *Network organization of the human autophagy system.* Nature, 2010. **466**(7302): p. 68-76.
148. Kraft, C., et al., *Binding of the Atg1/ULK1 kinase to the ubiquitin-like protein Atg8 regulates autophagy.* Embo j, 2012. **31**(18): p. 3691-703.
149. Nakatogawa, H., et al., *The autophagy-related protein kinase Atg1 interacts with the ubiquitin-like protein Atg8 via the Atg8 family interacting motif to facilitate autophagosome formation.* J Biol Chem, 2012. **287**(34): p. 28503-7.
150. Suzuki, H., et al., *Structural basis of the autophagy-related LC3/Atg13 LIR complex: recognition and interaction mechanism.* Structure, 2014. **22**(1): p. 47-58.
151. Stolz, A., A. Ernst, and I. Dikic, *Cargo recognition and trafficking in selective autophagy.* Nat Cell Biol, 2014. **16**(6): p. 495-501.
152. Hasegawa, J., et al., *Selective autophagy: lysophagy.* Methods, 2015. **75**: p. 128-32.
153. Meijer, W.H., et al., *ATG genes involved in non-selective autophagy are conserved from yeast to man, but the selective Cvt and pexophagy pathways also require organism-specific genes.* Autophagy, 2007. **3**(2): p. 106-16.
154. Bjorkoy, G., et al., *p62/SQSTM1 forms protein aggregates degraded by autophagy and has a protective effect on huntingtin-induced cell death.* J Cell Biol, 2005. **171**(4): p. 603-14.
155. Kirkin, V., et al., *A role for NBR1 in autophagosomal degradation of ubiquitinated substrates.* Mol Cell, 2009. **33**(4): p. 505-16.
156. Lamark, T., et al., *NBR1 and p62 as cargo receptors for selective autophagy of ubiquitinated targets.* Cell Cycle, 2009. **8**(13): p. 1986-90.
157. Newman, A.C., et al., *TBK1 kinase addiction in lung cancer cells is mediated via autophagy of Tax1bp1/Ndp52 and non-canonical NF-kappaB signalling.* PLoS One, 2012. **7**(11): p. e50672.
158. Thurston, T.L., et al., *The TBK1 adaptor and autophagy receptor NDP52 restricts the proliferation of ubiquitin-coated bacteria.* Nat Immunol, 2009. **10**(11): p. 1215-21.
159. Wild, P., et al., *Phosphorylation of the autophagy receptor optineurin restricts Salmonella growth.* Science, 2011. **333**(6039): p. 228-33.
160. Loilome, W., et al., *PRKAR1A is overexpressed and represents a possible therapeutic target in human cholangiocarcinoma.* Int J Cancer, 2011. **129**(1): p. 34-44.
161. Mavrakis, M., et al., *Depletion of type IA regulatory subunit (RIalpha) of protein kinase A (PKA) in mammalian cells and tissues activates mTOR and causes autophagic deficiency.* Hum Mol Genet, 2006. **15**(19): p. 2962-71.
162. Mavrakis, M., et al., *mTOR kinase and the regulatory subunit of protein kinase A (PRKAR1A) spatially and functionally interact during autophagosome maturation.* Autophagy, 2007. **3**(2): p. 151-3.
163. Day, M.E., et al., *Isoform-specific targeting of PKA to multivesicular bodies.* J Cell Biol, 2011. **193**(2): p. 347-63.
164. Lamark, T., et al., *Interaction codes within the family of mammalian Phox and Bem1p domain-containing proteins.* J Biol Chem, 2003. **278**(36): p. 34568-81.
165. Bhujabal, Z., et al., *FKBP8 recruits LC3A to mediate Parkin-independent mitophagy.* EMBO Rep, 2017. **18**(6): p. 947-961.
166. Hanahan D, *Techniques for transformation of E. coli*, in *DNA cloning: A practical approach*, Glover DM, Editor. 1985, IRL Press,: Washington, DC. p. 109-135,.
167. Hartley, J.L., G.F. Temple, and M.A. Brasch, *DNA cloning using in vitro site-specific recombination.* Genome Res, 2000. **10**(11): p. 1788-95.
168. Magnani, E., L. Bartling, and S. Hake, *From Gateway to MultiSite Gateway in one recombination event.* BMC Mol Biol, 2006. **7**: p. 46.
169. Zhang, S. and M.D. Cahalan, *Purifying plasmid DNA from bacterial colonies using the QIAGEN Miniprep Kit.* J Vis Exp, 2007(6): p. 247.

170. Yılmaz, M., C. Ozic, and İ. Gok, *Principles of Nucleic Acid Separation by Agarose Gel Electrophoresis*. 2012. 33-40.
171. Waters, D.L. and F.M. Shapter, *The polymerase chain reaction (PCR): general methods.* Methods Mol Biol, 2014. **1099**: p. 65-75.
172. Liu, H. and J.H. Naismith, *An efficient one-step site-directed deletion, insertion, single and multiple-site plasmid mutagenesis protocol.* BMC Biotechnol, 2008. **8**: p. 91.
173. Kinoshita, E., E. Kinoshita-Kikuta, and T. Koike, *Separation and detection of large phosphoproteins using Phos-tag SDS-PAGE.* Nat Protoc, 2009. **4**(10): p. 1513-21.
174. Shapiro, A.L., E. Vinuela, and J.V. Maizel, Jr., *Molecular weight estimation of polypeptide chains by electrophoresis in SDS-polyacrylamide gels.* Biochem Biophys Res Commun, 1967. **28**(5): p. 815-20.
175. Luo, L., et al., *Single-step protease cleavage elution for identification of protein-protein interactions from GST pull-down and mass spectrometry.* Proteomics, 2014. **14**(1): p. 19-23.
176. Kaelin, W.G., Jr., et al., *Identification of cellular proteins that can interact specifically with the T/E1A-binding region of the retinoblastoma gene product.* Cell, 1991. **64**(3): p. 521-32.
177. Mahmood, T. and P.-C. Yang, *Western Blot: Technique, Theory, and Trouble Shooting.* North American Journal of Medical Sciences, 2012. **4**(9): p. 429-434.
178. Kim, T.K. and J.H. Eberwine, *Mammalian cell transfection: the present and the future.* Anal Bioanal Chem, 2010. **397**(8): p. 3173-8.
179. Sanderson, M.J., et al., *Fluorescence microscopy.* Cold Spring Harb Protoc, 2014. **2014**(10): p. pdb.top071795.
180. Peter, S., K. Harter, and F. Schleifenbaum, *Fluorescence microscopy.* Methods Mol Biol, 2014. **1062**: p. 429-52.
181. Paddock, S.W., *Principles and practices of laser scanning confocal microscopy.* Mol Biotechnol, 2000. **16**(2): p. 127-49.
182. Wright, S.J. and D.J. Wright, *Introduction to confocal microscopy.* Methods Cell Biol, 2002. **70**: p. 1-85.
183. Odell, I.D. and D. Cook, *Immunofluorescence techniques.* J Invest Dermatol, 2013. **133**(1): p. e4.
184. Gerace, E. and D. Moazed, *Affinity pull-down of proteins using anti-FLAG M2 agarose beads*, in *Methods in enzymology*. 2015, Elsevier. p. 99-110.
185. Patronas, Y., et al., *In vitro studies of novel PRKAR1A mutants that extend the predicted RIalpha protein sequence into the 3'-untranslated open reading frame: proteasomal degradation leads to RIalpha haploinsufficiency and Carney complex.* J Clin Endocrinol Metab, 2012. **97**(3): p. E496-502.
186. Sancho, A., et al., *DOR/Tp53inp2 and Tp53inp1 constitute a metazoan gene family encoding dual regulators of autophagy and transcription.* PLoS One, 2012. **7**(3): p. e34034.
187. Shacka, J.J., B.J. Klocke, and K.A. Roth, *Autophagy, bafilomycin and cell death: the "a-B-cs" of plecomacrolide-induced neuroprotection.* Autophagy, 2006. **2**(3): p. 228-30.
188. Yuan, N., et al., *Bafilomycin A1 targets both autophagy and apoptosis pathways in pediatric B-cell acute lymphoblastic leukemia.* Haematologica, 2015. **100**(3): p. 345-56.
189. Han, Y.H., et al., *The effect of MG132, a proteasome inhibitor on HeLa cells in relation to cell growth, reactive oxygen species and GSH.* Oncol Rep, 2009. **22**(1): p. 215-21.
190. Davis, S., J. Wang, and S. Ferro-Novick, *Crosstalk between the Secretory and Autophagy Pathways Regulates Autophagosome Formation.* Dev Cell, 2017. **41**(1): p. 23-32.
191. Mei, S., et al., *Autophagy is activated to protect against endotoxic acute kidney injury.* Sci Rep, 2016. **6**: p. 22171.
192. Bjorkoy, G., et al., *Monitoring autophagic degradation of p62/SQSTM1.* Methods Enzymol, 2009. **452**: p. 181-97.

193. Chittaranjan, S., S. Bortnik, and S.M. Gorski, *Monitoring Autophagic Flux by Using Lysosomal Inhibitors and Western Blotting of Endogenous MAP1LC3B.* Cold Spring Harb Protoc, 2015. **2015**(8): p. 743-50.
194. Loos, B., A. du Toit, and J.H. Hofmeyr, *Defining and measuring autophagosome flux-concept and reality.* Autophagy, 2014. **10**(11): p. 2087-96.
195. Klionsky, D.J., et al., *Guidelines for the use and interpretation of assays for monitoring autophagy.* Autophagy, 2012. **8**(4): p. 445-544.
196. Pugsley, H.R., *Assessing Autophagic Flux by Measuring LC3, p62, and LAMP1 Co-localization Using Multispectral Imaging Flow Cytometry.* J Vis Exp, 2017(125).
197. Joachim, J. and S.A. Tooze, *Control of GABARAP-mediated autophagy by the Golgi complex, centrosome and centriolar satellites.* Biol Cell, 2018. **110**(1): p. 1-5.
198. Weidberg, H., et al., *LC3 and GATE-16/GABARAP subfamilies are both essential yet act differently in autophagosome biogenesis.* The EMBO Journal, 2010. **29**(11): p. 1792-1802.
199. Lamark, T., S. Svenning, and T. Johansen, *Regulation of selective autophagy: the p62/SQSTM1 paradigm.* Essays Biochem, 2017. **61**(6): p. 609-624.
200. Lee, Y. and C.C. Weihl, *Regulation of SQSTM1/p62 via UBA domain ubiquitination and its role in disease.* Autophagy, 2017. **13**(9): p. 1615-1616.
201. Tooze, S.A., *SNAREing an ARP requires a LIR.* J Cell Biol, 2018. **217**(3): p. 803-805.
202. Rogov, V.V., et al., *Phosphorylation of the mitochondrial autophagy receptor Nix enhances its interaction with LC3 proteins.* Sci Rep, 2017. **7**(1): p. 1131.
203. Ji, C.H. and Y.T. Kwon, *Crosstalk and Interplay between the Ubiquitin-Proteasome System and Autophagy.* Mol Cells, 2017. **40**(7): p. 441-449.
204. Nam, T., et al., *Emerging Paradigm of Crosstalk between Autophagy and the Ubiquitin-Proteasome System.* Mol Cells, 2017. **40**(12): p. 897-905.
205. Itakura, E. and N. Mizushima, *p62 Targeting to the autophagosome formation site requires self-oligomerization but not LC3 binding.* J Cell Biol, 2011. **192**(1): p. 17-27.
206. Padman, B.S., T.N. Nguyen, and M. Lazarou, *Autophagosome formation and cargo sequestration in the absence of LC3/GABARAPs.* Autophagy, 2017. **13**(4): p. 772-774.
207. Stephan, J.S., et al., *The Tor and PKA signaling pathways independently target the Atg1/Atg13 protein kinase complex to control autophagy.* Proc Natl Acad Sci U S A, 2009. **106**(40): p. 17049-54.
208. Tanida, I., T. Ueno, and E. Kominami, *LC3 and Autophagy.* Methods Mol Biol, 2008. **445**: p. 77-88.
209. Humphries, W.H., C.J. Szymanski, and C.K. Payne, *Endo-Lysosomal Vesicles Positive for Rab7 and LAMP1 Are Terminal Vesicles for the Transport of Dextran.* PLoS ONE, 2011. **6**(10): p. e26626.
210. Jimenez-Orgaz, A., et al., *Control of RAB7 activity and localization through the retromer-TBC1D5 complex enables RAB7-dependent mitophagy.* Embo j, 2018. **37**(2): p. 235-254.
211. Clague, M.J. and S. Urbe, *Multivesicular bodies.* Curr Biol, 2008. **18**(10): p. R402-r404.

7. Appendix

Table 7.1: Raw data for quantitation of LC3B puncta in fifty transfected cells co-expressed with GFP-PRKAR1A with and without catalytic subunit of PKA under FM and starved conditions. EGFP vector is used as negative control.

No. of cells	EGFP-PRKAR1A+ Cat PKA+ FM	EGFPPRKAR1A + Cat PKA+ HBSS	EGFP-PRKAR1A+FM	EGFP-PRKAR1A+HBSS	EGFP+FM	EGFP+HBSS
1	3	3	3	6	19	18
2	2	2	3	3	13	12
3	1	2	10	2	10	13
4	7	3	5	2	10	15
5	12	2	12	4	13	8
6	15	1	3	4	8	22
7	10	2	6	3	12	15
8	7	3	8	6	10	16
9	9	3	5	2	8	13
10	11	3	3	2	5	18
11	11	2	3	2	9	10
12	11	5	5	10	5	9
13	3	4	3	7	5	5
14	7	2	7	2	7	4
15	4	3	4	4	5	19
16	7	2	4	8	6	16
17	5	4	7	3	4	24
18	3	4	8	3	12	18
19	10	5	5	5	8	12
20	8	3	5	6	6	10
21	9	4	6	4	25	16
22	3	5	7	2	8	18
23	20	7	7	1	14	15
24	18	2	4	8	4	16
25	9	2	13	6	8	2
26	7	1	16	10	8	8
27	10	8	8	5	9	16
28	2	8	4	8	5	8
29	8	18	15	4	7	7
30	3	4	5	13	11	9
31	2	10	6	10	10	4
32	5	3	8	5	8	13
33	2	5	8	8	11	15
34	1	3	10	5	7	14
35	2	7	7	3	10	16
36	4	10	5	2	8	18
37	3	4	2	6	10	20
38	3	3	4	5	8	5
39	7	3	3	2	12	18
40	9	5	8	5	12	12
41	5	10	18	4	17	10
42	7	4	3	8	12	14
43	9	5	21	13	8	9
44	16	5	16	5	9	5
45	7	5	22	2	15	8

46	3	17	8	3	6	12
47	1	10	10	8	18	24
48	6	6	5	12	7	17
49	15	3	7	1	10	10
50	9	4	6	3	6	8
Average	7.02	4.78	7.42	5.1	9.56	12.88
Std dev	4.55573198	3.518406411	4.712510488	3.098715995	4.116467675	5.286254799
SEM	0.644277795	0.497577806	0.666449625	0.429546044	0.582156442	0.732784108

8. Supplementary figures

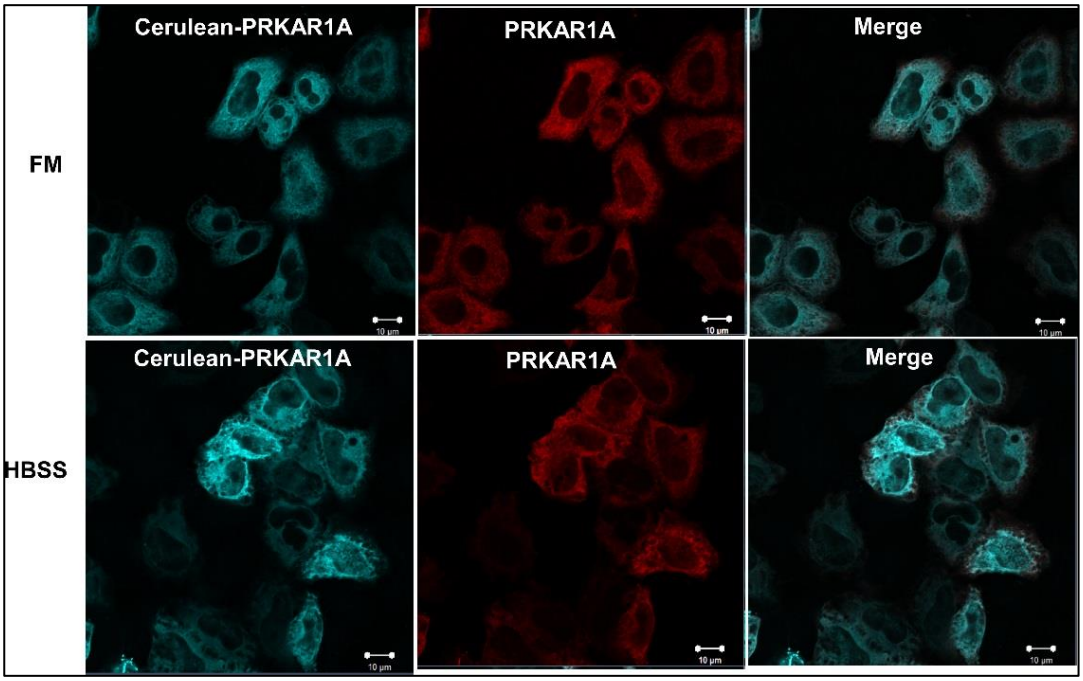

Supplementary Figure S1: PRKAR1A is localized to cytoplasm. HeLa cells were transiently transfected with Cerulean-PRKAR1A expressing constructs and cultured in FM (A) and starved for 4 hours in HBSS (B), fixed with methanol and subjected to immunofluorescence using anti-PRKAR1A and Rabbit Alexa 647 secondary antibody. Scale bar 10µm.

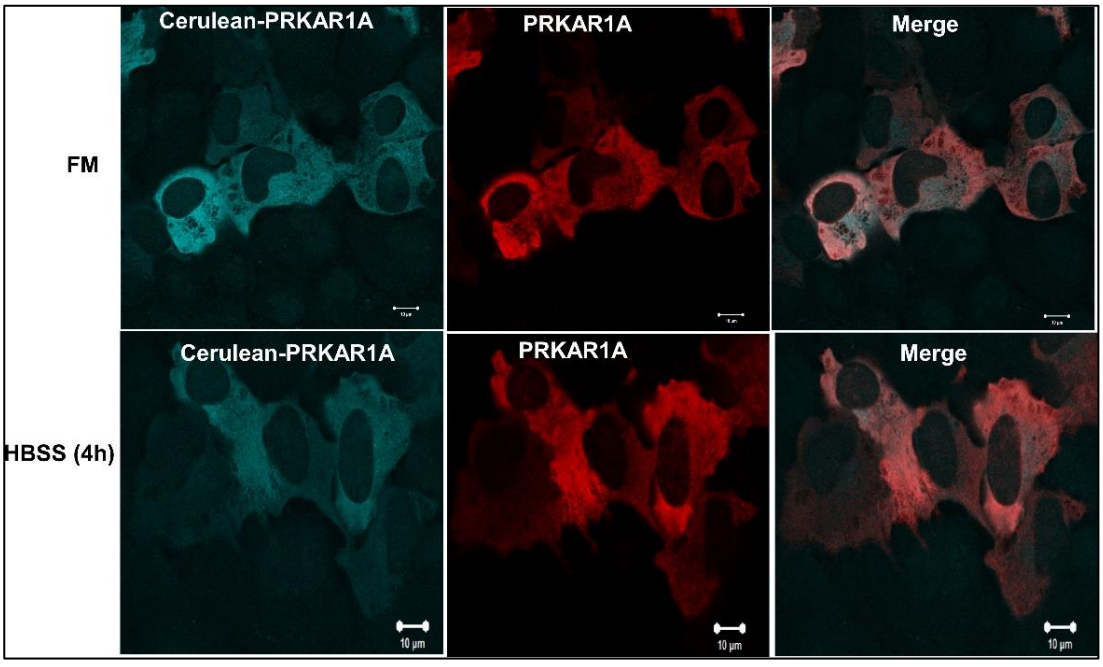

Supplementary Figure S2: PRKAR1A is localized to cytoplasm. U2OS cells were transiently transfected with Cerulean-PRKAR1A expressing constructs and cultured in FM and starved for 4 hours in HBSS, fixed with methanol and subjected to immunofluorescence using anti-PRKAR1A and Rabbit Alexa 647 secondary antibody. Scale bar 10 µm.

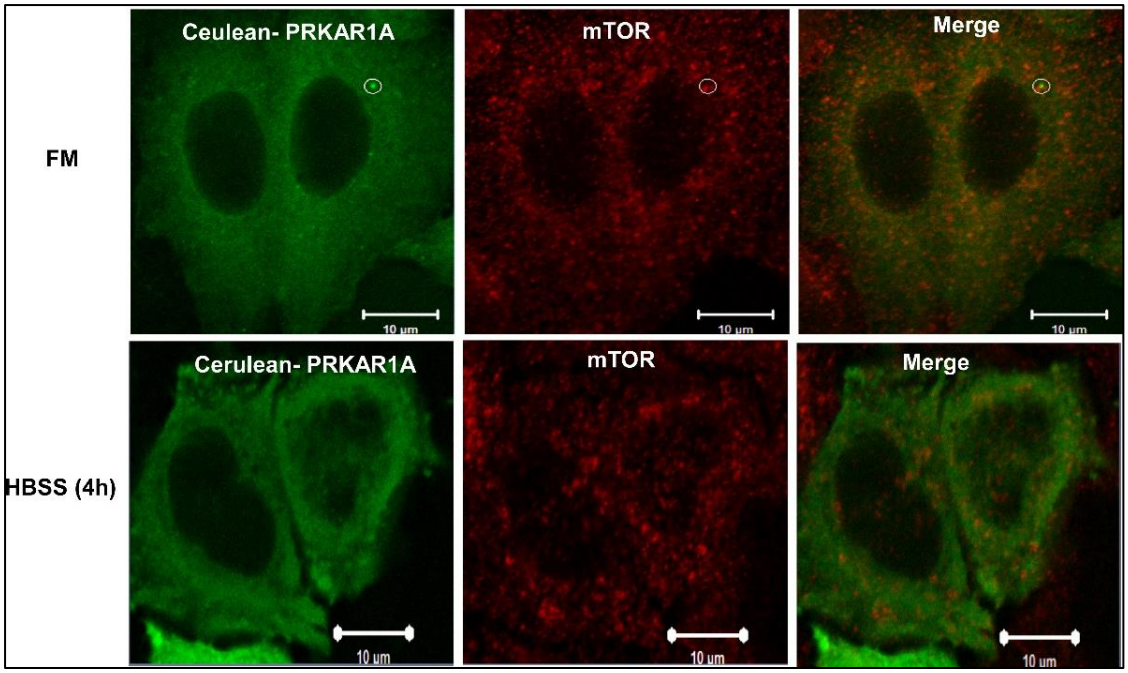

Supplementary Figure S3: Colocalization with mTOR was difficult to determine. HeLa cells were transiently transfected with Cerulean-PRKAR1A expressing constructs and cultured in FM and starved for 4 hours in HBSS, fixed with methanol and subjected to immunofluorescence using anti-mTOR and Alexa 555 secondary antibody. White rings indicate no colocalization. Scale bar 10 µm.